Contents

Chapter 1

Introduction

These "notes" are developed for a graduate course primarily focused on the physical processes in stellar atmospheres. The goals are for the students to develop a comprehensive understanding of the physics that give rise to the overall continuum shape, absorption lines, and "breaks" in stellar spectra.

Since the spectra are dominated by the region of the star where the optical depth approaches unity, we will focus on the physics in this region of stars, i.e., the atmosphere and photosphere. The overall stellar mass and radius dictates the pressure gradient in the atmosphere, which then dictates the temperature, density, chemical ionization balance, occupation of excited atomic states, and radiation field in the stellar atmosphere. The behavior of absorption lines are governed by gas convective motions (microturbulence), pressure broadening, and rotation speed of the star. For most stars, atomic processes dominate, though in cooler stars molecular processes dominate.

All this physical processes lends itself to the phenomonology of spectral classification. Though classification is not an end in and of itself, it does provide a means to catagorize the physical regime of the atmosphere of a star (and therefore the entire star, i.e., mass, metallicity, radius, luminosity) once the spectrum is placed in the context of its classification.

1.1 Topics Covered

Topics that will be covered include

Physics Governing Absorption Lines ; Anatomy of a Spectrum; The Photosphere; Anatomy of Stellar Spectra;

HR Diagram ; Photometry; Hydrogenic Atoms; Multi-Electron Atoms;

Gas Physics ; Abundances; Radiative Processes; Detailed Balancing in Thermal Equilibrium; Non-Equilibrium Gas;

The Radiation Field ; Moments of the Radiation Field; Macroscopic Terms of Radiation Transfer; General Equation of Radiative Transfer; Macroscopic versus Microscopic Terms; Equating Macro and Micro Terms;

Plane Parallel Approximation ; Eddington's Treatment; Moments of the Transfer Equation; The Grey Approximation; The Grey Atmosphere Model;

Flux Transport ; Convection Transport; Mixing Length Models; Superadiabatic Transport;

Cross Sections ; Absorption Cross Sections for Lines; Thermal and Turbulent Redistribution; Collisional/Pressure Broadening; The Total Line Absorption Cross Section; Overview of Continuous Cross Sections; Bound-Free Cross Section Hydrogenic Atoms; Free-Free Cross Section Hydrogenic Atoms; Bound-Free Cross Section of H^-; Free-Free Cross Section of H^-; Sum of H and H^- Cross Sections; Continuum Scattering Cross Section Bound-Free Cross Section of HeII; Bound-Free Cross Section of HeI; Free-Free Cross Section of HeII and HeI; Bound-Free Cross Section of He^-; Free-Free Cross Section of He^-;

Specteal Classification ; First-Order Spectral Classification; Higher-Order Spectral Classification;

1.2 Recommended Texts

- *Stellar Atmospheres*, by D. Mihalas. This is a highly theoretical book, but has extended discussions that aid in building physical intuition. This is an advance graduate level textbook. There is a great deal of mathematical treatment, but the author does an excellent job of explaining the context and meaning of the expressions. If you study out of this book it will be very rewarding in the long run. Especially focused on this class material is Chapters 1 through 5. Advanced topics, such as non thermal equilibrium and stellar winds are treated in later chapters.

- *The Observation and Analysis of Stellar Photospheres*, by D. Gray. This is an excellent introductory book for advance undergraduates or entering graduate students. It covers a wide range of topics, including comprehensive treatment of absorption line formation and the continuum opacity of stars. This book has special emphasis on interpretation of observations.

- *Introduction to Stellar Atmospheres*, by E. Novotny. This is an excellent introductory level book that is easily accessible and clear. It is an upper division undergraduate book. The explanations and diagrams (especially those detailing radiative transfer) are very helpful for stellar atmosphere modeling. The book is a little light on theory and the notation could be improved.

- *Stellar Structure and Evolution*, by R. Kippenhahn and A. Weigert. The main focus on this book is stellar structure, though the physics and modeling of stellar atmospherses is covered in some detail. It is written for capabable graduate students. The book provides a thorough and accessible treatment of thermodynamics and hydrodynamics, and the equation of state for an ideal gas with radiation in the stellar envelope and atmosphere.

- *Principles of Stellar Evolution and Nucleosynthesis*, by D. Clayton. This book was the standard for decades. Written for the capable and advance graduate student, it is terse (to the point) and comprehensive. Treatment of individual topics includes a cross between brief insights of the fundamental theoretical background and approximation formulae, with much of the details in between left to the reader to hunt down elsewhere. Still, the book is an excelent resource.

- *The Fundamentals of Stellar Astrophysics*, by G. W. Collins. The main focus on this book is stellar structure, though the physics and modeling of stellar atmospherses is covered in sufficient detial. It is written for advanced undegraduates and entering graduate students. As of this writing, this book can also be found on-line book as free PDF downloads. Especially check out chapters 9, 10, 12, 13, and 14. This is a very clearly written book that emphasizes conceptual understanding and presents many of the most important equations.

- *Interpreting Astronomical Spectra*, by D. Emerson. This is probably one of the best books for explaining how to analyze and interpret spectra from any and all astronomical sources. I recommend this book above all as a general source– it is long on explanation and all the relevant equations are presented for a wide range of physical conditions (including much emphasis on stellar). However, the treatment can be patchy such that some topics might require reading from other resources.

- *The Solar Atmosphere*, by H. Zirin. This is an older book, but the treatment of the stellar atmosphere is amongst the clearest I have seen. The most relevant chapters are 4, 5, and 10.

- *Foundations of Radiation Hydrodynamics*, by D. Mihalas and B. Weibel-Mihalas. This is book is amazing. It is targetted at the advanced graduate student, and then only for those who endeavor to model gas physics for a profession.

Chapter 2

Introduction to Spectral Analysis

Spectroscopic data provide the quantity I_λ, the observed counts as a function of wavelength. It is usually not difficult to obtain a reasonably accurate measurement of the continuum counts, I^0_λ, so that the ratio I_λ/I^0_λ is known.

A common goal of analyzing spectroscopic data is to extract as much information as possible about the physical conditions in the gas, i.e., to study the atomic matter using the observed[1] radiation. The tool for interpreting spectra is the transfer equation, which is a macroscopic relationship couched in generalized terms of the extinction (absorption and scattering) and emission coefficients, $\chi_\lambda(\mathbf{x})$ and $\eta_\lambda(\mathbf{x})$, respectively. If all the physical states of all absorbers are known, then the extinction and emission coefficients can be calculated and the observed spectrum fully predicted. Successfully predicting the observed spectra from the physical state of the gas is the goal of spectral analysis. In practice, however, the observed spectra are used to constrain the gaseous physical conditions.

The difficulty of this task is that the formalism of radiative transfer is based upon the total optical depth, τ_λ (Eq. 3.34), which is an integrated quantity in which the cloud geometry and the complex physical state of the gas are converted into a single number at each wavelength λ.

In the case of pure absorption (no source function), the spectra provide the ratio $I_\lambda/I^0_\lambda = \exp\{-\tau_\lambda\}$ from which the total optical depth, τ_λ, is measured as a function of wavelength. The optical depth, being the integral of $\chi_\lambda(\mathbf{x})$ over the total path length observed through the absorbing cloud (Eq. 3.34), contains the

[1] For quasar absorption line studies, we make the distinction between the observed radiation and the local radiation field. While the radiation from the source, i.e., distant background quasar, interacts with and is absorbed by the atoms in the gas, it is *not* coupled to the gas equilibrium conditions; it simply probes them. It is the local radiation field that governs the physical conditions of the gas. If the quasar is local to the probed gas, then such a distinction is blurred as the quasar radiation can then be a non–negligible fraction of the local radiation field.

information of *all* the desired physical conditions. This is because the extinction coefficient,[2] as written in Eq. 3.32, is the sum of the number densities of all atomic absorbers in states that interact with photons at wavelength λ weighted by their cross sections at λ. Thus, the number density of each *individual* absorber (which as we will see in Chapter **??**, each is a function of the kinematics, chemical and ionization conditions, temperature, and local radiation field) is lost in the weighted summation over all states to obtain $\chi_\lambda(\mathbf{x})$. Additionally, spatial information is lost in the integration of $\chi_\lambda(\mathbf{x})$ along the total (unknown) path length to obtain τ_λ.

2.1 Column Density

For a given absorbing gas cloud, spectral absorption features can arise from a plethora of different absorbers, and these absorbers can be atoms in a wide range of physical states (excitation levels, ionization stages, etc.). However, in a finite spectral wavelength over which any individual absorption feature is measured, it is almost always the case that the feature arises from a single absorber type. In such cases, one of the fundamental quantities that *can* be extracted directly from a spectrum is the column density, N, of the absorber (say, neutral hydrogen in the ground state). The column density is the number density of absorbers integrated along the path length of the observed light beam. The units are [atoms cm^{-2}].

As illustrated in Figure 2.1, consider a cloud of gas with a number density of a specific type of absorbing atoms, $n(\mathbf{x})$, which may vary significantly with location in the cloud. If a beam of radiation covers a total path length of L through the cloud in the $\hat{\mathbf{s}}$ direction, then the beam will intercept a column density of

$$N = \int_{\mathbf{x}_1}^{\mathbf{x}_2} n(\mathbf{x})\, ds = \int_0^L n(s)\, ds, \tag{2.1}$$

where $s = 0$ at location $\mathbf{x}_1$, the path length is $L\,\hat{\mathbf{s}} = \mathbf{x}_2 - \mathbf{x}_1$ and $n(s)$ is the number density as a function of the line of sight position through the cloud.

In the practice of quasar absorption line observations, one has no knowledge of $n(\mathbf{x})$, the path length through the cloud, L, nor any idea of how to formulate a geometry of the gaseous structure. Thus, it is virtually impossible to obtain the column density from physical principles alone; it must be deduced from the observed spectrum.

If I_λ/I_λ^0 is measured, then, assuming no emission within the cloud, the total optical depth at each wavelength can be obtained by inverting Eq. 3.56,

$$\tau_\lambda = \ln\left[\frac{I_\lambda^0}{I_\lambda}\right]. \tag{2.2}$$

An example of the application of this equation is illustrated in Figure 2.2. This measured value of the optical depth at each wavelength can then be compared

[2]For this discussion we assume scattering is negligible.

Figure 2.1: A schematic of the geometry of the line of sight intersection of an absorbing cloud. The beam passes through the cloud with density distribution $n(\mathbf{x})$ in the $\hat{\mathbf{s}}$ direction within some arbitrary coordinate system, which if known, could be used to obtain the path length through the cloud, L, and the density profile of the cloud of the line of sight, $n(s)$. In practice, no information is available and only the integral, Eq. 2.1, giving the column density, N, can be measured from the data (see text).

to the definition of optical depth (Eq. 3.34)

$$\tau_\lambda = \int_{\mathbf{x}_1}^{\mathbf{x}_2} \kappa_\lambda(\mathbf{x})\, ds, \tag{2.3}$$

which relates the spectroscopic data to the extinction coefficient $\kappa_\lambda(\mathbf{x})$, given by Eq. 3.32. Provided the extinction is due to a single type of absorber only, and not a combination of absorbers, then Eq. 3.32 simplifies to

$$\kappa_\lambda(\mathbf{x}) = n(\mathbf{x})\alpha(\lambda), \tag{2.4}$$

where $\alpha(\lambda)$ is the absorption cross section per absorber. Substituting $\kappa_\lambda(\mathbf{x}) = n(\mathbf{x})\alpha(\lambda)$ into the integral for τ_λ and invoking Eq. 2.1 , we have

$$\tau_\lambda = \int_{\mathbf{x}_1}^{\mathbf{x}_2} n(\mathbf{x})\alpha(\lambda)\, ds = \alpha(\lambda) \int_{\mathbf{x}_1}^{\mathbf{x}_2} n(\mathbf{x})\, ds = \alpha(\lambda)\, N. \tag{2.5}$$

Thus, for an individual absorption feature arising from a single absorber type, we can write Eq. 3.56 as a function of wavelength in terms of the column density and absorption cross section per absorber,

$$I_\lambda = I_\lambda^0 \exp\left\{-N\alpha(\lambda)\right\}. \tag{2.6}$$

This equation is the most commonly applied form of the transfer equation under the conditions of a background emitting source observed through an absorbing cloud (no internal emission and unity covering fraction).

2.2 Absorber Cross Sections: Additional Physics

From Eq. 2.6, it is clear that the cross section per absorber, $\alpha(\lambda)$, must be known in order to deduce N from τ_λ. Computing the value of $\alpha(\lambda)$ is generally straight forward and depends only upon the intrinsic, or atomic, properties of the absorbers. This is a desirable trait, rendering $\alpha(\lambda)$ independent of the physical properties of the gas (the computation of $\alpha(\lambda)$ for various absorption processes will be discussed in Chapter **??**). However, the wavelength functional form of τ_λ is also influenced by the physical properties of the gas. In certain conditions, this can be because the atomic absorption properties actually are modified by the gas properties (pressure broadening, etc). However, over a wide range of gas conditions, the atomic absorption properties are not detectably modified by the gas properties; it is the probability of which wavelengths will be absorbed by the atoms that is modified. For example, one of the most influential properties is the temperature T. The thermal motions of the atoms modify the wavelength dependence of the absorption cross section. Though this renders analysis more involved and challenging, it is also a desirable attribute because it means that certain physical properties of the gas can also be constrained from the spectroscopic data.

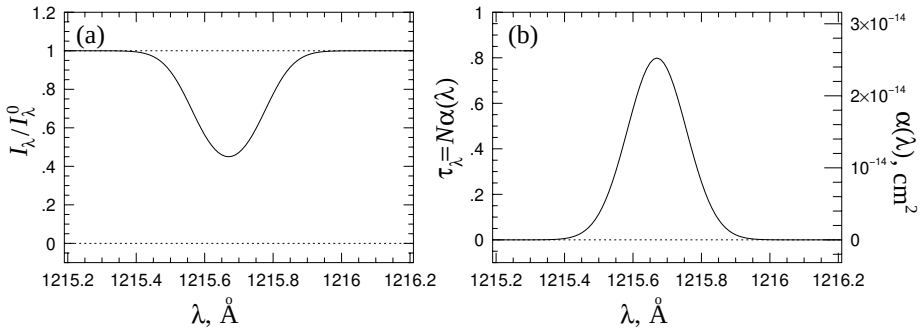

Figure 2.2: (*a*) An absorption feature from neutral the hydrogen Lyα bound–bound transition centered on 1215.67 [Å]. The plotted spectrum is I_λ/I_λ^0 versus wavelength λ. The absorption line corresponds to a column density $N = 3.16 \times 10^{13}$ [atoms cm^{-2}] and a gas temperature of $T = 55,000$ [K]. (*b*) The optical depth, τ_λ, for the the hydrogen absorption feature obtained directly from Eq. 2.2. Since $\tau_\lambda = N\alpha(\lambda)$, the shape of the absorption line directly reflects the wavelength dependence of the cross section for the Lyα transition, the value of which is given on the right hand axis. If the cross section were from the atomic properties of hydrogen only, the FWHM of $\alpha(\lambda)$ would be $\Delta\lambda \sim 10^{-3}$ [Å]. However, the FWHM of the above profile is $\Delta\lambda \sim 0.12$ [Å]. Clearly, additional physics is influencing the absorption line shape; in this case, it is the Doppler broadening due to thermal motions of the absorbers (see text).

Additional physics is incorporated into τ_λ by convolving the atomic cross section with a wavelength dependent redistribution function that depends upon the gas properties. For example, the thermal motions of atoms in the gas will Doppler shift the wavelength dependence of the atomic cross section,

$$\alpha(\lambda) = \alpha_{ijk}(\lambda) \otimes f_T(\lambda' - \lambda), \tag{2.7}$$

where $\alpha_{ijk}(\lambda)$ is the atomic absorption cross section for an absorbing atom designated ijk, and $f_T(\lambda' - \lambda)$ is a wavelength redistribution function of gas temperature that obeys $\int_{-\infty}^{\infty} f_T(\lambda' - \lambda)\, d\lambda' = 1$ for all λ.

To illustrate the above point, a small region of a spectrum, I_λ / I_λ^0, is schematically shown in Figure 2.2*a* for the absorption profile due to the Lyα transition of neutral hydrogen for which $\alpha_{\mathrm{Ly}\,\alpha}(\lambda)$ peaks at 1215.67 [Å]. The column density is $N = 3.16 \times 10^{13}$ [atoms cm^{-1}]. From the atomic properties of hydrogen, the FWHM width of $\alpha_{\mathrm{Ly}\,\alpha}(\lambda)$ is $\Delta\lambda \sim 10^{-3}$ [Å]. However, the FWHM width of the absorption feature is 0.12 [Å], a value more typically observed. In Figure 2.2*b*, τ_λ is plotted by directly inverting the absorption profile in Figure 2.2*a*. Since, $\tau_\lambda = N\alpha(\lambda)$, the value of $\alpha(\lambda)$ is also given on the right hand vertical axis.

Assuming a Gaussian distribution for $f_T(\lambda' - \lambda)$ with wavelength, and correcting for the convolution with $\alpha_{\mathrm{Ly}\,\alpha}(\lambda)$, the absorption profile width of 0.12 [Å], corresponds to a temperature of $T = 55,000$ [K].

2.3 Putting It All Together

The example of the previous subsection illustrates that spectral features record both the microscopic atomic properties of the chemical elements in the gas and the macroscopic physical state of the gas; as such, high quality spectra hold great potential for revealing the chemical, ionization, structural, kinematic, and thermal conditions of the absorbing gas. The process of determining the properties involves correctly formulating τ_λ as a function of both the atomic absorber and gas properties and then constraining the gas properties accurately as possible from the observed measured wavelength functionality of τ_λ.

The key to interpreting τ_λ is embedded in the solution of the transfer equation in the form of the extinction coefficient (and if there is emission, in the emission coefficient and source function). The extinction coefficient is a single number at each wavelength interval, $\lambda \rightarrow \lambda + d\lambda$ that is potentially the sum of countless microscopic atomic states that are in balance with the overall radiation field in the cloud. However, in practice, as described above, for most isolated spectral features, the absorption coefficient is based upon a single atomic state. For example, for the Lyα transition, the single atomic state being probed is neutral hydrogen with its electron in the ground state. As such, the column density deduced from the absorption line is the column density of ground state neutral hydrogen only.

Below is a brief summary of key concepts incorporated in the analysis of astronomical spectra. In the remaining chapters of this book, we will introduce the physical principles and develop the formalism for carrying out such analysis.

- The number density of the absorbers and the path length through the absorbing cloud are coupled together as the column density, N. The column density is a multiplicative factor for the optical depth, and thus primarily governs the magnitude of τ_λ and therefore the strength of the observed absorption feature.

- The wavelength dependence of the absorption cross section dominates the profile shape of the absorption feature. Absorption features rarely have the profile shapes of the atomic cross section, which depends only upon the atomic properties of the absorber. Thus, additional gas physics properties that influence and perhaps dominate the profile shape are parameterized in a "total" absorption cross section.

- This total absorption cross section is obtained via the convolution of the atomic cross section with a normalized wavelength redistribution function. Multiple redistribution functions can be convolved together to formulate a "total" absorption cross section that is a function of multiple gas properties. A most influential gas property that is parameterized in the total absorption cross section is the gas temperature.

- In addition to the the profile shape being governed by the column density and the atomic and gas properties, the spectrograph itself introduces a "blurring" of the incoming light distribution (this has not been discussed up to this point). In other words, an additional wavelength redistribution function must be incorporated to fully model an observed absorption profile! This redistribution function is called the instrumental spread function. The instrumental spread function is *not* convolved with the absorption coefficient; it is not part of the radiative transfer. See § **??** for further details.

If the spectroscopic data are populated by absorption features from many species of absorbing atoms over a wide range of ionization and excitation conditions, then the column densities of various chemical elements in various ionization stages can be measured. In addition, the gas properties can be determined with added robustness (though the properties may systematically change with ionization stage of a given species). Altogether, such data can then be used to constrain *models* of the gas, including the kinematics, average density, metallicity and chemical abundances, and ionization conditions. The density and ionization conditions are useful for constraining the mean intensity and spectral energy distribution of the local radiation field. Once such information is deduced, then the astrophysical context of the gas cloud can be examined and incorporated into solving the science issues.

Bibliography

Gray, D. F. 1992, *The Observational and Analysis of Stellar Photospheres*, Cambridge University Press

Mihalas, D. 1978, *Stellar Atmospheres*, W. H. Freeman & Company

Novotny, E. 1973, *Introduction to Stellar Atmospheres and Interiors*, W. H. Freeman & Company

Peraiah, A. 2002, *An Introduction to Radiative Transfer: Methods and Applications in Astrophysics*, Cambridge University Press

Rybicki, G. B, & Lightman, A. P. 2004, *Radiative Processes in Astrophysics*, Wiley–VCH Verlag GmbH & Company

Shu, F. H. 1991, *The Physics of Astrophysics I.: Radiation*, University Science Books

Chapter 3

Radiative transfer

Astronomers are handicapped physicists. It is as if they have no sense of sound, smell, taste, nor touch— only sight; and they have both hands tied behind their backs. Perhaps this is why experimental astronomers are known as "observers". Astronomers essentially have no control over the astrophysical laboratories they study, i.e., no methods of manipulating the physical conditions of astronomical objects. Furthermore, virtually all astronomical data are in reality nothing more than a trickle of photons that are painstakingly collected, focused, and then... counted.

Fundamentally, a spectrum is nothing more than a record of the number of photons counted in wavelength bins. At face value, it would then seem that spectra do not contain an overwhelming amount of information! But an astronomical spectrum is not taken at face value; it is a richly coded message that only needs to be interpreted in order to uncover countless physical details— details locked in a beam of light when the universe was a small fraction of its present age as it penetrates across billions of light years.

Microscopic quantum physics governs the interactions between light and matter, and serves as the tool for deducing the physical conditions giving rise to observed spectral features. Because the physics is so detailed and because there are degeneracies between various physical processes and the resulting observed spectral features, not all the physical properties and conditions can be deduced. These difficulties are usually mitigated by simplifying the geometry of the interaction, by utilizing macroscopic and integrated quantities, and by parameterizing multiple physical details with a single coefficient or variable. Such is the art of so–called radiative transfer, the powerful formalism by which simple number counts of photons are "inverted" to obtain the dynamical, chemical, thermal, environmental, and ionization conditions of the matter.

In this chapter we introduce the quantitative formalism of the radiation field, including higher moments such as the mean intensity and the flux. The intuitive

generalized concept of a beam is presented as well as the idealized plane wave beam. Modification of the radiation field is the result of interaction with matter and is dependent upon the detailed microscopic state of the matter, which in turn is a function of the conditions of the radiation field in a non–linear cause and effect loop. Determining the detailed states of the matter is extremely complex and will be the subject of Chapters **??** and **??**. The formalism of radiative transfer as introduced in this chapter employs macroscopic integrated wavelength dependent quantities known as the extinction coefficient, optical depth, emission coefficient, and source function.

Finally, the transfer equation is then derived in terms of the macroscopic quantities. The one–dimensional radiative transfer problem is then solved for plane parallel geometry. In the final section, the concepts introduced in this chapter are combined together to define the so–called column density, and demonstrate the need for convolution of atomic physics and macroscopic gas physics to formulate the absorber cross section. A conceptual application of the transfer equation to astronomical spectra is presented, which serves as a harbinger of the analysis methods detailed later chapters, such as Chapters **??**, **??**, and **??**.

Additional resources that extend beyond the scope of this chapter are numerous, given the general nature of the topic. A highly recommended and most comprehensive treatment of the subject is provided by Peraiah (2002). Also highly recommended resources are books focused on stellar atmospheres by Gray (1992), Mihalas (1978), and especially by Novotny (1973). Other classic resources include Rybicki & Lightman (2004) and Shu (1991).

3.1 Defining the radiation field

A full description of a radiation field requires both the energy (i.e., magnitude) and propagation direction of photons. Thus, the radiation field is a vector field. Let the propagation direction of a "beam" of photons be denoted by the unit vector $\hat{\mathbf{s}}$. In most applications, the $\hat{\mathbf{s}}$ direction of a beam of photons under consideration will be the line of sight to the observer. The propagating photons will pass through some point in position and time, the coordinate of which we will denote with the ordered pair ($\mathbf{x}$;t), where $\mathbf{x}$ represents the three coordinates for the spatial location, i.e., x_1, x_2, and x_3. The two most convenient coordinate systems for describing the radiation field are the Cartesian, $\mathbf{x} = (x, y, z)$, and spherical, $\mathbf{x} = (r, \phi, \theta)$, systems. These two coordinate systems and the relationship between their coordinates are illustrated in Figure 3.1.

The unit vector $\hat{\mathbf{s}}$ is most conveniently written in terms of the orthogonal unit base vectors of the Cartesian coordinate system

$$\hat{\mathbf{s}} = \cos\alpha\,\hat{\mathbf{i}} + \cos\beta\,\hat{\mathbf{j}} + \cos\gamma\,\hat{\mathbf{k}}, \tag{3.1}$$

where $\cos\alpha$, $\cos\beta$, and $\cos\gamma$ are the direction cosines, which obey the relation

$\cos^2\alpha + \cos^2\beta + \cos^2\gamma = 1$. By definition,

$$\begin{aligned} \hat{\mathbf{s}}\cdot\hat{\mathbf{i}} &= \cos\alpha \\ \hat{\mathbf{s}}\cdot\hat{\mathbf{j}} &= \cos\beta \\ \hat{\mathbf{s}}\cdot\hat{\mathbf{k}} &= \cos\gamma. \end{aligned} \tag{3.2}$$

The relationship between Cartesian and spherical coordinates is

$$\begin{aligned} x &= r\sin\theta\cos\phi & r &= (x^2+y^2+z^2)^{1/2} \\ y &= r\sin\theta\sin\phi & \theta &= \cos^{-1}(z/r) \\ z &= r\cos\theta & \phi &= \tan^{-1}(y/x) \end{aligned} \tag{3.3}$$

and the relationship between the unit base vectors between the two coordinate systems is

$$\begin{aligned} \hat{\mathbf{i}} &= \sin\theta\cos\phi\,\hat{\mathbf{r}} + \cos\theta\cos\phi\,\hat{\boldsymbol{\Theta}} - \sin\phi\,\hat{\boldsymbol{\Phi}} \\ \hat{\mathbf{j}} &= \sin\theta\sin\phi\,\hat{\mathbf{r}} + \cos\theta\sin\phi\,\hat{\boldsymbol{\Theta}} + \cos\phi\,\hat{\boldsymbol{\Phi}} \\ \hat{\mathbf{k}} &= \cos\theta\,\hat{\mathbf{r}} - \sin\theta\,\hat{\boldsymbol{\Theta}} \end{aligned} \tag{3.4}$$

$$\begin{aligned} \hat{\mathbf{r}} &= \sin\theta\cos\phi\,\hat{\mathbf{i}} + \sin\theta\sin\phi\,\hat{\mathbf{j}} + \cos\theta\,\hat{\mathbf{k}} \\ \hat{\boldsymbol{\Theta}} &= \cos\theta\cos\phi\,\hat{\mathbf{i}} + \cos\theta\sin\phi\,\hat{\mathbf{j}} - \sin\theta\,\hat{\mathbf{k}} \\ \hat{\boldsymbol{\Phi}} &= -\sin\phi\,\hat{\mathbf{i}} + \cos\phi\,\hat{\mathbf{j}}. \end{aligned}$$

As illustrated in Figure 3.1, the unit base vector directions in the Cartesian system are defined parallel to the principle axes of the system. As such, they are independent of the location $\mathbf{x}$. On the contrary, in the spherical coordinates system the directions of the unit base vectors depend upon the position $\mathbf{x}$ (note the example at $\mathbf{x}$ and the example in the $z = 0$ plane). The (θ, ϕ) dependence of $\hat{\mathbf{r}}$, $\hat{\boldsymbol{\Theta}}$, and $\hat{\boldsymbol{\Phi}}$ are given in Eq. 3.4.

Detailed descriptions of the radiation field incorporate not only the energy and direction, but also angular averages, or moments. These moments relate to how a beam traveling in the $\hat{\mathbf{s}}$ direction propagates into a two–dimensional angular element called the solid angle. The general definition of solid angle, Ω, is the ratio of the physical area through which the beam passes to the distance squared, D^2, from either the source or the observer's location, i.e., $\Omega = A/D^2$, depending upon the application of the analysis. In the spherical coordinate system, the area element on a sphere of radius R is

$$\mathbf{dA} = dA\,\hat{\mathbf{n}} = R^2\sin\theta\,d\theta\,d\phi\,\hat{\mathbf{n}}, \tag{3.5}$$

where $\hat{\mathbf{n}} = \hat{\mathbf{r}}$ is the vector normal to the sphere surface at location R, ϕ, θ. The area element is illustrated in Figure 3.2. Viewed from the center of the sphere, the solid angle subtended by the surface area element is

$$d\Omega = \frac{dA}{R^2} = \sin\theta\,d\theta\,d\phi. \tag{3.6}$$

The same area element, as viewed by an observer located at distance D along a line of sight vector direction $\hat{\mathbf{s}}$ passing through the area element on the sphere,

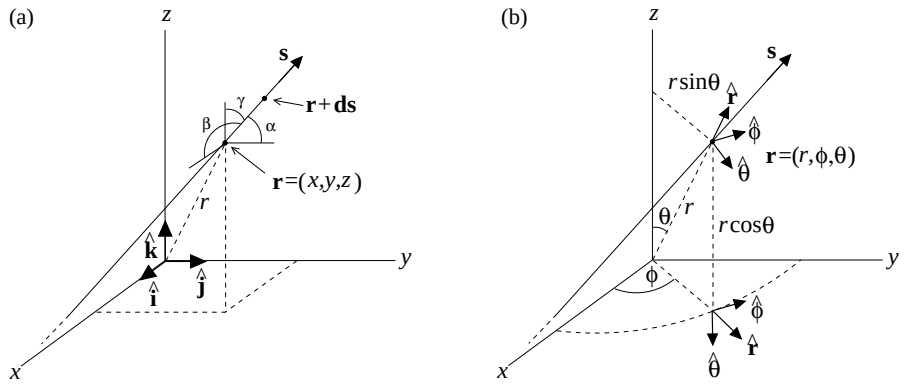

Figure 3.1: The unit vector $\hat{\mathbf{s}}$ represents a propagating "beam" of radiation that passes through point $\mathbf{x}$ in some arbitrary direction. (*a*) In the Cartesian coordinate system the point $\mathbf{x}$ is represented by the ordered pair (x, y, z). Unit vector $\hat{\mathbf{s}}$ is written in terms of the orthogonal unit base vectors $\hat{\mathbf{i}}$, $\hat{\mathbf{j}}$, and $\hat{\mathbf{k}}$. (*b*) In the spherical coordinate system the point $\mathbf{x}$ is represented by the ordered pair (r, ϕ, θ), where r is the radial distance from the origin, ϕ is the azimuthal angle that sweeps counterclockwise from $0 \leq \phi \leq 2\pi$ rotated around the z axis ($\hat{\mathbf{k}}$ vector) with $\phi = 0$ in the $\hat{\mathbf{i}}$ direction, and θ is the polar (or zenith) angle that sweeps from the $\hat{\mathbf{k}}$ direction through the range $0 \leq \theta \leq \pi$ (to the $-\hat{\mathbf{k}}$ direction). The orthogonal unit base vectors are $\hat{\mathbf{r}}$, $\hat{\mathbf{\Phi}}$, and $\hat{\mathbf{\Theta}}$. Note that, unlike the Cartesian base vectors that are independent of $\mathbf{x}$, the direction of the spherical coordinate base vectors depend upon $\mathbf{x}$, as illustrated with the additional point in the $z = 0$ plane.

will subtend solid angle

$$d\Omega = \frac{dA'}{D^2} = \frac{R^2(\hat{\mathbf{s}} \cdot \hat{\mathbf{n}}) \sin\theta \, d\theta \, d\phi}{D^2}, \tag{3.7}$$

where dA' is the projected area from the observer's perspective. If the angle between $\hat{\mathbf{s}}$ and $\hat{\mathbf{n}}$ is ψ, then $\hat{\mathbf{s}} \cdot \hat{\mathbf{n}} = \cos\psi$.

3.1.1 The concept of a beam

In the following discussions, we will consider the propagation of photons through space and time. Within any given volume at any instant, countless photons may be propagating in as many countless directions. The concept of a "beam" is convenient to describe photons having a wide range of wavelengths all traveling in a quasi–parallel direction in a localized spatial location. Since none of the photons travel in exactly parallel directions, a beam is not strictly coherent. Across an infinitesimal cross sectional area centered at location $\mathbf{x}$, photons are "entering" the beam originating from an infinitesimal solid angle while other photons are "exiting" the beam through an infinitesimal solid angle. This process manifests as the illusion of a semi–coherent beam of radiative energy, yet we describe the direction with a simple vector $\hat{\mathbf{s}}$. This concept is useful for describing the interaction of radiation with matter from the point of view of an observer located "downstream" along the $\hat{\mathbf{s}}$ vector.

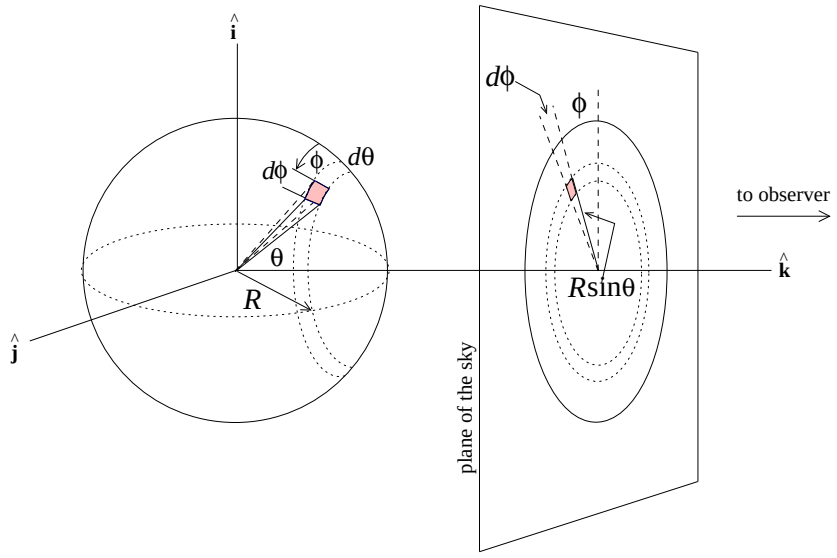

Figure 3.2: A schematic of the area element, dA, on a sphere or radius R. The area element can be placed in the context of an annulus of angular width $d\theta$ about the azimuth angle ϕ (the $\hat{\mathbf{k}}$ vector). The arc length on the sphere over angle $d\theta$ (the zenith angle) is $R\,d\theta$, since the arc lies on a great circle of the sphere. The arc length in the azimuthal direction is $R\sin\theta\,d\phi$. This latter arc length does not lie on a great circle, but on a circle of radius $R\sin\theta$, as illustrated on the two–dimensional collapsed view from the $\hat{\mathbf{k}}$ point of view. The area element is the product of the two arc lengths and has unit vector direction $\hat{\mathbf{n}}$ normal to the surface, i.e., $\hat{\mathbf{r}}$.

If a single source generates photons, and this source *appears* as a point source to the observer, then the description of the propagating photons as a beam is more intuitive. If the distance to the source is much greater than the source size, then photons do not "enter" the beam (as described above) along the line of sight. However, such a beam is still an incoherent bundle of radiative energy. As such, the photons do not travel in strictly parallel paths and some "exit" the beam through an infinitesimal solid angle. The number of photons reaching the observer decreases with distance to the source. Still, the direction of the beam is described by the vector $\hat{\mathbf{s}}$.

Note that any quantitative description of the energy transported via a beam must necessarily incorporate its cross sectional nature and its semi-coherent directionality, the solid angle of the dispersion of photon paths. To account for the dynamic aspect of the radiative energy carried in a beam (the magnitude of the vector), it is convenient to quantify the beam in terms of radiation passing through some infinitesimal cross sectional area, dA, propagating into some infinitesimal solid angle, $d\Omega$.

As defined quantitatively in § 3.1.2, the "magnitude" of any given light beam comprising radiation in the wavelength interval $\lambda \rightarrow \lambda + d\lambda$ and propagating in the $\hat{\mathbf{s}}$ direction at location $\mathbf{x}$ at time t is called the specific intensity, denoted $I_\lambda(\mathbf{x}; t)$. Over a time interval from $t \rightarrow t + dt$, the photons will propagate a distance $\mathbf{ds} = c \cdot dt\,\hat{\mathbf{s}}$ from location $\mathbf{x}$ to $\mathbf{x} + \mathbf{ds}$. Thus, in the absence of any

modification to the beam (in a vacuum), the radiation field obeys

$$I_\lambda(\mathbf{x}+\mathbf{ds};t+dt)\,dA\,d\Omega\,d\lambda\,dt = I_\lambda(\mathbf{x};t)\,dA\,d\Omega\,d\lambda\,dt. \tag{3.8}$$

In the presence of matter, this relationship does not hold due to modifications to the specific intensity of the beam. Describing the *observed* modification to the beam as it propagates in the $\hat{\mathbf{s}}$ direction is the goal of radiative transfer calculations.

3.1.2 Specific intensity

Consider a point in space at $\mathbf{x}$ at time t. Let electromagnetic radiation pass through this point propagating in $\hat{\mathbf{s}}$ direction. The fundamental quantity describing the propagation of this radiation is called the specific intensity, $I_\lambda(\mathbf{x};t)$. The specific intensity is defined as the incremental amount of energy, $d\epsilon_\lambda(\mathbf{x};t)$, transported in direction $\hat{\mathbf{s}}$ by radiation of wavelength range $\lambda \rightarrow \lambda + d\lambda$ passing through an infinitesimal projected area centered on position $\mathbf{x}$ into solid angle $d\Omega$ in time interval dt,

$$d\epsilon_\lambda(\mathbf{x};t) = I_\lambda(\mathbf{x};t)\,(\hat{\mathbf{s}}\cdot dA\hat{\mathbf{n}})\,d\Omega\,d\lambda\,dt, \tag{3.9}$$

where $\hat{\mathbf{n}}$ is the normal direction of the area element, dA. The units of specific intensity are [erg cm^{-2} sec^{-1} rad^{-2} Å^{-1}].

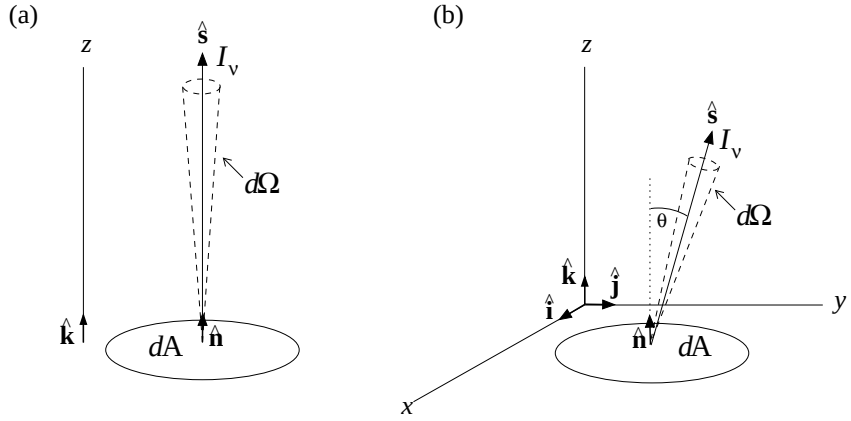

Figure 3.3: (*a*) A schematic of a pencil beam of radiative energy of specific intensity I_λ propagating in the $\hat{\mathbf{s}}$ direction through area element dA into solid angle $d\Omega$. In this example, the propagation is parallel to $\hat{\mathbf{n}}$, the area normal unit vector, and parallel to a (or the) principle axis of the coordinate system (z axis in the $\hat{\mathbf{k}}$ direction). This illustrates the case in which the geometry is defined with respect to the propagation direction. (*b*) In a geometry in which the orientation of the area element is defined, the propagation direction may not be parallel to $\hat{\mathbf{n}}$. In such cases, the radiative energy $d\epsilon_\lambda$ transported by the beam of specific intensity I_λ in the $\hat{\mathbf{s}}$ direction is modulated by the factor $\hat{\mathbf{s}}\cdot\hat{\mathbf{n}} = \cos\theta$, which accounts for the projection of the area element, dA, along the line of sight.

A schematic is presented in Figure 3.3*a* for which $\hat{\mathbf{s}}\cdot dA\hat{\mathbf{n}} = dA$, i.e., $\hat{\mathbf{s}}$ is parallel to $\hat{\mathbf{n}}$ and $\hat{\mathbf{s}}\cdot\hat{\mathbf{n}} = 1$. This scenario provides a one dimensional description

of the phenomena of radiative energy transport in which the viewing angle defines the principal axis of the coordinate system. In three dimensions, the viewing angle may not align with any of the principle axes of the coordinate system, i.e., the direction of propagation under consideration is not parallel to the normal of the area element. Figure 3.3*b* provides a schematic in which the direction of propagation, $\hat{\mathbf{s}}$, subtends and angle θ with the area element normal. In this case $(\hat{\mathbf{s}} \cdot dA\hat{\mathbf{n}}) = dA\cos\theta$.

When discussing the propagation of radiative energy through a medium, i.e., the transfer equation, the extinction and emission are always measured over a path length along a line of sight (the $\hat{\mathbf{s}}$ direction, as defined by the "downstream" location of the observer). Both the vector nature of the radiation field and geometric factors are invoked when the line of sight path length is not parallel to any one of the principal axis of the adopted coordinate system. This point will be made more clear in the subsequent discussion on flux (§ 3.1.4).

3.1.3 Mean intensity

The mean intensity, $J_\lambda(\mathbf{x};t)$, provides the unweighted (zeroth moment) angular average of the specific intensity. Consider a single point, $\mathbf{x}$, at time t. Specific intensity propagating in any direction may pass through (or originate from) this point (actually an area element centered on the point). If we add all solid angle contributions of the specific intensity, $I(\mathbf{x};t)\,d\Omega$, that emanate from the point $\mathbf{x}$ at time t then divide by the sum of all solid angles, we obtain the mean intensity

$$J_\lambda(\mathbf{x};t) = \langle I_\lambda(\mathbf{x};t)\rangle = \frac{\oint I_\lambda(\mathbf{x};t)\,d\Omega}{\oint d\Omega} = \frac{1}{4\pi}\oint I_\lambda(\mathbf{x};t)\,d\Omega, \tag{3.10}$$

where $\oint d\Omega$ indicates closed surface[1] integration over the complete range of polar angle $0 \le \theta \le \pi$ and azimuthal angle $0 \le \phi \le 2\pi$. Substituting is Eq. 3.6 for $d\Omega$, we have

$$\oint d\Omega = \int_0^{2\pi} d\phi \int_0^{\pi} \sin\theta d\theta = 2\pi\,(-\cos\theta)\Big|_0^{\pi} = 4\pi, \tag{3.11}$$

which provides the normalizing factor 4π in Eq. 3.10. The units of mean intensity are [erg cm^{-2} sec^{-1} Å^{-1}]. Since we are summing all the contributions of $I_\lambda(\mathbf{x};t)$ that radially emanate from location $\mathbf{x}$ at time t, we implicitly assume that $\hat{\mathbf{s}} = \hat{\mathbf{r}}$ and $\hat{\mathbf{n}} = \hat{\mathbf{r}}$ giving $\hat{\mathbf{s}} \cdot \hat{\mathbf{n}} = 1$ for all θ and ϕ. This is the meaning of the zeroth moment.

[1] As mentioned in the text, $\oint d\Omega$, indicates closed surface integration over the complete range of the polar and azimuthal angles. In other applications, the integration may be over a limited range of the polar and azimuthal angles, in which case the integral is written $\iint_\Omega d\Omega$, or in the case in which the integration is over the area ($dA = r^2 d\Omega$), the integral is written $\iint_A dA$.

In some astrophysical environments, the specific intensity may have a well defined angular distribution. For example, just beyond the surface layers of a stellar atmosphere, the directions range between perpendicular to radially outward from the stellar center. As distance increases above the stellar surface, the distribution of photon directions become progressively more radial. However, in locations far from luminous sources, such as the intergalactic medium, the radiation field may be essentially isotropic (no angular dependence). In this case, the solid angle contributions of specific intensity are the same for all θ and ϕ, so that Eq. 3.10 evaluates to $J_\lambda(\mathbf{x};t) = I_\lambda(\mathbf{x};t)$. That is, the angular average of the specific intensity emanating isotropically from a point is simply equal to the specific intensity propagating in any single direction.

3.1.4 Flux and power

The flux, $\mathbf{F}_\lambda(\mathbf{x};t)$, is a vector defined such that, $d\mathcal{P}_\lambda(t)$, the *net* rate of the energy carried by radiation across a projected surface area element per unit wavelength per unit time is $\mathbf{F}_\lambda(\mathbf{x};t)\cdot\mathbf{dA}$. $d\mathcal{P}_\lambda(t)$ can be thought of as the monochromatic (in wavelength range $\lambda \rightarrow \lambda + d\lambda$) power element crossing a projected surface area element. From this definition, we have

$$d\mathcal{P}_\lambda(t) = \oint \frac{d\epsilon_\lambda(\mathbf{x};t)}{d\lambda\, dt} = \mathbf{F}_\lambda(\mathbf{x};t)\cdot\mathbf{dA}, \tag{3.12}$$

where $d\epsilon_\lambda(\mathbf{x};t)$ is the incremental amount of energy transported in direction $\hat{\mathbf{s}}$ by radiation of wavelength range $\lambda \rightarrow \lambda + d\lambda$ passing through a projected area element, dA, centered on position $\mathbf{x}$ into solid angle $d\Omega$ in time interval dt (Eq. 3.9),

$$d\epsilon_\lambda(\mathbf{x};t) = I_\lambda(\mathbf{x};t)\,(\hat{\mathbf{s}}\cdot dA\hat{\mathbf{n}})\,d\Omega\,d\lambda\,dt. \tag{3.13}$$

Since the integral in Eq. 3.12 is over a closed surface, the independent variables are spatial. From Eq. 3.13, and invoking $\mathbf{dA} = dA\hat{\mathbf{n}}$, we have

$$\frac{d\epsilon_\lambda(\mathbf{x};t)}{d\lambda\, dt} = I_\lambda(\mathbf{x};t)\,(\hat{\mathbf{s}}\cdot\mathbf{dA})\,d\Omega. \tag{3.14}$$

Substituting into Eq. 3.12 yields

$$\oint I_\lambda(\mathbf{x};t)\,(\hat{\mathbf{s}}\cdot\mathbf{dA})\,d\Omega = \mathbf{F}_\lambda(\mathbf{x};t)\cdot\mathbf{dA}. \tag{3.15}$$

Equating the vectors in Eq. 3.15, we see that the flux vector is

$$\mathbf{F}_\lambda(\mathbf{x};t) = \oint I_\lambda(\mathbf{x};t)\,\hat{\mathbf{s}}\,d\Omega, \tag{3.16}$$

with units [erg cm^{-2} sec^{-1} Å^{-1}]. This flux vector is the first moment of the specific intensity; the integral is over all solid angles but includes only the specific intensity propagating in the $\hat{\mathbf{s}}$ direction.

The power passing through a given area is then

$$\mathcal{P}_\lambda(t) = \iint_A \mathbf{F}_\lambda(\mathbf{x};t)\cdot\mathbf{dA}. \tag{3.17}$$

Since luminosity is a measure of power, Eq. 3.17 can be invoked to compute the luminosity of a source.

In Cartesian coordinates, the flux vector can be written as the vector sum

$$\mathbf{F}_\lambda(\mathbf{x};t) = F^x_\lambda(\mathbf{x};t)\,\hat{\mathbf{i}} + F^y_\lambda(\mathbf{x};t)\,\hat{\mathbf{j}} + F^z_\lambda(\mathbf{x};t)\,\hat{\mathbf{k}}, \tag{3.18}$$

where the orthogonal flux components, $F^x_\lambda(\mathbf{x};t)$, $F^y_\lambda(\mathbf{x};t)$, and $F^z_\lambda(\mathbf{x};t)$ provide the net rate of radiative energy per unit wavelength per unit time crossing a projected unit area for beams propagating in the $\hat{\mathbf{s}}$ equals $\hat{\mathbf{i}}$, $\hat{\mathbf{j}}$, and $\hat{\mathbf{k}}$ directions, respectively. Since the unit area vector is $\hat{\mathbf{n}}$, the components are written

$$\begin{aligned} F^x_\lambda(\mathbf{x};t) &= \oint I_\lambda(\mathbf{x};t)\,(\hat{\mathbf{i}}\cdot\hat{\mathbf{n}})\,d\Omega \\ F^y_\lambda(\mathbf{x};t) &= \oint I_\lambda(\mathbf{x};t)\,(\hat{\mathbf{j}}\cdot\hat{\mathbf{n}})\,d\Omega \\ F^z_\lambda(\mathbf{x};t) &= \oint I_\lambda(\mathbf{x};t)\,(\hat{\mathbf{k}}\cdot\hat{\mathbf{n}})\,d\Omega, \end{aligned} \tag{3.19}$$

where the first unit vector in the dot product is the propagation direction of the beam (the direction of the $\hat{\mathbf{s}}$ vector in Eq. 3.16) and the second, $\hat{\mathbf{n}}$, is the vector direction of the unit area through which the beam passes. If the beam is passing through the surface of a sphere centered at the origin of the coordinate system, then the unit area vector is $\hat{\mathbf{n}} = \hat{\mathbf{r}}$, and from Eq. 3.4 we have

$$\hat{\mathbf{i}}\cdot\hat{\mathbf{n}} = \sin\theta\cos\phi \qquad \hat{\mathbf{j}}\cdot\hat{\mathbf{n}} = \sin\theta\sin\phi \qquad \hat{\mathbf{k}}\cdot\hat{\mathbf{n}} = \cos\theta, \tag{3.20}$$

where $d\Omega = \sin\theta\,d\theta\,d\phi$ (Eq. 3.6).

For example, consider the flux of radiation propagating in the outward radial direction from a central point $\mathbf{x}$ so that $\hat{\mathbf{s}} = \hat{\mathbf{r}}$. The radial component of the flux is then

$$F^r_\lambda(\mathbf{x};t) = \oint I_\lambda(\mathbf{x};t)\,(\hat{\mathbf{r}}\cdot\hat{\mathbf{r}})\,d\Omega. = \oint I_\lambda(\mathbf{x};t)\,d\Omega = 4\pi J_\lambda(\mathbf{x};t). \tag{3.21}$$

Thus, we see that the radial flux normalized by the integral over all solid angle is equivalent to the mean intensity about the central point $\mathbf{x}$.

3.1.4.1 The astrophysical flux

The astrophysical flux, $\mathcal{F}_\lambda$, is the surface flux through one hemisphere of a spherical source of radiation in the wavelength range $\lambda \to \lambda + d\lambda$ heading in a single chosen direction, $\hat{\mathbf{s}}$. The surface flux is defined as the flux passing

through the surface area of an emitting source. Regardless of the radius, R_s, of the source, the the solid angle element subtended by a unit area on the surface is $d\Omega = \sin\theta\, d\theta\, d\phi$, given by Eq. 3.6. The unit vector of the unit area element is $\hat{\mathbf{n}} = \hat{\mathbf{r}}$.

The astrophysical flux quantifies the surface flux from a source intercepted by an observer. A randomly placed observer at some distance from the source will intercept sight lines that originate from only the near–side hemisphere of the source. We aim to compute the surface flux from the source for lines of sight that intercept an observer (who is at some arbitrary distance from the source). For ease of calculation, assume the observer is located along the z axis. Thus, the vector direction of the observed lines of sight, which is the propagation direction of the observed emitted beams, is $\hat{\mathbf{s}} = \hat{\mathbf{k}}$ (we assume all beams reaching the observer are parallel, meaning the observer is at a distance much greater than the radius of the source). The geometry for this scenario is illustrated in Figure 3.2.

To further simplify, assume the specific intensity leaving the surface of the source is isotropic and time independent, so that $I_\lambda(R_s, \phi, \theta, t) = I_\lambda(R_S)$. From Eq. 3.19, the surface flux of the observed hemisphere from the source is equal to the z component of the flux evaluated at $\mathbf{x} = (R_s, \phi, \theta)$; that is $\mathcal{F}_\lambda = F^z_\lambda(R_s)$. We have

$$\mathcal{F}_\lambda = \iint_\Omega I_\lambda(R_s)(\hat{\mathbf{k}} \cdot \hat{\mathbf{r}})\, d\Omega = \int_0^{2\pi}\int_0^{\pi/2} I_\lambda(R_s)\cos\theta\sin\theta\, d\theta\, d\phi, \tag{3.22}$$

where the integration over the polar angle ($0 \leq \theta \leq \pi/2$) includes only the observable hemisphere. Evaluating, we find that the net rate of radiative energy per unit area emerging from the surface of the spherical source in the z direction is

$$\mathcal{F}_\lambda = 2\pi I_\lambda(R_s)\left\{\frac{1}{2}\sin^2\theta\,\Big|_0^{\pi/2}\right\} = \pi I_\lambda(R_s). \tag{3.23}$$

Any point on the surface of the source emits angular specific intensity contributions, $I_\lambda(R_s, \phi, \theta)\,\hat{\mathbf{s}}\, d\Omega$, in *all* directions into all solid angles[2]. If we assume the specific intensity at the surface is isotropic, then we find that the surface flux of parallel beams passing across one hemisphere of a spherical source is equal to the geometric factor π times the specific intensity at the surface.

3.1.4.2 Observed flux: resolved & unresolved source

The observed flux is a measurement of the energy per unit area per unit wavelength per unit time intercepted by a detector. Because flux is the first angular moment of the specific intensity emitted by a source, the observed flux necessarily depends upon the solid angle of the collected beam.

All detectors have a theoretical limiting resolution, a minimum solid angle over which they can collect focused light. In practice, the resolution is limited

[2]Note that this expression is simply the integrand of Eq. 3.16.

by the atmospheric seeing, which has a FWHM angular width on the order of $1''$. Consider an instrument with focal length f that has a limiting FWHM angular resolution that projects to a resolution element area on the detector $A_r = \pi(d_r/2)^2 = \pi r_r^2$, where d_r is the diameter of the resolution element corresponding to the FHWM of the angular resolution, and where r_r is the radius of the resolution element. As such, the minimum solid angle for the collection of light from a distant source is $\Omega_r = A_r/f^2 = \pi r_r^2/f^2$.

Consider a spherical emitting source of radius R_s at a distance D from the focal point of the instrument that subtends a total solid angle several factors greater than Ω_r. This scenario is illustrated in Figure 3.4*a*. The source is said to be resolved. Since each resolution element will image a solid angle Ω_r, the collected light in each resolution element will be emitted from an area on the source, $A_s = \Omega_r D^2$ (the equality presumes $D \gg R_s$).

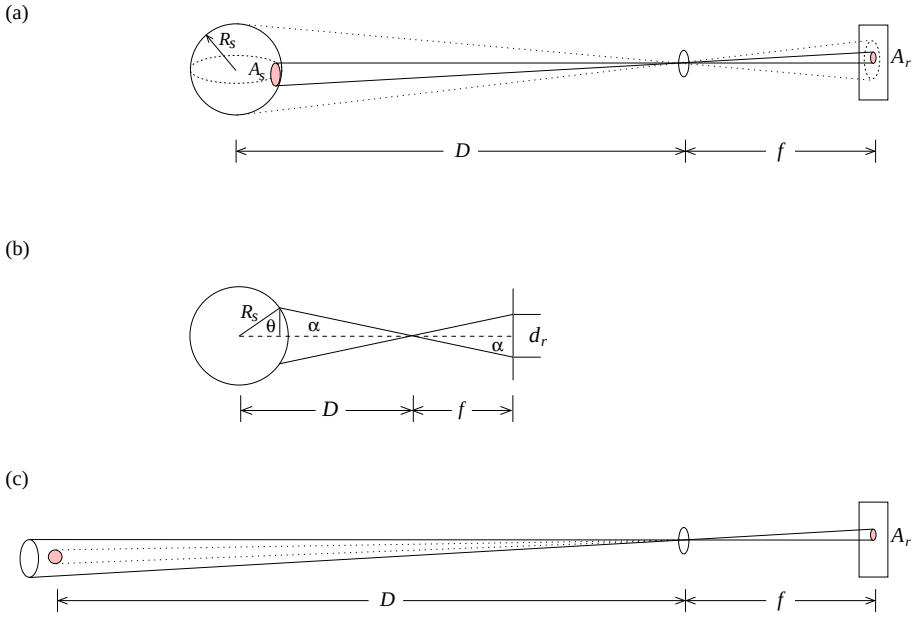

Figure 3.4: (*a*) The relationships between the area of the resolution element, A_r, of an instrument with focal length f and the observed area on the source, A_s, of radius R_s at distance D when the source is resolved. (*b*) An expanded view of the geometry for the resolved source showing the relationship between the angle θ, distance, focal length, source radius, and linear diameter of the instrument resolution element. (*c*) The same as for the schematic in panel (*a*) when the source is unresolved.

In order to compute the observed flux from the resolved source, we invoke principles similar to those applied in § 3.1.4.1. Assume the observer is at the focal point of the instrument at distance D from the source on the z axis. Also assume that the collected light beams are parallel toward the observer and that the surface specific intensity is isotropically emitted from the surface. Thus, we again have $\hat{\mathbf{s}} = \hat{\mathbf{k}}$ and $\hat{\mathbf{n}} = \hat{\mathbf{r}}$, so that $(\hat{\mathbf{s}} \cdot \hat{\mathbf{n}}) = \cos\theta$. Therefore, the computation

of the observed flux is almost identical to Eq. 3.22 for the surface flux except that (1) the observed area element on the source is now from the position of the observer, and (2) the integration over the surface of the source is limited to the area A_s.

As illustrated in Figure 3.2, $dA_s = R_s^2 \sin\theta \, d\theta \, d\phi$ is the area element on the source. From a distance D along the radial vector, the observed solid angle element is

$$d\Omega = \frac{dA_s}{D^2} = \frac{R_S^2}{D^2} \sin\theta \, d\theta \, d\phi. \tag{3.24}$$

The integration limits are determined from the geometric relationships illustrated in Figure 3.4*b*. From similar triangles reflected about the focal point, $\tan\alpha = (r_r/f) = R_s \sin\theta/(D - R_S \cos\theta)$. Provided $D \gg R_s$, we obtain the polar angle limit of integration corresponding to the solid angle of a resolution element,

$$\theta_r = \sin^{-1}\left(\frac{D}{R_s}\tan\alpha\right) = \sin^{-1}\left(\frac{D}{R_s}\frac{r_r}{f}\right). \tag{3.25}$$

The observed flux collected at $z = D$ is then

$$F_\lambda^{obs} = \frac{R_s^2}{D^2}\int_0^{2\pi}\int_0^{\theta_r} I_\lambda(R_s)\cos\theta\sin\theta \, d\theta \, d\phi. \tag{3.26}$$

Carrying out the integration, we obtain

$$\begin{aligned} F_\lambda^{obs} &= \pi I_\lambda(R_s)\frac{R_s^2}{D^2}\sin^2\left\{\sin^{-1}\left(\frac{D}{R_s}\frac{r_r}{f}\right)\right\} \\ &= \frac{r_r^2}{f^2}\pi I_\lambda(R_s) = \frac{A_r}{f^2}I_\lambda(R_s) = \Omega_r I_\lambda(R_s) = \Omega_r\frac{\mathcal{F}_\lambda}{\pi}. \end{aligned} \tag{3.27}$$

Note that the observed flux is simply the solid angle of a resolution element times the specific intensity at the source surface. As such, when an object is resolved, the flux measurement provides a direct determination of the specific intensity. We also see that the astrophysical flux of a resolved source can be measure directly from the observed flux from $\mathcal{F}_\lambda = F_\lambda^{obs}/\tan^2\alpha$. Most importantly, note that the observed flux is independent of both the physical size of the source and the distance to the source. Intuitively, this is due to the constancy of Ω_s, which equals the solid angle of the resolution element, Ω_r. For a given resolved source, as the distance is increased (decreased), the area of the emitting region corresponding to a collecting resolution element increases (decreases) equally.

If the above source is moved to much greater distance, the full disk of the source will eventually subtend a solid angle less than Ω_r. Thus, the emerging intensity from the full hemisphere of the source will be recorded in a single resolution element. This scenario is illustrated in Figure 3.4*c*. Since the full hemisphere is contributing to the observed flux, we replace θ_r with $\pi/2$ for the upper limit of integration in Eq. 3.26. Performing the integration, we obtain

$$F_\lambda^{obs} = \frac{R_s^2}{D^2}\pi I_\lambda(R_s) = \frac{R_s^2}{D^2}\mathcal{F}_\lambda = \Omega_s I_\lambda(R_s) = \Omega_S\frac{\mathcal{F}_\lambda}{\pi}. \tag{3.28}$$

We see that the observed flux of a source is measurable whether it is resolved or unresolved. In both cases, observed flux is proportional to the specific intensity scaled by the solid angle of the collected beam. In the case of a resolved source, the solid angle is the solid angle of the detector resolution element so that the observed flux is independent of both the source size and distance. In the case of an unresolved source, the solid angle is that subtended by the disk of the source. In order to measure either the astrophysical flux or the specific intensity of an unresolved source, one must know both the source size and distance.

3.2 Terms of radiative transfer

3.2.1 The extinction coefficient

When matter (in a gaseous phase) is present in a radiation field, the energy carried in the field will be redistributed via absorption and scattering processes. The absorption and scattering events are probabilistic by nature, and are directionally isotropic in a static medium (but not in a dynamic medium, which we do not address). However, extinction is a directional phenomenon; the infinitesimal quantity of energy removed (or redistributed) from the radiation field must be described relative to two infinitesimally separated points, $\mathbf{x}$ and $\mathbf{x}+\mathbf{ds}$, where $\mathbf{ds} = c \cdot dt\,\hat{\mathbf{s}}$ is the infinitesimal distance and direction between the two points (along the line of sight to an observer).

The extinction coefficient, $\chi_\lambda(\mathbf{x};t)$, also called the opacity or the total absorption coefficient, is a macroscopic quantity describing the mean reduction of energy removed along a direction of propagation. The extinction coefficient is defined such that the incremental amount of energy, $d\epsilon_\lambda(\mathbf{x};t)$ associated with the specific intensity propagating $\mathbf{ds}$ in time interval $t \rightarrow t + dt$ is mitigated according to

$$dE_\lambda = \chi_\lambda(\mathbf{x};t)\, d\epsilon_\lambda(\mathbf{x};t)\, ds \tag{3.29}$$

where $d\epsilon_\lambda(\mathbf{x};t)$ is given by Eq. 3.9. We have

$$dE_\lambda = \chi_\lambda(\mathbf{x};t)\, \{I_\lambda(\mathbf{x};t)\, dA\; d\Omega\, d\lambda\, dt\}\, ds. \tag{3.30}$$

Thus, the extinction coefficient is defined such that an element of material of cross section dA and length ds through which radiation of specific intensity $I_\lambda(\mathbf{x};t)$ is propagating perpendicular to dA (in the $\hat{\mathbf{s}}$ direction) will remove energy dE_λ from the radiation field in the solid angle $d\Omega$ in the wavelength range $\lambda \rightarrow \lambda + d\lambda$ in time interval dt. The units of $\chi_\lambda(\mathbf{x};t)$ are $[\mathrm{cm}^{-1}]$.

In order to make a distinction between absorption and scattering, the extinction coefficient is often written as the sum of an absorption component, $\kappa_\lambda(\mathbf{x};t)$, and a scattering component, $\sigma_\lambda(\mathbf{x};t)$,

$$\chi_\lambda(\mathbf{x};t) = \kappa_\lambda(\mathbf{x};t) + \sigma_\lambda(\mathbf{x};t). \tag{3.31}$$

Consider the absorption component of the extinction coefficient, $\kappa_\lambda(\mathbf{x};t)$. The magnitude of the extinction at any location in a gas depends upon the

number density of absorbers and varies significantly with wavelength. Here, we emphasize that an absorber is an atom of species k that is in one of all possible ionization stages, j, and excitation states, i. The interaction probability of any possible absorber, ijk, at wavelength λ is described by a wavelength dependent absorption cross section $\alpha_{ijk}(\lambda)$, which has units [cm^2 per absorber]. The total extinction coefficient is the sum (over all possible absorbers) of the product of the absorption cross section per absorber and the number density of absorbers [cm^{-3}],

$$\kappa_\lambda(\mathbf{x};t) = \sum_{ijk} n_{ijk}(\mathbf{x};t)\,\alpha_{ijk}(\lambda). \tag{3.32}$$

The calculations of n_{ijk} and $\alpha_{ijk}(\lambda)$ will be addressed in Chapters **??** and **??**. Eq. 3.32 clearly highlights the non–linear balancing act required to determine the extinction coefficient. The complex wavelength dependence of $\chi_\lambda(\mathbf{x};t)$, and therefore the nature and attenuation of the radiation field depends upon the chemical composition and the distribution of occupied atomic ionization stages and excitations states. But, the distribution of atomic states depends upon the detailed balancing of ionizations, recombinations, and scatterings in a gas affected by the intensity and spectral energy distribution of the radiation field (see Chapter **??** for details).

3.2.2 The optical depth

The inverse of the extinction coefficient is the mean free path,

$$\ell(\mathbf{x};t) = \chi_\lambda^{-1}(\mathbf{x};t), \tag{3.33}$$

which is the average distance a photon of wavelength λ propagates before it is absorbed or scattered from the $\hat{\mathbf{s}}$ direction.

We now define the absorptivity along the path length ds as $d\tau_\lambda = \chi_\lambda(\mathbf{x};t)\,ds$. The optical depth is defined as the integrated absorptivity over the path length from location $\mathbf{x}_1$ to location $\mathbf{x}_2$,

$$\tau_\lambda = \int_{\mathbf{x}_1}^{\mathbf{x}_2} \chi_\lambda(\mathbf{x};t)\,ds. \tag{3.34}$$

The integrand of Eq. 3.34 is equivalent to the ratio of the path length element to the mean free path, $ds/\ell(\mathbf{x};t)$. Thus, the optical depth is a statistical quantity that is interpreted as the number of mean free paths photons of wavelength λ travel before being absorber or scattered out of the beam.

3.2.3 The emission coefficient

Energy can be redirected or introduced into a definite direction in a material (gas) by electron scattering, continuum emission processes such as recombination, or line emission processes. The incremental emission of radiative energy dE_λ from an element of material of cross section dA and length ds propagating

perpendicular to dA (in the $\hat{\mathbf{s}}$ direction) into the solid angle $d\Omega$ in the wavelength range $\lambda \rightarrow \lambda + d\lambda$ in time interval dt is parameterized by the emission coefficient, $\eta_\lambda(\mathbf{x}; t)$,

$$dE_\lambda = \eta_\lambda(\mathbf{x}; t)\, dA\, ds\, d\Omega\, d\lambda\, dt, \tag{3.35}$$

where $\eta_\lambda(\mathbf{x}; t)$ has units [erg cm^{-3} rad^{-2} Å^{-1} sec^{-1}].

For absorption and emission processes (i.e., excluding scattering processes), in a steady state thermal equilibrium, in which there is no net energy gain or loss in the material, the time independent versions of Eqs. 3.35 and 3.30 are equal, giving

$$\eta_\lambda(\mathbf{x})\, dA\, ds\, d\Omega\, d\lambda = \kappa_\lambda(\mathbf{x})\, \{I_\lambda(\mathbf{x})\, dA\ d\Omega\, d\lambda\}\, ds, \tag{3.36}$$

or

$$\eta_\lambda(\mathbf{x}) = \kappa_\lambda(\mathbf{x}) I_\lambda(\mathbf{x}). \tag{3.37}$$

This relation states that in thermal equilibrium, and in the absence of an external radiation source, that the ratio of the emission coefficient to the absorption component of the extinction coefficient is the net specific intensity in the material at location $\mathbf{x}$.

3.2.4 The source function

In general, the ratio of the emission coefficient to the extinction coefficient,

$$S_\lambda(\mathbf{x}; t) = \frac{\eta_\lambda(\mathbf{x}; t)}{\chi_\lambda(\mathbf{x}; t)} = \frac{\eta_\lambda(\mathbf{x}; t)}{\kappa_\lambda(\mathbf{x}; t) + \sigma_\lambda(\mathbf{x}; t)}, \tag{3.38}$$

is called the source function, which has the units of specific intensity [erg cm^{-2} rad^{-2} Å^{-1} sec^{-1}]. The source function is a convenient quantity for describing the net specific intensity emitted into the medium at location $\mathbf{x}$ and time t under general thermodynamic conditions.

3.3 The transfer equation

Define $\Delta\epsilon_\lambda$ as the difference between the radiative energy in the wavelength interval $\lambda \rightarrow \lambda + d\lambda$ at position $\mathbf{x}$ and time t and the radiative energy in the wavelength interval $\lambda \rightarrow \lambda + d\lambda$ propagating in direction $\hat{\mathbf{s}}$ that emerges into solid angle $d\Omega$ across area dA at position $\mathbf{x} + \mathbf{ds}$ and time $t + dt$. This difference is equivalent to the amount of radiative energy created by emission processes (Eq. 3.35) less the amount absorbed (Eq. 3.30) in the volume element $dA\, ds$,

$$\Delta\epsilon_\lambda = [\eta_\lambda(\mathbf{x}; t) - \chi_\lambda(\mathbf{x}; t) I_\lambda(\mathbf{x}; t)]\ dA\, d\Omega\, d\lambda\, dt\, ds. \tag{3.39}$$

Invoking the definition of the specific intensity (Eq. 3.9), the quantity $\Delta\epsilon_\lambda$

can be written

$$\begin{aligned}\Delta\epsilon_\lambda &= d\epsilon_\lambda(\mathbf{x}+\mathbf{ds};t+dt) - d\epsilon_\lambda(\mathbf{x};t) \\ &= \left[I_\lambda(\mathbf{x}+\mathbf{ds};t+dt) - I_\lambda(\mathbf{x};t)\right]\, dA\, d\Omega\, d\lambda\, dt \\ &= \left[\frac{1}{c}\frac{\partial I_\lambda(\mathbf{x};t)}{\partial t} + \frac{\partial I_\lambda(\mathbf{x};t)}{\partial s}\right]\, ds\, dA\, d\Omega\, d\lambda\, dt,\end{aligned} \tag{3.40}$$

where the last step follows from finite differencing,

$$\frac{1}{c}\frac{\partial I_\lambda(\mathbf{x};t)}{\partial t} + \frac{\partial I_\lambda(\mathbf{x};t)}{\partial s} = \frac{I_\lambda(\mathbf{x}+\mathbf{ds};t+dt) - I_\lambda(\mathbf{x};t)}{ds}. \tag{3.41}$$

A schematic of the finite difference expressed in Eq. 3.40 is illustrated in Figure 3.5. Note that for purposes of describing the modification of a beam as it propagates in a fixed direction, the volume element of material, $dA\, ds$, is oriented perpendicular to the propagation direction; that is, $\hat{\mathbf{s}} = \hat{\mathbf{n}}$.

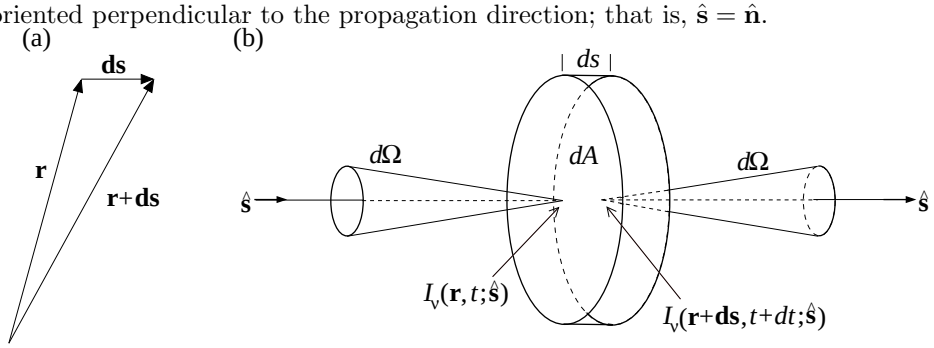

Figure 3.5: A schematic of the absorbing and emitting material and the geometric configuration for the equation of transfer. In a time interval dt, an incident beam of specific intensity $I_\lambda(\mathbf{x};t)$ propagating in the $\hat{\mathbf{s}}$ direction within solid angle $d\Omega$ travels a distance $ds = c \cdot dt$ through a volume element of cross sectional area dA. Following absorption, scattering, and/or emission processes due to interactions with the material, the beam exits at position $\mathbf{x}+\mathbf{ds}$ with modified specific intensity $I_\lambda(\mathbf{x}+\mathbf{ds};t+dt)$ into the same solid angle $d\Omega$.

The general expression for the spatial portion of the partial derivative is

$$\frac{\partial I_\lambda(\mathbf{x};t)}{\partial s} = \hat{\mathbf{s}}\cdot\nabla I_\lambda(\mathbf{x};t). \tag{3.42}$$

Equating Eqs. 3.39 and 3.40, and substituting Eq. 3.42, we have the generalized equation of radiative transfer

$$\frac{1}{c}\frac{\partial I_\lambda(\mathbf{x};t)}{\partial t} + \hat{\mathbf{s}}\cdot\nabla I_\lambda(\mathbf{x};t) = \eta_\lambda(\mathbf{x};t) - \chi_\lambda(\mathbf{x};t) I_\lambda(\mathbf{x};t). \tag{3.43}$$

Dividing by the extinction coefficient (which is the equivalent of multiplying by the mean free path), we obtain

$$\frac{1}{\chi_\lambda(\mathbf{x};t)}\left[\frac{1}{c}\frac{\partial I_\lambda(\mathbf{x};t)}{\partial t} + \hat{\mathbf{s}}\cdot\nabla I_\lambda(\mathbf{x};t)\right] = S_\lambda(\mathbf{x};t) - I_\lambda(\mathbf{x};t), \tag{3.44}$$

where $S_\lambda(\mathbf{x};t)$ is the source function (Eq. 3.38).

In Cartesian coordinates, we have

$$\hat{\mathbf{s}} \cdot \nabla I_\lambda(\mathbf{x};t) = \cos\alpha \frac{\partial I_\lambda(\mathbf{x};t)}{\partial x} + \cos\beta \frac{\partial I_\lambda(\mathbf{x};t)}{\partial y} + \cos\gamma \frac{\partial I_\lambda(\mathbf{x};t)}{\partial z} \tag{3.45}$$

where $\cos\alpha$, $\cos\beta$, and $\cos\gamma$ are the direction cosines (Eq. 3.2) of the propagation direction $\hat{\mathbf{s}}$. In spherical coordinates, we have

$$\hat{\mathbf{s}} \cdot \nabla I_\lambda(\mathbf{x};t) = \frac{\partial I_\lambda(\mathbf{x};t)}{\partial r}(\hat{\mathbf{s}} \cdot \hat{\mathbf{r}}) + \frac{\partial I_\lambda(\mathbf{x};t)}{r\,\partial\theta}(\hat{\mathbf{s}} \cdot \hat{\mathbf{\Theta}}) + \frac{\partial I_\lambda(\mathbf{x};t)}{r\sin\theta\,\partial\phi}(\hat{\mathbf{s}} \cdot \hat{\mathbf{\Phi}}). \tag{3.46}$$

3.3.1 Applying plane parallel geometry

In the scenario of quasar absorption line studies of intervening absorbers, the only known geometric information is the line of sight direction to the quasar. There is no *a priori* knowledge of the geometry of an absorber in the case of an intergalactic or individual galactic halo "cloud". It is common practice to assume a plane parallel geometry.

For purposes of illustration, assume a steady state (equilibrium) condition in a plane parallel one dimensional gas "cloud" of thickness L. Let the depth into the cloud be measured by the coordinate z in the Cartesian system, where $z = 0$ is the cloud "face". Further, assume the photon propagation direction (line of sight being measured) is in the $\hat{\mathbf{s}}$ direction, such that $\hat{\mathbf{s}} \cdot \hat{\mathbf{k}} = \cos\theta$, where θ is the angle between $\hat{\mathbf{s}}$ and the coordinate direction $\hat{\mathbf{k}}$. A schematic of the scenario is illustrated in Figure 3.6. A beam incident on the cloud face has specific intensity $I_\lambda(0)$. In order to obtain a general form of the solution to the transfer equation, we will assume that emission, $S_\lambda(z)$, occurs as a general function of z within the cloud.

The equation of transfer for this scenario is written

$$\frac{1}{\chi_\lambda(z)}\left[(\hat{\mathbf{s}} \cdot \hat{\mathbf{k}})\,\frac{dI_\lambda(z)}{dz}\right] = S_\lambda(z) - I_\lambda(z). \tag{3.47}$$

As written, a simple analytical solution for $I_\lambda(z)$ is impossible because the integrand, $\chi_\lambda(z)[S_\lambda(z) - I_\lambda(z)]\,dz/\cos\theta$, is undetermined. Invoking the definition of the absorptivity and accounting for the propagation direction with respect to the geometric coordinate, we have $d\tau_\lambda = \chi_\lambda(z)\,ds = \chi_\lambda(z)\,dz/\cos\theta$. Thus, as illustrated in Figure 3.49, the optical depth along the photon propagation vector can be written in terms of the physical depth[3]. From Eq. 3.34, we have

$$\tau_\lambda(z) = \frac{1}{\cos\theta}\int_0^z \chi_\lambda(z')\,dz', \tag{3.48}$$

[3] As mentioned above, the distinction of a photon propagation (line of sight) direction different than the coordinate direction is not commonly invoked for intervening quasar absorption line systems, i.e., $\cos\theta = 1$. We introduce the distinction simply for illustrative purpose. Alternative definitions, such as for stellar atmosphere work, do not incorporate the direction cosine into the definition of the optical depth, but leave it as a geometric factor in the transfer equation, i.e., $d\tau_\lambda = \chi_\lambda(z)\,dz$. This definition provides a "projected" optical depth, which is useful where optical depth changes as a function of viewing angle on the stellar disk for a fixed physical depth into the atmosphere.

where we have explicitly included the z dependence of the optical depth.

We thus can rewrite the transfer equation as a function of the optical depth as the independent variable,

$$\frac{dI_\lambda(\tau_\lambda)}{d\tau_\lambda} = S_\lambda(\tau_\lambda) - I_\lambda(\tau_\lambda). \tag{3.49}$$

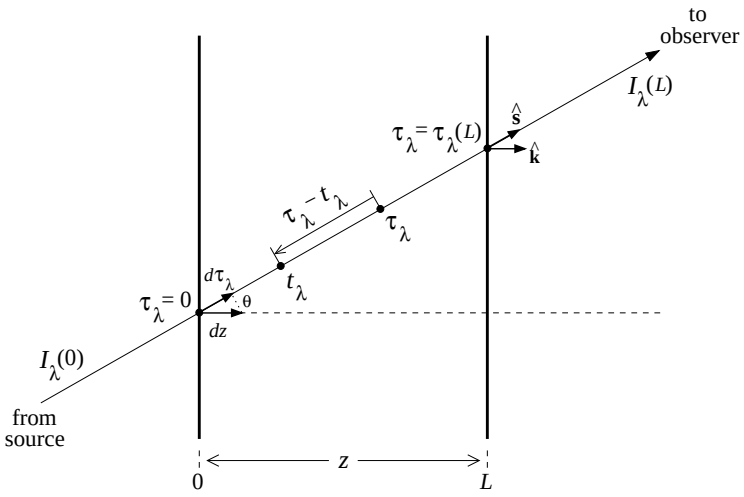

Figure 3.6: Schematic of a one dimensional plane parallel "cloud" of thickness L through which a pencil beam of radiative energy of specific intensity $I_\lambda(z)$ is propagating in the $\hat{\mathbf{s}}$ direction such that $\hat{\mathbf{s}} \cdot \hat{\mathbf{k}} = \cos\theta$, where $\hat{\mathbf{k}}$ is the unit vector along the geometric axis of the cloud. The specific intensity at an optical depth τ_λ measured from the cloud "face" ($\tau_\lambda = 0$) is the sum of the extinction $I_\lambda(0)\exp\{-\tau_\lambda\}$ of the incident specific intensity and the integrated contribution of the extinctions from the emission, $S_\lambda(t_\lambda)$, at each $\tau_\lambda - t_\lambda$, i.e., $\int S_\lambda(t_\lambda)\exp\{-(\tau_\lambda - t_\lambda)\}\,dt_\lambda$.

3.3.2 Solution in one dimension

The form of the transfer equation, written as Eq. 3.49, is now such that we can apply the standard integrating factor technique and assume a solution of the form,

$$I_\lambda(\tau_\lambda) = Q_\lambda(\tau_\lambda) \cdot \exp\{p\tau_\lambda\}\,. \tag{3.50}$$

Differentiating, we have

$$\frac{dI_\lambda(\tau_\lambda)}{d\tau_\lambda} = \frac{dQ_\lambda(\tau_\lambda)}{d\tau_\lambda}\exp\{p\tau_\lambda\} + p\,Q_\lambda(\tau_\lambda) \cdot \exp\{p\tau_\lambda\}\,. \tag{3.51}$$

Equating Eqs. 3.49 and 3.51, we have the relations

$$\begin{aligned} S_\lambda(\tau_\lambda) &= \frac{dQ_\lambda(\tau_\lambda)}{d\tau_\lambda}\exp\{p\tau_\lambda\} \\ -I_\lambda(\tau_\lambda) &= p\,Q_\lambda(\tau_\lambda) \cdot \exp\{p\tau_\lambda\}\,. \end{aligned} \tag{3.52}$$

From Eq. 3.50, the latter relation yields $p = -1$, which after substitution into the former relation for $S_\lambda(\tau_\lambda)$ and solving for $Q_\lambda(\tau_\lambda)$ yields the integral

$$Q(\tau_\lambda) = C + \int_0^{\tau_\lambda} S_\lambda(t_\lambda) \cdot \exp\{t_\lambda\}\, dt_\lambda. \tag{3.53}$$

Substituting Eq. 3.53 into Eq. 3.50 gives

$$I_\lambda(\tau_\lambda) = C \exp\{-\tau_\lambda\} + \exp\{-\tau_\lambda\} \int_0^{\tau_\lambda} S_\lambda(t_\lambda) \exp\{t_\lambda\}\, dt_\lambda. \tag{3.54}$$

Evaluating at the boundary $\tau_\lambda = 0$ where the specific intensity incident upon the cloud face is $I_\lambda(0)$, we have $C = I_\lambda(0)$. Following substitution, and rearranging the second term, the solution to the transfer equation is written

$$I_\lambda(\tau_\lambda) = I_\lambda(0) \exp\{-\tau_\lambda\} + \int_0^{\tau_\lambda} S_\lambda(t_\lambda) \exp\{-(\tau_\lambda - t_\lambda)\}\, dt_\lambda. \tag{3.55}$$

3.3.3 Interpreting the solution: simple cases

Employing the optical depth as the dependent variable in Eq. 3.55 may seem somewhat less intuitive than solving the transfer equation as a function of physical depth. In fact, note that τ_λ is an integral from the cloud face to the corresponding path length (or deprojected physical depth), and requires knowledge of the extinction coefficient as a function of physical depth. However, in practice, the transfer equation is simply a tool applied to observational spectra, which directly provide the optical depth as a function of wavelength, λ. We discuss this further in § **??**

The λ subscripts denote that Eq. 3.55 is written for radiation in the wavelength range $\lambda \to \lambda + d\lambda$. If the extinction coefficient is wavelength dependent, then the physical depth corresponding to a given optical depth will also be wavelength dependent. This means that the average photon observed at given wavelength will originate from a different depth in the cloud than an average photon at a different wavelength.

Interpreting Eq. 3.55, it is clear that two components govern the behavior of the specific intensity as a function of optical depth (or physical depth) along a line of sight. In the case that there is no emission within the cloud, $S_\lambda(\tau_\lambda) = 0$ (an absorbing cloud), then

$$I_\lambda(\tau_\lambda) = I_\lambda(0) \exp\{-\tau_\lambda\}. \tag{3.56}$$

For heuristic illustration, assume the extinction coefficient is a path length averaged value, which we will denote $\bar{\chi}_\lambda$, and is constant throughout the cloud. Then $\tau_\lambda(s) = \bar{\chi}_\lambda\, s$, were $s = z/\cos\theta$ is the coordinate position along the line of sight that the photons have traveled through the cloud medium. For $\bar{\chi}_\lambda$ constant, Eq. 3.56 can be written as a function of the path length s,

$$I_\lambda(s) = I_\lambda(0) \exp\{-\bar{\chi}_\lambda\, s\}. \tag{3.57}$$

When $s = \bar{\chi}_\lambda^{-1}$, the photons have traveled one complete mean free path and the specific intensity has suffered extinction by the factor $e^{-1} = 0.367$. For every multiple additional mean free path the beam travels, the extinction is an additional factor of 0.367. If a beam travels a distance $s = L$ through an absorbing cloud, then the total optical depth of the cloud is $\tau_\lambda = \bar{\chi}_\lambda L$. That is, the total optical depth of a cloud of total path length L is directly proportional to the magnitude of the extinction coefficient.

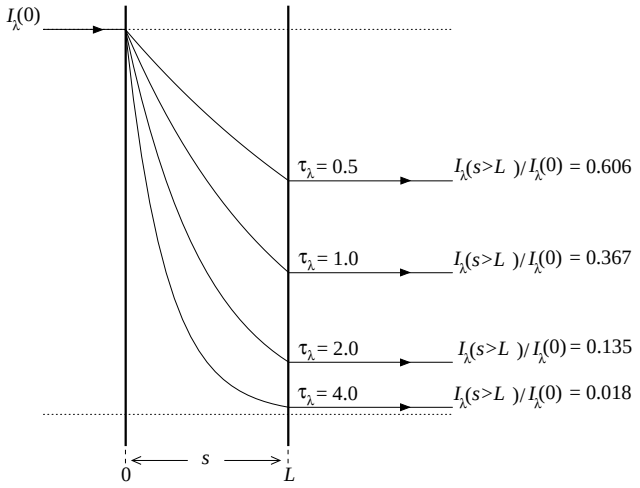

Figure 3.7: A schematic of radiative transfer through an absorbing cloud, i.e., $S_\lambda(\tau_\lambda) = 0$, of total path length L, for which the total optical depth is $\tau_\lambda = 0.5$, 1.0, 2.0, and 4.0. The incoming beam $I_\lambda(0)$ (propagating from left to right) suffers extinction through the cloud according to Eq. 3.57. Since τ_λ is the integral of $\bar{\chi}_\lambda$ over the path length from $0 \leq s \leq L$, the examples are for different opacities (extinction coefficients).

In Figure 3.7, the behavior of Eq. 3.57 is illustrated as a function of path length for four different extinction coefficients in an absorbing cloud through which the total path length is L. The different extinction coefficients result in different extinction rates and therefore in different total optical depths, τ_λ. Four cases are shown, $\tau_\lambda = 0.5$, 1.0, 2.0, and 4.0. The specific intensity of the incident beam is $I_\lambda(0)$. The ratios of the specific intensity of the emerging beam to the incident beam, $I_\lambda(s \geq L)/I_\lambda(0)$, are given for the four total optical depths. Eq. 3.56 is the workhorse expression for analysis of quasar absorption line data. That is, in most all observational situations, emission into the line of sight to the observer is so negligible that the source function can be omitted from the radiative transfer.

In the case where the source function is not negligible, the second term of Eq. 3.55 accounts for specific intensity added to the beam at different locations along the line of sight, s. If the source function is a constant, S_λ, throughout the cloud, then integration of Eq. 3.55 yields

$$I_\lambda(s) = I_\lambda(0) \exp\{-\bar{\chi}_\lambda s\} + S_\lambda \cdot \left[1 - \exp\{-\bar{\chi}_\lambda s\}\right], \tag{3.58}$$

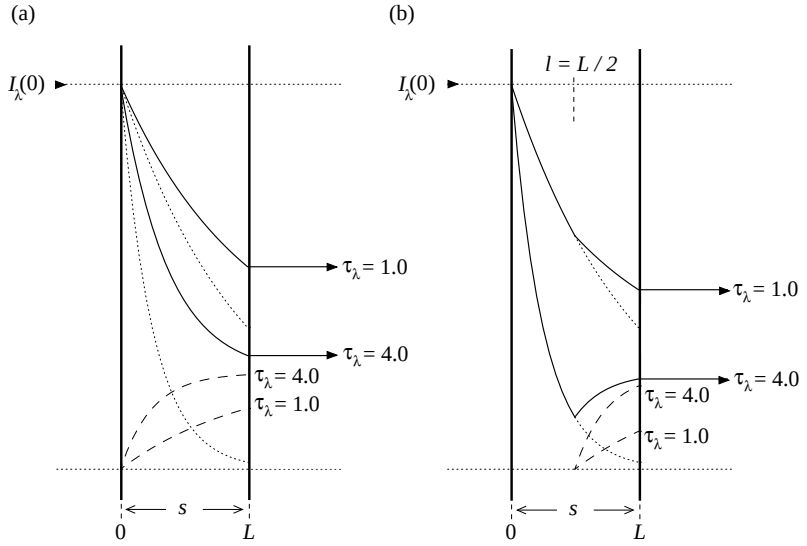

Figure 3.8: Schematics of radiative transfer through a cloud of total path length L with constant source function, $S_\lambda = 0.25 I_\lambda(0)$, where $I_\lambda(0)$ is the specific intensity incident on the cloud face. Examples with total optical depths $\tau_\lambda = 1.0$, and 4.0 are shown. (*a*) The source function is a constant over the full path length $0 \le s \le L$. Solid curves are $I_\lambda(s)$ given by Eq. 3.58, dotted curves are the first term, $I_\lambda(0) \exp\{-\bar{\chi}_\lambda\, s\}$, and dashed curves are the second term $S_\lambda \cdot [1 - \exp\{-\bar{\chi}_\lambda\, s\}]$. (*b*) The source function is $S_\lambda = 0$ for $s < l$ and $S_\lambda = 0.25 I_\lambda(0)$ for $l \le s \le L$, where $l = L/2$ for this example. $I_\lambda(s)$ obeys Eq. 3.57 for $s < l$ and Eq. 3.59 for $l \le s \le L$. The curves represent the same terms as in panel *a*.

where, following the integration, we again assumed $\tau_\lambda = \bar{\chi}_\lambda\, s$. Eq. 3.58 is illustrated in Figure 3.8*a* with $S_\lambda = 0.25 I_\lambda(0)$ for total optical depths $\tau_\lambda = 1.0$ and 4.0.

The most general case is that the source function is a smooth function of physical depth. In the case of a strong discontinuity in the source function at some location in the cloud, the behavior of $I_\lambda(s)$ can be approximated by treating the cloud as two adjoining media. For example, consider a scenario in which $S_\lambda = 0$ for $0 \le s < l$ and $S_\lambda =$ constant for $l \le s \le L$, where $0 \le l \le L$. We will assume $\bar{\chi}_\lambda$ is the same in both "media", but this assumption is not required. The specific intensity will suffer extinction according to Eq. 3.57 until $s = l$, at which point $I_\lambda(l) = I_\lambda(0) \exp\{-\bar{\chi}_\lambda\, l\}$. For the remaining path length $l \le s \le L$, the specific intensity will be

$$\begin{aligned} I_\lambda(s) &= I_\lambda(l) \exp\{-\bar{\chi}_\lambda\,(s-l)\} + S_\lambda \cdot \Big[1 - \exp\{-\bar{\chi}_\lambda (s-l)\}\Big] \\ &= I_\lambda(0) \exp\{-\bar{\chi}_\lambda\, s\} + S_\lambda \cdot \Big[1 - \exp\{-\bar{\chi}_\lambda (s-l)\}\Big], \end{aligned} \tag{3.59}$$

where the second form is obtained following substitution of $I_\lambda(l)$. Eq. 3.59 is illustrated in Figure 3.8*b* for $l = L/2$ and $S_\lambda = 0.25 I_\lambda(0)$ for total optical depths

$\tau_\lambda = 1.0$ and 4.0. Note that in the case of $\tau_\lambda = 4.0$, the specific intensity quickly converges to the value of the source function.

It is the general behavior that when $S_\lambda \neq 0$, $I_\lambda(s)$ converges toward the value S_λ with increasing path length, s, through the cloud. The convergence (or path length required for convergence) depends upon both the magnitude of the absorption coefficient and the ratio $I_\lambda(s)/S_\lambda$ at the boundary layer where $S_\lambda \neq 0$. For larger $\bar{\chi}_\lambda$, the *rate* of convergence is more rapid. The further the ratio $I_\lambda(s)/S_\lambda$ is from unity at the boundary, the more path length that is required to converge for a given $\bar{\chi}_\lambda$.

The convergence of S_λ to $I_\lambda(s)$ is directly described by Eq. 3.58. The term $I_\lambda(0)\exp\{-\bar{\chi}_\lambda\, s\}$ ranges from $I_\lambda(0) \rightarrow 0$ and the rate at which it vanishes with increasing path length is more rapid for larger $\bar{\chi}_\lambda$. The term $S_\lambda \cdot [1 - \exp\{-\bar{\chi}_\lambda\, s\}]$ ranges from $0 \rightarrow S_\lambda$ at a rate parallel with the vanishing of the first term. As such, for internally emitting optically thick clouds, which is to say for clouds with a mean ratio $\bar{\chi}_\lambda / L \gg 1$, the incident specific intensity is quickly attenuated, the specific intensity quickly equals the source function throughout the cloud, and the emerging specific intensity from the cloud face will be the mean value of the source function.

3.4 What astronomical spectra record

An astronomical spectrum is a recording of the flux of the source. The observed flux from an unocculted, unresolved spherical source of radius R_s at a distance D from the observer was derived in § 3.1.4.2. For a non–isotropic specific intensity distribution, the observed flux for beams emitted from ϕ, θ locations on the surface of the source *that intercept the observer* is

$$F_\lambda^{obs} = \frac{R_s^2}{D^2} \int_0^{2\pi} \int_0^{\pi/2} I_\lambda(R_s, \phi, \theta) \cos\theta \sin\theta \, d\theta \, d\phi. \tag{3.60}$$

It is assumed that the geometric relationship between source and observer is that the observer is located a distance D from the source on the z axis, i.e., in the direction $\theta = 0$ (see Figure 3.2). Recall that the polar angle ranges from $0 \leq \theta \leq \pi/2$ for integration over the "near–side" hemisphere of the source.

If an intervening absorption cloud resides between source and observer, we simply incorporate the solution of the transfer equation for pure absorption, given by Eq. 3.56, into Eq. 3.60. We have

$$F_\lambda^{obs} = \frac{R_s^2}{D^2} \int_0^{2\pi} \int_0^{\pi/2} I_\lambda(R_s, \phi, \theta) \exp\{-\tau_\lambda(\phi, \theta)\} \cos\theta \sin\theta \, d\theta \, d\phi. \tag{3.61}$$

The quantity F_λ^{obs} is the source flux incident upon the upper atmosphere of Earth (it is almost what is recorded in an astronomical spectrum). To the extent that Eq. 3.61 is fully solvable, we see that the observed flux in each wavelength interval, $\lambda \rightarrow \lambda + d\lambda$, is an integral over the surface of the source for which the optical depth through the intervening cloud for each beam must be

mapped back the beam ϕ, θ point of origin on the source surface. In practice, the mapping is an intractable problem.

As such, the common practice is to assume the source is radiating isotropically, so that $I_\lambda(R_s, \phi, \theta) = I_\lambda(R_s)$. It is also common practice to assume the optical depth through the intervening cloud is independent of the the beam ϕ, θ point of origin on the surface of the source. This is tantamount to assuming a uniform, or an averaged, absorbing cloud over the source cross section, or $\bar{\tau}_\lambda = \langle \chi L \rangle$, where χ is the extinction coefficient L is the total path length through the cloud. This may seem to be an obvious set of assumptions, but it is worth explicitely clarifying that virtually all published extragalactic work utilizing unresolved sources rests upon them.

Applying the above assumptions and evaluating Eq. 3.61, the observed flux incident on the upper atmosphere is

$$F_\lambda^{obs} = \pi \frac{R_s^2}{D^2} I_\lambda(R_s) \exp\left\{-\bar{\tau}_\lambda\right\} = \frac{\sigma_s}{D^2} I_\lambda(R_s) \exp\left\{-\bar{\tau}_\lambda\right\}, \tag{3.62}$$

where σ_s is the integrated cross section of the source, or the beam cross section ($\Omega_s = \pi R_s^2/D^2 = \sigma_s/D^2$ is the solid angle subtended by the source). Before this flux is recorded for subsequent analysis, the beam suffers wavelength dependent attenuated transmission through the atmosphere, followed by wavelength dependent reflection, transmission, and finally detection through various optical and electronic elements of the telescope faclility. The spectrum, then, is a modified observed flux, I_λ, which we call the "observed counts",

$$I_\lambda = \epsilon(\lambda) F_\lambda^{obs} = \epsilon(\lambda) \frac{\sigma_s}{D^2} I_\lambda(R_s) \exp\left\{-\bar{\tau}_\lambda\right\} = I_\lambda^0 \exp\left\{-\bar{\tau}_\lambda\right\}, \tag{3.63}$$

where the efficiency function $\epsilon(\lambda)$ accounts for flux loss due to atmospheric extinction and telescope throughput, and where I_λ^0 is the counts in the absence of an intervening cloud, $\tau_\lambda = 0$,

$$I_\lambda^0 = \epsilon(\lambda) \frac{\sigma_s}{D^2} I_\lambda(R_s), \tag{3.64}$$

which we will call the "continuum counts".

Bibliography

Gray, D. F. 1992, *The Observational and Analysis of Stellar Photospheres*, Cambridge University Press

Mihalas, D. 1978, *Stellar Atmospheres*, W. H. Freeman & Company

Novotny, E. 1973, *Introduction to Stellar Atmospheres and Interiors*, W. H. Freeman & Company

Peraiah, A. 2002, *An Introduction to Radiative Transfer: Methods and Applications in Astrophysics*, Cambridge University Press

Rybicki, G. B, & Lightman, A. P. 2004, *Radiative Processes in Astrophysics*, Wiley–VCH Verlag GmbH & Company

Shu, F. H. 1991, *The Physics of Astrophysics I.: Radiation*, University Science Books

Chapter 4

Atomic Absorption Lines

Line opacities are first and formost dependent upon the rates of the transistions. These rates, either absorption or emission, can be decribed using several formalisms, but perhaps the most intuitive and well known formalism is the Einstein coefficients. From these coefficients (describing microphysics of atomic transitions) the macroscopic rates at which energy is absorbed from or emitted into the observer's line of sight can be expressed in terms of the emission coefficient, η_ν, and the absorption coefficient, κ_ν, from which the radiative transfer equation can be solved.

In practice, the optical depth across an absorption line is described by the frequency-depdendent absorption cross section, $\sigma(\nu)$ [cm^2], which describes the fractional power removed from the line of sight specific intensity per absorbing atom/ion. There are three atomic constants employed to compute the cross section, the damping constant, Γ [s^{-1}], the oscillator strength, f [unitless], and the transition frequency ν [Hz] or wavelenth, λ [Å]. As we will show in this chapter, the natural atomic cross section for absorption has the identical functional form as that of the classical oscillator (derived in Appendix 13), namely a Lorentzian distribution as a function of frequency.

For a multi-electron atom (as well as hydrogenic atoms), a transition is represented by the notation

$$^{2S+1}\mathrm{L}_J \; -^{2S'+1}\mathrm{L}'_{J'} \, . \tag{4.1}$$

We will employ the simplified notation for an atomic state such that n denotes the lower state (excited or ground) for quantum state $nLJS$ and n' denotes an upper excited state corresponding to the atomic state $n'L'J'S'$. Recall that for allowed transitions (those subject to the dipole slection rules), we have $\Delta L = \pm 1$, $\Delta J = 0, \pm 1$, $\Delta S = 0$. There is no constraint on Δn.

For a given transition, consider for example, a rate R. We adopt the notation $R_n^{n'} \equiv R_n^{n'}(\uparrow)$ to denote an upward transition from n to n'. For downward transitions, $R_n^{n'} \equiv R_n^{n'}(\downarrow)$, we instead adopt $R_{n'}^{n} \equiv R_{n'}^{n}(\uparrow)$ to denote a transition from upper state n' to lower state n. Thus, the transitions proceed from subscript to superscript. However, we will not generally employ the $(\uparrow)$ notation.

For our discussion, we will treat absorption and emission processes only and assume no line or continuum scattering. Thus, the total opacity χ_ν is given by κ_ν, the absorption opacity only.

4.1 Line Coefficients

Accounting for line emission and continuum emission, we define the total emission coefficient as

$$\eta_\nu = \eta^n_{n'}(\nu) + \eta^c_\nu \,, \tag{4.2}$$

where $\eta^n_{n'}(\nu)$ is the line emission coefficient and η^c_ν is the continuum emission coefficient. We interpret η_ν [erg cm^{-3} s^{-1} Hz^{-1} str^{-1}] as the monochromatic energy density emitted into the line of sight per unit time ($t \to t + dt$) per unit frequency ($\nu \to \nu + d\nu$) per unit solid angle ($\Omega \to \Omega + d\Omega$).

Accounting for line absorption and continuum absorption, we define the total absorption coefficient, or opacity, as

$$\kappa_\nu = \kappa^{n'}_n(\nu) + \kappa^c_\nu \,, \tag{4.3}$$

where $\kappa^{n'}_n(\nu)$ is the line absorption coefficient and κ^c_ν is the continuum absorption coefficient. We interpret κ_ν [cm^{-1}] as the inverse of the free mean path of photons between absorption events, $\ell_\nu = \kappa_\nu^{-1}$.

In terms of the above notation, the transfer equation is written

$$\frac{1}{w}\frac{dI_\nu}{dz} = \left[\eta^n_{n'}(\nu) + \eta^c_\nu\right] - \left[\kappa^{n'}_n(\nu) + \kappa^c_\nu\right] I_\nu \,, \tag{4.4}$$

which describes the gradient of the monochromatic specific intensity along the observer's line of sight per unit time per unit frequency per unit solid angle. The quantity $\kappa^{n'}_n(\nu) I_\nu$, having units [erg cm^{-3} s^{-1} Hz^{-1} str^{-1}], is the monochromatic energy density absorbed from the line of sight per unit time per unit frequency per unit solid angle.

In spectral regions corresponding to line absorption or emission, the source function, $S_\nu = \eta_\nu / \kappa_\nu$ is

$$S_\nu = \frac{\eta^n_{n'}(\nu) + \eta^c_\nu}{\kappa^{n'}_n(\nu) + \kappa^c_\nu} \,. \tag{4.5}$$

The source function includes both the continuum emission and absorption across the line profile as well as the line emission and/or absorption. We will treat the continuum in § **??**.

Condsider the line emission coefficient, $\eta^n_{n'}(\nu)$. Let $A^n_{n'}$ [s^{-1}] be the rate of spontaneous downward transitions from upper state n' to lower state n for an atom/ion in state n'. Due to the probabilistic nature of the atom, the frequency of the emitted photon may not be precisely $\nu^n_{n'} = E^n_{n'}/h = (E_{n'} - E_n)/h$. As we will show in § 4.2, the probability distribution of the emitted frequency can be described by a "natural line broadening" function, $\phi^n_{n'}(\nu)$ [Hz^{-1}], which is

the relative number of photons in the line per unit frequency with peak at $\nu^n_{n'}$, where

$$\int_0^\infty \phi^n_{n'}(\nu)\, d\nu = 1\,. \tag{4.6}$$

The rate at which a photon will be emitted with frequency $\nu \rightarrow \nu + d\nu$ is $A^n_{n'}\phi^n_{n'}(\nu)$ [s^{-1} Hz^{-1}]. If the number density of atoms/ions in state n' is $n_{n'}$, then the rate per unit volume is $n_{n'}A^n_{n'}\phi^n_{n'}(\nu)$ [cm^{-3} s^{-1} Hz^{-1}]. To obtain the rate at which the monochromatic energy density per unit solid angle is emitted, i.e., $\eta^n_{n'}(\nu)$, the rate per unit volume is multiplied by the energy $h\nu$ and divided by the integral overall solid angle, $\oint d\Omega = 4\pi$, yielding

$$\boxed{\eta^n_{n'}(\nu) = \left(\frac{h\nu}{4\pi}\right) n_{n'} A^n_{n'} \phi^n_{n'}(\nu) \qquad \text{(spontaneous emission)}\,.} \tag{4.7}$$

Stimulated emission can also occur, in which a photon with frequency $\simeq \nu^n_{n'}$ at or near the peak of $\phi^n_{n'}(\nu)$ induces a downward transition ($n' \rightarrow n$), resulting in the emission of a photon with frequency $\simeq \nu^n_{n'}$ also at or near the peak of $\phi^n_{n'}(\nu)$. Being proportional to the rate of incident photons, the rate of stimulated transitions for an atom/ion in state n' is $4\pi B^n_{n'} I_\nu$ [s^{-1}]. Note that, since $4\pi I_\nu$ has units [erg cm^{-2} s^{-1} Hz^{-1}], this definition requires $B^n_{n'}$ to have units [cm^2 erg^{-1} s^{-1}], which we interpret as a cross section per unit energy per unit time. Following the reasoning used to obtain the spontaneous emission coefficient, we multiply by $h\nu/4\pi$ and obtain the monochromatic energy density emitted into the line of sight per unit time per unit frequency per unit solid angle for stimulated emission is

$$\boxed{\eta^n_{n'}(\nu) = h\nu\, n_{n'} B^n_{n'} I_\nu \phi^n_{n'}(\nu) \qquad \text{(stimulated emission)}\,.} \tag{4.8}$$

The rate of absorption for ion/atom in lower state n is also proportional to the rate of incident photons, yielding $4\pi B^{n'}_n I_\nu$ [s^{-1}]. As with spontaneous and stimulated emission, due to the probabilistic nature of the atom, the frequency of the absorbed photon may not be precisely $\nu^{n'}_n = E^{n'}_n/h = (E_n - E_{n'})/h$. We require a "natural line broadening" function, $\phi^{n'}_n(\nu)$ [Hz^{-1}]. Though it is not obvious *a priori* that $\phi^{n'}_n(\nu)$ is identical to $\phi^n_{n'}(\nu)$, we show in § 4.2 that $\phi^{n'}_n(\nu) = \phi^n_{n'}(\nu)$ for natural broadening. Following the above steps, we obtain the monochromatic energy density absorbed along the line of sight per unit time per unit frequency per unit solid angle,

$$\kappa^{n'}_n(\nu) I_\nu = h\nu\, n_n B^{n'}_n I_\nu \phi^{n'}_n(\nu)\,, \tag{4.9}$$

which yields

$$\boxed{\kappa^{n'}_n(\nu) = h\nu\, n_n B^{n'}_n \phi^{n'}_n(\nu) \qquad \text{(absorption)}\,.} \tag{4.10}$$

Since both stimulated emission and absorption are proportional to the specific intensity in the line-of-sight direction, whereas spontaneous emission is isotropic, in certain applications we treat stimulated emission as the reverse

process of absorption, giving $\kappa_n^{n'}(\nu) = h\nu[n_n B_n^{n'} \phi_n^{n'}(\nu) - n_{n'} B_{n'}^n I_\nu \phi_{n'}^n(\nu)]$. That is, stimulated emission can be treated as *reducing* the absorption by adding photons into the line of sight.

4.1.1 Einstein Coefficients

Einstein formulated the above definitions of transition rates [s^{-1}] in terms of the quantities $A_{n'}^n$, $B_{n'}^n$, and $B_n^{n'}$, which are known as the Einstein coefficients for spontaneous emission, stimulated emission, and absorption, respectively. Expressed in terms of these coefficients, the transitions rates [s^{-1}] are

$$\begin{aligned} A_{n'}^n &= \text{spontaneous emission rate} && A_{n'}^n, [\text{s}^{-1}] \\ 4\pi B_{n'}^n I_\nu &= \text{stimulated emission rate} && B_{n'}^n, [\text{cm}^2\ \text{erg}^{-1}\ \text{s}^{-1}] \\ 4\pi B_n^{n'} I_\nu &= \text{absorption rate} && B_n^{n'}, [\text{cm}^2\ \text{erg}^{-1}\ \text{s}^{-1}]\,. \end{aligned} \tag{4.11}$$

Each individual transition of a given atom/ion is decribed by a unique Einstein coefficient. The Einstein coefficient $A_{n'}^n$ provides the rate per unit time at which spontaneous emission occurs. The Einstein coefficients $B_{n'}^n$ and $B_n^{n'}$ provide a cross-sectional description per unit energy per unit time for stimulated emission and absorption, respectfully.

Consider spontaneous emission. Weak electromagnetic perturbations naturally occur within atoms/ions, and, when an electron is in an excited state, these can lead to spontaneous downward transitions. From the dipole approximation and perturbation theory in the weak limit, the isotropic spontaneous emission rate is computed from the overlap integral of the wave functions (Bethe & Salpeter 1957),

$$\begin{aligned} A_{n'}^n &= \frac{64}{3}\frac{\pi^4 e^2}{hc^3}\,(\nu_{n'}^n)^3 \int_0^\infty \psi_{n'}^* |r| \psi_n\, r^2 dr \\ &= \frac{64}{3}\frac{\pi^4 e^2}{hc^3}\,(\nu_{n'}^n)^3 \int_0^\infty \psi_{n'}^* \psi_n\, r^3 dr\,, \end{aligned} \tag{4.12}$$

where $\psi_{n'} = \psi_{n'}(\mathbf{r}) = \psi_{n'}(r, \phi, \theta)$, is the spatial (time-independent) wave function for upper state n', and ψ_n is that of lower state n. For the dipole approximation, $A_{n'}^n \neq 0$ only when $J = J'$ or $J' \pm 1$, and $L = L' \pm 1$; all other values vanish; these are the so-called dipole selection rules. For virtually all astronomically studied transitions, the $A_{n'}^n$ are tabulated. An excellent resource is the Atomic Spectra Database (ADS) provided by the National Institute of Standards and Technology (NIST)[1]. Typical values of $A_{n'}^n$ are $\simeq 10^8$ s^{-1}.

Given the $A_{n'}^n$, both $B_{n'}^n$ and $B_n^{n'}$ can be determined using the Einstein

[1] NIST/ASD: *http://physics.nist.gov/PhysRefData/ASD/lines_form.html* .

relations[2]

$$\boxed{\begin{aligned} B^n_{n'} &= \frac{c^2}{8\pi h\nu^3} A^n_{n'} \quad \text{stimulated} \leftrightarrow \text{spontaneous emission} \\ B^{n'}_n &= \frac{g_{n'}}{g_n} B^n_{n'} \qquad \text{absorption} \leftrightarrow \text{stimulated emission}\,, \end{aligned}} \tag{4.13}$$

where $g_n = 2J + 1$ and $g_{n'} = 2J' + 1$ are the multiplicities for states n and n', respectively. The Einstein relations are derived from atomic physics, and are therefore valid regardless of the local state variables of the gas, the nature of the radiation field, or whether the atom/ions are in equilibrium with the radiation field.

4.2 The Line Broadening Function

To determine the functional form of $\phi^n_{n'}(\nu)$, we must consider the time-dependent probability of an atom/ion in upper state n' that spontaneously decays to lower state n. Recall that the probability of finding an electron in quantum state n' is

$$P_{n'}\, dr = \psi^*_{n'} \psi_{n'}\, r^2 dr\,. \tag{4.14}$$

Consider the transition due to spontaneous decay from state n' to n, where both n' and n are excited states (that is, state n' can spontaneously decay to any allowed state $m < n'$ and state n could spontaneously decay to any allowed state $m < n$). Analgous to Eq. 4.14, the time-dependent joint probability for a transition due to spontaneous decay from state n' to n is

$$P^n_{n'}(t)\, dr = \Psi^*_n(\mathbf{r}, t) \Psi_{n'}(\mathbf{r}, t)\, r^2 dr\,, \tag{4.15}$$

where the time-dependent wave functions of state n' and n are

$$\begin{aligned} \Psi_{n'}(\mathbf{r}, t) &= \psi_{n'}(\mathbf{r}) \exp\{-(i/\hbar)\, E_{n'} t\} \exp\{-(\Gamma_{n'}/2)t\} \\ \Psi_n(\mathbf{r}, t) &= \psi_n(\mathbf{r}) \exp\{-(i/\hbar)\, E_n t\} \exp\{-(\Gamma_n/2)t\}\ , \end{aligned} \tag{4.16}$$

where $2/\Gamma_{n'}$ is the e-folding time for state n' to spontaneously decay and $2/\Gamma_n$ is the e-folding time for state n to spontaneously decay.

Lower state n is one of many possible states to which upper state n' can decay, for which the time-dependent probability is proportional to $\exp\{-(A^n_{n'}/2)t\}$. Since state n' can decay to any allowed lower state $m < n'$, we must account for the joint probability of all decay channels to obtain the actual e-folding time at which state n' will spontanesously decay. Thus,

$$\Psi_{n'}(\mathbf{r}, t) \propto \prod_{m=1}^{n'-1} \exp\{-(A^m_{n'}/2)t\}\,, \tag{4.17}$$

[2]The quantity $8\pi h\nu^3/c^2$ has units [erg cm^{-2}].

where the product is taken over all states $m < n'$ and we adopt the convention that $m = 1$ is the ground state. This is equivalent to summing the rates over all states $m < n'$, from which we obtain the total spontaneous decay rate for upper state n',

$$\boxed{\Gamma_{n'} = \sum_{m=1}^{n'-1} A^m_{n'}\,,} \tag{4.18}$$

which yields $\Psi_{n'}(\mathbf{r},t) \propto \exp\{-(\Gamma_{n'}/2)t\}$. Similar arguments apply for spontaneous decay of lower state n to states $m < n$,

$$\boxed{\Gamma_{n} = \sum_{m=1}^{n-1} A^m_{n}\,,} \tag{4.19}$$

yielding $\Psi_n(\mathbf{r},t) \propto \exp\{-(\Gamma_n/2)t\}$. Since typical values of $A^n_{n'}$ are $\simeq 10^8$ s^{-1}, the typical values of Γ are $\simeq 10^8$ s^{-1}, yielding e-folding times of $\simeq 10^{-8}$ s.

Substituting Eq. 4.16 into Eq. 4.15, and invoking $E^n_{n'} = E_{n'} - E_n$, we have

$$P^n_{n'}(t)\,dr = \psi^*_n\psi_{n'} \exp\left\{-\left(i/\hbar\right) E^n_{n'}t\right\} \exp\left\{-(\Gamma^n_{n'}/2)t\right\}\, r^2 dr\,, \tag{4.20}$$

where

$$\Gamma^n_{n'} = \Gamma_{n'} + \Gamma_n\,. \tag{4.21}$$

We can separate Eq. 4.20 into a spatial part and a time-dependent part, where the time-dependent part is

$$f(t) = \exp\left\{-\left(i/\hbar\right) E^n_{n'}t\right\} \exp\left\{-(\Gamma^n_{n'}/2)t\right\}\,. \tag{4.22}$$

The inverse Fourier transform of $f(t)$ is a complex function, $F(\nu)$, that is the frequency power spectrum of $f(t)$. The natural line broadening function is the amplitude of the frequency power spectrum, i.e., $\phi^n_{n'}(\nu) = F^*(\nu)F(\nu)$. Taking the transform,

$$F(\nu) = \frac{1}{2\pi}\int_0^\infty f(t) \exp\{2\pi i\nu t\}\,dt\,, \tag{4.23}$$

invoking $E^n_{n'}/h = \nu^n_{n'}$, and substituting $f(t)$, we obtain

$$F(\nu) = C\int_0^\infty \exp\left\{-2\pi i\left(\nu^n_{n'} - \nu\right)t\right\} \exp\left\{-(\Gamma^n_{n'}/2)t\right\}\, dt\,, \tag{4.24}$$

which yields

$$F(\nu) = \frac{C}{2\pi i\left(\nu^n_{n'} - \nu\right) + \left(\Gamma^n_{n'}/2\right)}\,. \tag{4.25}$$

where we have introduced the constant C so that we can inforce the normalization condition given by Eq. 4.6. Applying $\phi^n_{n'}(\nu) = F^*(\nu)F(\nu)$, we have

$$\begin{aligned}\phi^n_{n'}(\nu) &= \frac{C^2}{4\pi^2\left(\nu - \nu^n_{n'}\right)^2 + \left(\Gamma^n_{n'}/2\right)^2} \\ &= \frac{1}{\pi}\frac{C^2/4\pi}{\left(\nu - \nu^n_{n'}\right)^2 + \left(\Gamma^n_{n'}/4\pi\right)^2}\,.\end{aligned} \tag{4.26}$$

Eq. 4.26 has the functional form of the well known Lorentzian

$$\mathcal{L}(x) = \frac{1}{\pi}\frac{y}{(x-x_0)^2+y^2}\,, \qquad \int_0^\infty \mathcal{L}(x)\,dx = 1\,, \tag{4.27}$$

where x_0 is known as the location parameter yielding the maximum $\mathcal{L}(x_0) = 1/\pi y$, and where y is the half width at half maximum (HWHM). Normalizing Eq. 4.26 according to Eq. 4.27, we find $C^2 = \Gamma^n_{n'}$, yielding

$$\boxed{\phi^n_{n'}(\nu) = \frac{1}{\pi}\frac{(\Gamma^n_{n'}/4\pi)}{(\nu-\nu^n_{n'})^2 + (\Gamma^n_{n'}/4\pi)^2}\,.} \tag{4.28}$$

Note that $\Gamma^n_{n'}/2\pi$ is the full width at half maximum (FWHM) of the line broadening function. The quantity $\Gamma^n_{n'}$ is known as the damping constant. Given the Einstein A coefficients, which are obtainable in tables, the damping constant can be computed from Eq. 4.21. However, often the damping constant itself is directly tabulated (again, a good source is NIST/ASD).

The above derivation of the natural broadening function for emission accounted for the e-folding lifetimes, $2/\Gamma_{n'}$ and $2/\Gamma_n$, for a states n' and n only in terms of spontaneous decay. In an intense radiation field, the e-folding time can be shortened due to stimulated emission and due to absorption,

$$\begin{aligned}
\Gamma_{n'} &= \sum_{m=1}^{n'-1} A^m_{n'} + 4\pi \sum_{m=1}^{n'-1} B^m_{n'} I_\nu + 4\pi \sum_{m=n'+1}^{\infty} B^{n'}_m I_\nu \\
\Gamma_{n} &= \sum_{m=1}^{n-1} A^m_{n} + 4\pi \sum_{m=1}^{n-1} B^m_{n} I_\nu + 4\pi \sum_{m=n+1}^{\infty} B^{n}_m I_\nu\,,
\end{aligned} \tag{4.29}$$

both of which can potentially induce and electron to change states before spontaneous decay would naturally occur. However, in stellar atmospheres of most all stars, the stimulated emission and absorption rates are on the order of 1–0.1% of the spontaneous decay rates. In an A star ($T = 10,000$ K), where the Planck curve peaks at $\simeq 10^{15}$ Hz ($\simeq$ 3000 Å) with $I_\nu \simeq 10^{-4}$ erg s^{-1} cm^{-2} Hz^{-1} str^{-1}, the Einstein relations (Eq. 4.13) give $B^{n'}_n \simeq B^n_n \simeq 6A^n_{n'}$, so that $4\pi B^{n'}_n I_\nu \simeq 4\pi B^n_{n'} I_\nu \simeq 7\times 10^{-3} A^n_{n'}$. Note however, that most optical transitions do not reside at the peak of the Planck curve. In an O star, the stimulated emission and absorption rates can be has high as 10% of the spontaneous emission rates. Thus, the expression given by Eqs. 4.18 and 4.19 suffice for computing $\Gamma^n_{n'}$ and $\Gamma^{n'}_n$ for most all applications (and this is especially true for the conditions in the interstellar medium and intergalactive medium). Note that these are the values tabulated by NIST/ASD.

Note that according to Eq. 4.21, the damping constants for both the emission and absorption transitions are symmetric, i.e., $\Gamma^n_{n'} = \Gamma^{n'}_n$. And since, the emission and absorption frequencies are identical ($\nu^n_{n'} = \nu^{n'}_n$), we see that the natural absorption line function is identical to the natural emission line function,

$$\boxed{\phi^{n'}_n(\nu) = \phi^n_{n'}(\nu)\,.} \tag{4.30}$$

4.3 Absorption Cross Section

Consider an atom/ion in lower state n with number density n_n [cm^{-3}]. For an absorption transition from lower state n to upper state n', the transfer equation yields

$$I_\nu = I_\nu^0 \exp\{-\tau_\nu\}\,, \tag{4.31}$$

where τ_ν is the frequency-dependent optical depth across the line profile and I_ν^0 is the continuum specific intensity at the location of the line formation. The optical depth is the integral of the absorption opacity over the infinitessimal line-of-sight path lengths ds across the unknown line-of-sight thickness L, of the absorbing region,

$$\tau_\nu = \int_0^L \kappa_n^{n'}(\nu)\, ds\,, \tag{4.32}$$

where $\kappa_n^{n'}(\nu)$ [cm^{-1}] is the line absorption coefficient for the transition. Note that the number density of the absorbing atom/ion may vary with location in the absorbing region.

Interpreting $\kappa_n^{n'}(\nu)$ as the inverse of the mean free path $\ell_n^{n'}(\nu)$ of a photon with frequency ν in the line, the relation $\kappa_n^{n'}(\nu) = n_n \sigma_n^{n'}(\nu)$ follows from the well-known relation $\ell = 1/n\sigma$. The frequency dependence of $\kappa_n^{n'}(\nu)$ and $\sigma_n^{n'}(\nu)$ will govern the width and shape of the absorption profile. As we will discuss below, the total absorption cross section may depend upon location in the absorbing region (due to thermal, turbulent, pressure, and/or rotational line broadening). However, in what follows, we will focus on "natural" line broadening due only to atomic physics. Thus, for natural broadening, $\sigma_n^{n'}(\nu)$ is decoupled from the location in the absorbing region and we have

$$\tau_\nu = \int_0^L n_n(s)\sigma_n^{n'}(\nu)\, ds = \sigma_n^{n'}(\nu) \int_0^L n_n(s)\, ds = N_n \sigma_n^{n'}(\nu)\,, \tag{4.33}$$

which defines the column density N_n [cm^{-2}] of the absorbing atom/ion.

Thus, the naturally broadened absorption line can be modeled as the product of the column density of the absorbing atom/ion and the atomic absorption cross section. From Eq. 4.10, we have

$$\boxed{\sigma_n^{n'}(\nu) = \frac{\kappa_n^{n'}(\nu)}{n_n} = h\nu\, B_n^{n'} \phi_n^{n'}(\nu)} \tag{4.34}$$

A general derivation and interpretation of the cross section is presented in Appendix 12, where we show that, even though $\sigma(\nu)$ can be interpreted as the interaction "area" per absorbing atom/ion, the actual definition of the cross section is that it measures the power [erg s^{-1}] removed from the line of sight per unit incident flux per absorbing atom/ion.

4.4 Oscillator Strengths

Integrating Eq. 4.34 over all frequencies, we obtain the total cross section,

$$\sigma_n^{n'} = \int_0^\infty h\nu B_n^{n'} \phi_n^{n'}(\nu)\, d\nu = hB_n^{n'} \int_0^\infty \phi_n^{n'}(\nu)\, \nu d\nu\,, \tag{4.35}$$

which provides the rate at which energy is removed from the line-of-sight specific intensity per absorbing atom/ion by an absorption line (i.e., the fractional power removed from the beam). The full width half maximum of the natural broadening profile is typically on the order of $\Delta\lambda \simeq 10^{-4}$ Å, or $\Delta\nu/\nu = \Delta\lambda/\lambda \simeq 10^{-8}$ Hz for optical wavelengths. We thus can approximate the natural broadening profile as a δ function centered on the transition frequency, $\nu_n^{n'}$. Thus, to excellent accuracy, the total cross section is

$$\sigma_n^{n'} = h\nu_n^{n'} B_n^{n'} \int_0^\infty \phi_n^{n'}(\nu)\, d\nu = h\nu_n^{n'} B_n^{n'}\,. \tag{4.36}$$

It is convention to normalize the total cross section in terms of the classical oscillator, $\sigma = \pi e^2/m_e c$ (see Eq. 13.43), which we derived in Appendix 13 assuming a self-damping free electron in an oscillating electric field. However, since the fractional power removed from the beam differs from one transition to another, whereas the classical oscillator formalism makes no allowance for that fact, a constant of proportionality is introduced. This constant or proportionality is called the oscillator strength, $f_n^{n'}$, and it is simply defined through the relation

$$\sigma_n^{n'} = \frac{\pi e^2}{m_e c} f_n^{n'} = h\nu_n^{n'} B_n^{n'}\,, \tag{4.37}$$

which yields the oscillator strength for absorption,

$$f_n^{n'} = \frac{m_e c}{\pi e^2} h\nu_n^{n'} B_n^{n'}\,. \tag{4.38}$$

Similarly, we find that the oscillator strength for emission is

$$f_{n'}^{n} = \frac{m_e c}{\pi e^2} h\nu_{n'}^{n} B_{n'}^{n}\,. \tag{4.39}$$

From the Einstein relations (Eq. 4.13), we have $g_{n'} B_{n'}^n = g_n B_n^{n'}$, yielding the relationship between the oscillator strength for emission and absorption,

$$g_{n'} f_{n'}^n = g_n f_n^{n'}\,. \tag{4.40}$$

In terms of the commonly tabulated Einstein A coefficients,

$$f_n^{n'} = \frac{m_e c^3}{8\pi^2 e^2} \frac{g_{n'}}{g_n} \left(\nu_n^{n'}\right)^{-2} A_{n'}^n\,. \tag{4.41}$$

Typical values of the oscillator strength range from near unity to 10^{-6} in the case of the weakest transitions. Commonly observable transitions have $10^{-2} \leq f_{n'}^n < 1$.

Applying the above normalization, we have $\sigma_n^{n'}(\nu) = (\pi e^2/m_e c) f_n^{n'} \phi_n^{n'}(\nu)$ and obtain the final form of the cross sections for atomic absorption transitions

$$\boxed{\sigma_n^{n'}(\nu) = \frac{e^2}{m_e c} f_n^{n'} \frac{(\Gamma_n^{n'}/4\pi)}{(\nu - \nu_n^{n'})^2 + (\Gamma_n^{n'}/4\pi)^2}} \tag{4.42}$$

Defining $\Delta\nu = \nu - \nu_n^{n'}$, and invoking $\Delta\nu = [c/(\lambda_n^{n'})^2]\Delta\lambda$, where $\Delta\lambda = \lambda - \lambda_n^{n'}$, we obtain the absorption cross section as a function of wavelength,

$$\boxed{\sigma_n^{n'}(\lambda) = \frac{e^2}{m_e c^2} f_n^{n'} (\lambda_n^{n'})^2 \frac{[(\lambda_n^{n'})^2 \Gamma_n^{n'}/4\pi c]}{(\lambda - \lambda_n^{n'})^2 + [(\lambda_n^{n'})^2 \Gamma_n^{n'}/4\pi c]^2}\,,} \tag{4.43}$$

for which

$$\int_0^\infty \sigma_n^{n'}(\lambda)\, d\lambda = \frac{\pi e^2}{m_e c} \frac{(\lambda_n^{n'})^2}{c} f_n^{n'}\,. \tag{4.44}$$

As with the quantities $A_{n'}^n$ and $\Gamma_n^{n'} = \Gamma_{n'}^n$, the oscillator strengths and multiplicities of states, g_n and $g_{n'}$, are tabulated by NIST/ASD.

4.5 Naturally Broadened Lines

From Eqs. 4.31 and 4.33, for natural broadening, an observed absorption line profile will have frequency (or wavelength) dependence

$$I_\nu = I_\nu^0 \exp\left\{-N_n \sigma_n^{n'}(\nu)\right\} \quad \text{or} \quad I_\lambda = I_\lambda^0 \exp\left\{-N_n \sigma_n^{n'}(\lambda)\right\} \tag{4.45}$$

As we show in following chapters, additional broadening mechanisms modify the actual observed profile shape. Here, we characterize the natural broadening.

4.5.1 Column Density for Unity Optical Depth

Comparing Eqs. 4.42 and 4.27, we see that the peak amplitude occurs at $\nu = \nu_n^{n'}$, yielding $\sigma_n^{n'}(\nu_n^{n'}) = (4\pi e^2/m_e c)(f_n^{n'}/\Gamma_n^{n'})$. The identical result is obtained at $\lambda_n^{n'}$ using Eq. 4.43. The optical depth in the line core is therefore

$$\tau_c = \frac{4\pi e^2}{m_e c} \frac{f_n^{n'}}{\Gamma_n^{n'}} N_n\,. \tag{4.46}$$

For unity optical depth in the line core, where the depth at the line center is $I_\nu/I_\nu^c = e^{-1} = 0.368$, the required column density is

$$N_n(\tau_c{=}1) = \frac{m_e c}{4\pi e^2} \frac{\Gamma_n^{n'}}{f_n^{n'}} \simeq 2 \times 10^9 \left(\frac{\Gamma_n^{n'}}{10^8\ \mathrm{s}^{-1}}\right)\left(\frac{0.5}{f_n^{n'}}\right) \quad \mathrm{cm}^{-2}\,, \tag{4.47}$$

where the typical value of the damping constant is on the order of a few times 10^8 s^{-1} and the typical value of the oscillator strength is on the order of unity, we have $N_n(\tau_c{=}1) \sim 10^9$ cm^{-2}.

4.5.2 Natural Line Width

Comparing Eqs. 4.42 and 4.27, we see the FHWM of the cross section in frequency is $\Delta\nu = \Gamma_n^{n'}/2\pi \simeq 10^8$ Hz. Thus, at optical wavelengths, $\Delta\nu/\nu \sim 10^{-7}$ indicating that the natural broadening is very narrow indeed. Similarly, for Eq. 4.43, the FWHM in wavelength is $\Delta\lambda = (\lambda_n^{n'})^2\Gamma_n^{n'}/2\pi c \simeq 10^{-4}$ Å for optical wavelengths, or $\Delta\lambda/\lambda \sim 10^{-7}$.

Alternatively, we can heuristically invoke the Heisenberg uncertainty principle,

$$\Delta E_n^{n'} \Delta t_n^{n'} = \hbar \,, \tag{4.48}$$

where $\Delta E_n^{n'} = h\Delta\nu = [hc/(\lambda_n^{n'})^2]\Delta\lambda$ and $\Delta t_n^{n'} = 2/\Gamma_n^{n'}$. We have $\Delta\nu = \Gamma_n^{n'}/4\pi$ and $\Delta\lambda = (\lambda_n^{n'})^2\Gamma_n^{n'}/4\pi c$, both of which differ by a factor of two from the full quantum menchanical treatment.

4.5.3 Line Source Function

To compute the source function in the line, we treat the absorption (Eq. 4.10) as being mitigated by stimulated emission (Eq. 4.8), and write

$$\kappa_n^{n'}(\nu) = h\nu \left[n_n B_n^{n'} \phi_n^{n'}(\nu) - n_{n'} B_{n'}^n I_\nu \phi_{n'}^n(\nu) \right] . \tag{4.49}$$

That is, stimulated emission can be treated as *reducing* the absorption by adding photons into the line of sight. The source function, $S(\nu)$ across the line profile is then the ratio of spontaneous emission (Eq. 4.7) to the mitigated absorption,

$$S(\nu) = \frac{\eta_{n'}^n(\nu)}{\kappa_n^{n'}(\nu)} = \frac{(h\nu n_{n'}/4\pi) A_{n'}^n \phi_{n'}^n(\nu)}{h\nu \left[n_n B_n^{n'} - n_{n'} B_{n'}^n \right] \phi_{n'}^n(\nu)} \,, \tag{4.50}$$

where we have invoked $\phi_n^{n'}(\nu) = \phi_{n'}^n(\nu)$. We have

$$S(\nu) = \frac{(A_{n'}^n/4\pi B_{n'}^n)}{(n_n/n_{n'})(B_n^{n'}/B_{n'}^n) - 1} \,. \tag{4.51}$$

Applying the Einstein relations (Eq 4.13), the source function simplifies to

$$\boxed{S(\nu) = \frac{2h\nu^3}{c^2} \left[\frac{n_n}{n_{n'}} \frac{g_{n'}}{g_n} - 1 \right]^{-1} \,,} \tag{4.52}$$

which holds assuming isotropy (no scattering), regardless of whether the populations n' and n are in thermal equilibrium with the radiation field. If the populations are in equilibrium, then the Boltzmann Equation holds, giving

$$\frac{n_{n'}}{n_n} = \frac{g_{n'}}{g_n} \exp\left\{ -\frac{h\nu}{kT} \right\} \,, \tag{4.53}$$

and we obtain the Planck function,

$$S(\nu) = B_\nu(T) = \frac{2h\nu^3}{c^2} \frac{1}{\exp\{h\nu/kT\} - 1} \,. \tag{4.54}$$

When both isotropy (no scattering) and thermal equilibrium hold, the line source function is the Planck function across the absorption or emission line.

The full source function is

$$S_\nu = \frac{\eta^n_{n'}(\nu) + \eta^c_\nu}{\kappa^{n'}_n(\nu) + \kappa^c_\nu} \,, \tag{4.55}$$

where η^c_ν and κ^c_ν are the continuum emission and absorption coefficients, repsectively. These are the topic of § **??**. In the next two chapters, we discuss additional line braodening mechansims, which must be convolved with the natural broadening and therefore change the optical depth column density relationship and the line profile width.

Chapter 5

Rotational Broadening

5.1 Stellar Rotation

Discuss evidence for stellar rotation, Figures 18.21, 18.23, 18.24, 17.18 from Gray. Provide exmples of rotationally broadened lines, Figure 18.7 from Gray.

5.2 The Broadening Function

Consider an "intrinisc" absorption line profile given by

$$I_\lambda = I^0_\lambda \exp\{-\tau_{_\lambda}\}\,, \tag{5.1}$$

which we assume occurs uniformly at all locations on the seeing disk of a non-rotating star. Under rotation, an observed wavelength, λ, will be shifted an amount $\Delta\lambda = \lambda' - \lambda = (v_{\rm los}/c)\lambda_0$, where $v_{\rm los}$ is the line-of-sight velocity, λ' is the observed shifted wavlength, and λ is the unshifted wavelength. Clearly, $v_{\rm los}$ is a function of location on the seeing stellar disk, i.e., a maximum at the limbs of the equator and a minimum at the center of the seeing disk. Thus, the observer simultaneously views the range $-v_{_{\rm R}} \sin i \le v_{\rm los} \le v_{_{\rm R}} \sin i$, where we define $v_{_{\rm R}}$ as the rotation velocity of the star with inclination i. As such, the range of corresponding wavelength shifts must be weighted appropriately by the relative area-weighted surface flux to obtain the resulting observed absorption profile.

Let $\Phi_{_{\rm R}}(\Delta\lambda)d(\Delta\lambda)$ be the rotational broadenineg function, which is the wavelength probability redistribution function in the range $\Delta\lambda \to \Delta\lambda + d(\Delta\lambda)$. The observed profile is then the convolution of $\Phi_{_{\rm R}}(\Delta\lambda)$ with the intrinisc absorption line profile,

$$I_\lambda = \Phi_{_{\rm R}}(\Delta\lambda) * I^0_\lambda \exp\{-\tau_{_\lambda}\}\,, \tag{5.2}$$

with normalization

$$\int_{-\infty}^{\infty} \Phi_{_{\rm R}}(\Delta\lambda)\, d(\Delta\lambda) = 1\,, \tag{5.3}$$

required in order to conserve the total flux removed by the intrinisc absorption profile.

To derive $\Phi_{\rm R}(\Delta\lambda)$, we consider a star of radius R rotating as a solid body with constant angular velocity ω. Let the stellar surface flux, $F_* = \sigma T_{\rm eff}^4$, be uniform across the seeing disk (we relax this assumption in § 5.3). To simplify matters, we first assume that the rotation axis is not inclined relative to the observer. In Figure 5.1a, we show a schematic of the stellar seeing disk. Any point on the seeing disk is denoted $P(x, y)$ given by the projected coordinates x and y. Note that $y = y(x) = R\sqrt{1 - (x/R)^2}$. For solid-body rotator, contours of constant line-of-sight velocity are vertical strips of constant x, which yields $\Delta\lambda(x) = (\lambda/c)v_{\rm los}(x)$.

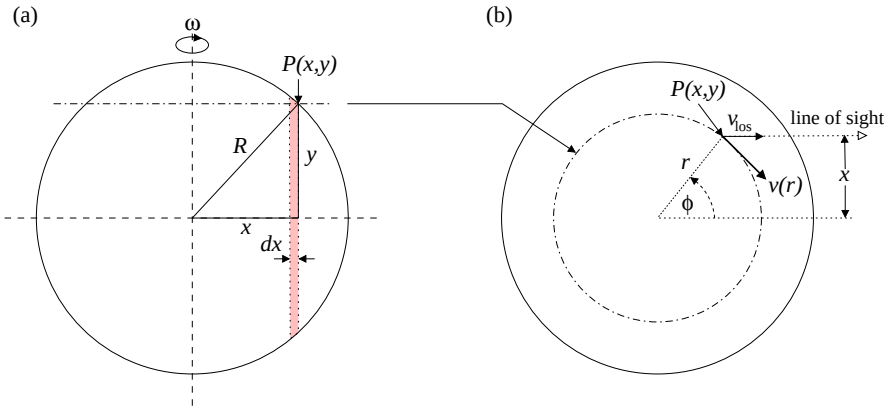

Figure 5.1: A schematic of the geometry for computing the rotational broadening function, $\Phi(\Delta\lambda)$. (a) Face-on view of a star of radius R rotating as a solid body with constant angular velocity ω with uniform surface flux F_*. An arbitrary point on the disk is denoted $P(x, y)$ given by the positions x (horizontal) and y (verticle). Countours of constant line-of-sight velocity are vetical strips with weighted-area surface flux contribution $l(x) = F_* dA = 2yF_* dx$. (b) View from the polar axis with the observer to the right. The intersection of the horizontal plane containing $P(x, y)$ is shown as the dot-dashed line. The line-of-sight velocity, $v_{\rm los}(x)$, is $v(r)\sin\phi$, where $v(r) = \omega r$.

Since $\Phi_{\rm R}(\Delta\lambda)$ is proportional to the relative area-weighted surface flux for each $\Delta\lambda(x)$, we write

$$\Phi_{\rm R}(\Delta\lambda)d(\Delta\lambda) = \Phi_0 \frac{l[\Delta\lambda(x)]}{l[\Delta\lambda(0)]} d(\Delta\lambda) \tag{5.4}$$

where $l[\Delta\lambda(x)]$ is the area-weighted surface flux corresponding to the shift $\Delta\lambda(x)$ contours at x, and $l[\Delta\lambda(0)]$ is the area-weighted surface flux at $x = 0$, the center of the seeing disk where $\Delta\lambda(0) = 0$. The constant Φ_0 is the normalization constant obtained via application of Eq. 5.3.

Consider an area-weighted surface flux contribution from an iso-shift strip at x with projected width dx. The contribution corresponding to the shift $\Delta\lambda(x)$ is $l[\Delta\lambda(x)] = F_* \cdot dA(x) = F_* \cdot 2y(x)dx = 2F_* R\sqrt{1 - (x/R)^2}dx$. The contribution

at $x = 0$ is $l[\Delta\lambda(0)] = F_* \cdot dA(0) = F_* \cdot 2y(0)\,dx = 2F_* R\,dx$. Thus,

$$\frac{l[\Delta\lambda(x)]}{l[\Delta\lambda(0)]} = \sqrt{1-(x/R)^2}\,, \tag{5.5}$$

in terms of geometric quantities. However, we wish to express Eq. 5.5 in terms of wavelength shifts $\Delta\lambda$.

Denote the rotational velocity at the equator as $v_{\rm R} = v(R) = R\omega$, which corresponds to the maximum wavelength shift $\Delta\lambda_{\rm R}$. We now show that x/R is equivalent to the ratio $v_{\rm los}(x)/v_{\rm R}$, which is equivalent to the ratio $\Delta\lambda/\Delta\lambda_{\rm R}$.

To obtain $v_{\rm los}(x)$, we consider the geometric relations illustrated in Figure 5.1b, which provides a view from the polar axis of the star. The perpendicular distance of an aribtrary point $P(x, y)$ from the roation axis is r, which has rotational velocity $v(r) = \omega r$. Thus, $v(r)/v_{\rm R} = r/R$. The line-of-sight velocity of this point is $v_{\rm los}(x) = v(r)\sin\phi$, where $\sin\phi = x/r$. Thus, $v_{\rm los}(x) = (x/r)v(r)$. From, $v(r) = (r/R)v_{\rm R}$, we have $v_{\rm los}(x) = (x/r)(r/R)v_{\rm R} = (x/R)v_{\rm R}$, which yields $x/R = v_{\rm los}(x)/v_{\rm R}$.

We now allow for the star rotation axis to be inclined by the angle i so that the actual maximum rotation velocity is $v_{\rm R}\sin i$. We thus obtain $x/R = v_{\rm los}(x)/v_{\rm R}\sin i$. Substituting into Eq. 5.5, we have

$$\frac{l[\Delta\lambda(x)]}{l[\Delta\lambda(0)]} = \frac{l[v_{\rm los}(x)]}{l[v_{\rm los}(0)]} = \sqrt{1-\left[\frac{v_{\rm los}(x)}{v_{\rm R}\sin i}\right]^2}\,, \tag{5.6}$$

where clearly $v_{\rm los}(0) = 0$. From the Doppler relation $v/c = \Delta\lambda/\lambda$, we have $v_{\rm los}(x) = (c/\lambda)\Delta\lambda$ and $v_{\rm R}\sin i = (c/\lambda)\Delta\lambda_{\rm R}$, yielding

$$\frac{l[\Delta\lambda(x)]}{l[\Delta\lambda(0)]} = \frac{l(\Delta\lambda)}{l(0)} = \sqrt{1-(\Delta\lambda/\Delta\lambda_{\rm R})^2}\,. \tag{5.7}$$

Substituting into Eq. 5.4,

$$\Phi_{\rm R}(\Delta\lambda)d(\Delta\lambda) = \Phi_0\sqrt{1-(\Delta\lambda/\Delta\lambda_{\rm R})^2}d(\Delta\lambda)\,. \tag{5.8}$$

To obtain Φ_0, we write Eq. 5.8 as $\Phi_{\rm R}(\Delta\lambda)d(\Delta\lambda) = \Phi_0\,\Delta\lambda_{\rm R}\sqrt{1-z^2}dz$, where $z = \Delta\lambda/\Delta\lambda_{\rm R}$ and $-1 \le z \le 1$. Using trignometric subtitution, $z = \cos u$, and invoking Eq. 5.3 we have

$$\Phi_0\,\Delta\lambda_{\rm R}\int_0^\pi \sin^2 u\,du = \Phi_0\,\Delta\lambda_{\rm R}\left(\frac{\pi}{2}\right) = 1\,. \tag{5.9}$$

Thus, $\Phi_0 = 2/\pi\Delta\lambda_{\rm R}$, and we obtain the rotational broadening function,

$$\boxed{\Phi_{\rm R}(\Delta\lambda) = \frac{2}{\pi\Delta\lambda_{\rm R}}\sqrt{1-(\Delta\lambda/\Delta\lambda_{\rm R})^2}\,,} \tag{5.10}$$

where $\Delta\lambda_{\rm R} = (\lambda/c)\,v_{\rm R}\sin i$ is the constraining observable quantity. Recall that the derivation of Eq. 5.10 assumed a uniform intrinisc line profile and surface flux across the stellar seeing disk *and* a solid-body rotation. We now relax the second assumption by incorporating limb darkening.

5.3 Accounting for Limb Darkening

$$\mu = \frac{r}{R} = \sqrt{1 - \frac{x^2 + h^2}{R^2}} \tag{5.11}$$

$$l[\Delta\lambda(x)] = F_0 dx \int_{-y(x)}^{y(x)} (a + b\mu)\, dh \tag{5.12}$$

where $y(x) = R\sqrt{1 - (x/R)^2}$

$$l[\Delta\lambda(x)] = F_0 dx \left\{ 2ay(x) + b \int_{-y(x)}^{y(x)} \left[1 - \frac{x^2 + h^2}{R^2} \right]^{1/2} dh \right\} \tag{5.13}$$

$$1 - \frac{x^2 + h^2}{R^2} = 1 - \frac{x^2}{R^2} - \frac{h^2}{R^2} = y^2(x) - \frac{h^2}{R^2}\,, \tag{5.14}$$

$$b \int_{-y(x)}^{y(x)} \left[1 - \frac{x^2 + h^2}{R^2} \right]^{1/2} dh = bR \int_{-y(x)}^{y(x)} \left[y^2(x) - \frac{h^2}{R^2} \right]^{1/2} \frac{dh}{R} \tag{5.15}$$

Chapter 6

Gas Physics and Ionization Balance

For the following, we assume an ideal gas with radiation. Under the assumption of theromdynamic equilibrium, the physical conditions at any arbitrary location in the atmosphere, can be quantitified by local variables, including the pressure, temperature, and mass density. These three "state variables" are related through the equation of state.

6.1 Thermodynamic Equilbrium

Discuss what is thermal equlibirium.

What is dynamic equilbirum. Dynamical time.

What is thermodynamic equilibrium. Cooling time less than Dynamical Time.

6.1.1 Temperature and LTE

Thermalization of the electrons, time scales.

6.2 The Radiation Field

In thermal equilibrium, the radiation field is isotropic, and is given by the Planck function [erg cm^{-2} sec^{-1} rad^{-2} Å^{-1}],

$$\boxed{B_\lambda(T) = \frac{2hc^2}{\lambda^5}\frac{1}{\exp\left(hc/\lambda kT\right) - 1},} \tag{6.1}$$

which depends only on the equilibrium temperature.

Integrating over all wavelengths we obtain the flux per unit solid angle [erg cm^{-2} sec^{-1} rad^{-2}],

$$B(T) = \int_0^\infty B_\lambda(T)\, d\lambda = \frac{\sigma}{\pi} T^4 = \frac{ac}{4\pi} T^4 \tag{6.2}$$

where $\sigma = 2\pi^5 k/(15h^3c^2)$, and where $a = 4\sigma/c$.

Integrating over solid angle (assuming isotropy), we obtain the energy density [erg cm^{-3}],

$$\boxed{u_r = \frac{4\pi}{c} B(T) = aT^4} \tag{6.3}$$

Check all that.

6.3 The Particle Field

The particles comprising a gas include atomic particles and free electrons. The free electrons are donated to the gas by the ionized atoms. For a given volume of gas, we will denote the number densities [particles cm^{-3}] and mass densities [g cm^{-3}] as

$$\boxed{\begin{array}{lcl} n_{\rm N} & = & \text{number density of all atomic/nuclear particles} \\ \rho_{\rm N} & = & \text{mass density of all atomic/nuclear particles} \\ n_e & = & \text{number density of free electrons} \\ \rho_e & = & \text{mass density of free electrons} \end{array}} \tag{6.4}$$

The total density of particles in the gas is

$$\begin{aligned} n &= n_{\rm N} + n_e \\ \rho &= \rho_{\rm N} + \rho_e \,. \end{aligned} \tag{6.5}$$

Whereas atomic/nuclear densities will be governed by the equation of state (see Eq. 6.48), primarily through the pressure and temperature of the gas, the total and electron densities will be also be dictated by the distribution of ionization stages of the atomic/nuclear particles.

6.3.1 Particle and Mass Density Conservation

We describe the ensemble of neutral and ionized atoms (ions) using an indexing scheme. Denote k as the index for a given atomic species, such as hydrogen, helium, etc. For ionization stages, we use the index j, which ranges from $j = 1$ for the neutral atom to $k + 1$ for the fully ioized atom. We also include the excitation levels using the index i in which $i = 1$ is the ground state.

Using this notation, we define n_{ijk} and ρ_{ijk} as the number and mass density of atomic species k in ionization stage j and excitation state i. We then define n_{jk} and ρ_{jk} as the number and mass density of atomic species k in ionization

stage j, accounting for all excitation states. And finally, we define n_k and ρ_k as the number and mass density of species k in all ionization stages and excitation states. The relationship between these densities are

$$n_{jk} = \sum_{i=1} n_{ijk} \qquad n_k = \sum_{j=1}^{k+1} n_{jk} \qquad n_{\rm N} = \sum_k n_k \tag{6.6}$$

and

$$\rho_{jk} = \sum_{i=1} \rho_{ijk} \qquad \rho_k = \sum_{j=1}^{k+1} \rho_{jk} \qquad \rho_{\rm N} = \sum_k \rho_k \,. \tag{6.7}$$

The number and mass densities are related through the mass of species, m_k. Writing $m_k = A_k m_{\rm a}$, where A_k is the atomic weight of species k in atomic mass units ($m_{\rm a} = 1.66054 \times 10^{-24}$ g),

$$n_{ijk} = \frac{\rho_{ijk}}{A_k m_{\rm a}} \qquad n_{jk} = \frac{\rho_{jk}}{A_k m_{\rm a}} \qquad n_k = \frac{\rho_k}{A_k m_{\rm a}} \tag{6.8}$$

The relative abundance of the various species is an important constraint on the particle densities and resulting electron density. Typically, logarithmic abundances, $\mathcal{A}_k$, are tabulated on a scale where hydrogen is 12,

$$\mathcal{A}_k = \log\left(\frac{n_k}{n_{\rm H}}\right) + 12 \tag{6.9}$$

where we explicitly write $n_{\rm H}$ for the number density of hydrogen. However, it is most convenient to invoke the abundance ratio, defined as

$$\alpha_k = \frac{n_k}{n_{\rm N}} \quad \text{where} \quad n_{\rm N} = \sum_k n_k \,, \tag{6.10}$$

which can be computed from the logarithmic abundances by writing

$$\boxed{\alpha_k = \frac{(n_k/n_{\rm H})}{(n_{\rm N}/n_{\rm H})} = \frac{10^{(\mathcal{A}_k - 12)}}{\sum_k 10^{(\mathcal{A}_k - 12)}}} \tag{6.11}$$

Note that $\sum_k \alpha_k = 1$.

In terms of mass densities, it is most convenient to invoke the mass fraction

$$x_k = \frac{\rho_k}{\rho_{\rm N}} \quad \text{where} \quad \rho_{\rm N} = \sum_k \rho_k \tag{6.12}$$

which can be computed from the tabulated abundances by writing

$$\boxed{x_k = \frac{(\rho_k/\rho_{\rm H})}{(\rho_{\rm N}/\rho_{\rm H})} = \frac{A_k 10^{(\mathcal{A}_k - 12)}}{\sum_k A_k 10^{(\mathcal{A}_k - 12)}}} \tag{6.13}$$

where we have invoked $\rho_k = n_k A_k m_a$ from Eq. 6.8. Note that $\sum_k x_k = 1$.

It is of interest to show the mass density of atomic/nuclear particles is directly related to the number density and mass fraction of any single species,

$$n_k = \frac{x_k}{A_k}\frac{\rho_N}{m_a} \quad \longleftrightarrow \quad \rho_N = \frac{A_k}{x_k} m_a n_k \tag{6.14}$$

and that the number density of atomic/nuclear particles is directly related to the mass density and abundance fraction of any single species,

$$\rho_k = \alpha_k A_k m_a n_N \quad \longleftrightarrow \quad n_N = \frac{\rho_k}{\alpha_k A_k m_a} \tag{6.15}$$

Note that if mass fractions are given, but abundance fractions are desired,

$$\alpha_k = \frac{x_k/A_k}{\sum_k x_k/A_k}\,, \tag{6.16}$$

using $n_k = (x_k/A_k)(\rho_N/m_a)$. Or if abundance fractions are given and mass fractions are desired,

$$x_k = \frac{\alpha_k A_k}{\sum_k \alpha_k A_k}\,, \tag{6.17}$$

using $\rho_k = \alpha_k A_k m_a n_N$.

6.3.2 Charge Conservation and Ionization Balance

To obtain the equilibrium state of the particle field in a gas, all densities must be specified. Since each ion contributes a number of electrons in proportion to its ionization stage, we must know the number densities, n_{jk}, of all ionization stages of all atomic/nuclear species. However, as we will show in detail in § 7.8, the ionization balance in thermal equilibrium depends on the electron densities (and the temperature). We therefore must derive a balancing equation in which the n_{jk} and n_e can be solved for simultaneously. The resulting balancing equation is based upon the principle of charge density conservation.

In a given volume, each ion contributes $(j-1)n_{jk}$ to the electron density. Note that the nuetral stage of an atom makes no contribution. Summing over all contributions, that is over all ionization stages for all species, we have

$$n_e = \sum_k \sum_{j=1}^{k+1} (j-1) n_{jk}\,. \tag{6.18}$$

We introduce the ionization fractions

$$f_{jk}(n_e, T) = \frac{n_{jk}}{n_k}\,, \tag{6.19}$$

where we explicitly write the fraction as a function of n_e and T. Computation of the ionization fractions for a gas in thermal equilibrium will be detailed in § 7.8. Adopting the notation, we obtain

$$n_e = \sum_k n_k \sum_{j=1}^{k+1} (j-1) f_{jk}(n_e, T) \,. \tag{6.20}$$

This relation provides the electron density *if* we know the ionization fractions; but, since the ionization fractions depend upon the electron density and temperature, we need to know n_e in order to sum the $f_{jk}(n_e, T)$. This implies that we are required to root solve Eq. 6.20. However, we have yet to fully constrain the particle densities, which we do using particle density conservation.

If the abundance fractions, α_k, are known for all atomic species, then particle conservation is expressed

$$n_k = \alpha_k n_{\rm N} = \alpha_k \left(n - n_e \right) \,, \tag{6.21}$$

where the last step follows from $n = n_{\rm N} + n_e$. Substituting, we obtain the non-linear balancing equation for the electron density

$$\boxed{n_e = (n - n_e) \sum_k \alpha_k \sum_{j=1}^{k+1} (j-1) f_{jk}(n_e, T)} \tag{6.22}$$

which must be root solved using interative numerical methods.

Once the equilibrium ionization balance is determined, n_e and the f_{jk} are known, from which the individual number densities can be obtained by employing particle conservation

$$\boxed{\begin{aligned} n_{\rm N} &= n - n_e \\ n_k &= \alpha_k n_{\rm N} \\ n_{jk} &= f_{jk} n_k \end{aligned}} \tag{6.23}$$

Note that the quantities α_k, n, and T must be specified. That is, the abundance fractions dictate the *relative* contributions of the ions for each atomic species. The total particle number density constrains the *magnitude* of the individual densities. Equation 6.22 is closed by the equation of state, which provides n and T for a given thermodynamic and hydrodynamic equilibrium condition of the gas (see Chapter 8). As such, the ionization balance is coupled to the gas hydrodynamical state.

6.3.3 Velocity Distributions

Consider an isothermal gas with no bulk motion comprising particles of species k having mass m_k. Assume a cartesian coordinate system for describing the particle velocities. If $n_k(v_x)$ is the number of particles of species k having mass m_k in the interval $v_x \to v_x + dv_x$, and n_k is the total number of particles of

species k in the gas volume, then the fraction of particles, $f_k(v_x) = n_k(v_x)/n_k$, of species k in the interval $v_x \to v_x + dv_x$, is

$$f_k(v_x)\, dv_x = \left(\frac{m_k}{2\pi kT}\right)^{1/2} \exp\left\{-\frac{m_k v_x^2}{2kT}\right\} dv_x\,. \tag{6.24}$$

As will be shown in § 6.3.4, the product kT is proportional to the mean non-relativistic kinetic energy of particles in a gas with temperature T. The distribution of particle *velocities* in any single direction (and subsequently, along any line of sight through the gas) is simply a Gaussian distribution. The normalization is

$$\int_0^\infty f_k(v_x)\, dv_x = 1. \tag{6.25}$$

The distribution of particle speeds, $f_k(v) = n_k(v)/n_k$ in the interval $v_x \to v_x + dv_x$, $v_y \to v_y + dv_y$, and $v_z \to v_z + dv_z$, is

$$f_k(v_x) f_k(v_y) f_k(v_z)\, dv_x dv_y dv_z = f_k(v)\, 4\pi v^2 dv \tag{6.26}$$

where $v^2 = v_x^2 + v_y^2 + v_z^2$, and $dv_x dv_y dv_z = 4\pi v^2 dv$, is obtained by replacing the cartesian velocity elements $dv_x dv_y dv_z$ by the spherical element $4\pi v^2 dv$, which can be visualized as a shell of thickness $v \to v + dv$. The distribution of particle velocities is then

$$\boxed{f_k(v)\, dv = \left(\frac{m_k}{2\pi kT}\right)^{3/2} \exp\left[-\frac{m_k v^2}{2kT}\right] 4\pi v^2 dv,} \tag{6.27}$$

known as a Maxwellian distribution, which has normalization,

$$\int_0^\infty f_k(v)\, dv = 1. \tag{6.28}$$

For a particle of mass m, the most probable, average, and RMS speeds are

$$v_0 = \left(\frac{2kT}{m}\right)^{1/2} \qquad \langle v\rangle = \left(\frac{8}{\pi}\frac{kT}{m}\right)^{1/2} \qquad v_{\rm RMS} = \left(\frac{3kT}{m}\right)^{1/2}. \tag{6.29}$$

Note that more massive particles have smaller v_0, $\langle v\rangle$, and $v_{\rm RMS}$ at a given T.

6.3.4 Energy Density

For given particle species k of mass m_k having non-relativistic speed v, its non-relativistic kinetic energy is $\frac{1}{2} m_k v^2$. The mean kinetic energy of particles of mass m_k in an isothermal gas of temperature T is

$$\langle \mathrm{KE}\rangle = \frac{1}{2} m_k \left\langle v_k^2 \right\rangle\,, \tag{6.30}$$

with

$$\left\langle v_k^2 \right\rangle = \frac{\displaystyle\int_0^\infty v^2 f_k(v)\, dv}{\displaystyle\int_0^\infty f_k(v)\, dv}, \tag{6.31}$$

where $f_k(v)$ is the Maxwellian distribution for particles of species k, given by Eq. 6.27. The denominator is unity. Invoking Eq. 6.29, we have

$$\left\langle v_k^2 \right\rangle = \int_0^\infty v^2 f_k(v)\, dv = \frac{4}{\sqrt{\pi}} \frac{1}{v_0^3} \int_0^\infty \exp\left\{ -\left(v/v_0\right)^2 \right\} v^4 dv. \tag{6.32}$$

The integral evaluates to $\frac{3}{8}\sqrt{\pi} v_0^5$, which yields

$$\left\langle v_k^2 \right\rangle = \frac{3}{2} v_0^2 = \frac{3kT}{m_k}, \tag{6.33}$$

from which we obtain the average kinetic energy per pariticle

$$\langle \mathrm{KE} \rangle = \frac{3}{2} kT\,. \tag{6.34}$$

An interesting property of the mean kinetic energy is that it is independent of particle mass. Thus, the mean kinetic energy of all particle species are the same, being dependent only upon the first power of gas temperature.

The energy density [erg cm^{-3}] of the gas particles is obtained by multiplying the average kntetic energy per particle by the particle number density. For nuclear particles (atoms and ions) and free electrons, we have

$$u_{\mathrm{N}} = \frac{3}{2} n_{\mathrm{N}} kT \qquad u_e = \frac{3}{2} n_e kT\,, \tag{6.35}$$

repectively. The total particle energy density is then

$$\boxed{u_g = \frac{3}{2}\left(n_{\mathrm{N}} + n_e\right) kT = \frac{3}{2} nkT.} \tag{6.36}$$

6.3.5 Pressure: The Equation of State

Pressure, P, is defined as force, F, per unit area, where force is the rate of momentum transfer, $F = dp/dt = m(dv/dt)$. In a gas, this can be visualized as the rate at which particles transfer momentum across an imaginary unit area within a unit volume.

The flux of particles of species k crossing both directions through a unit area per unit time is

$$\frac{dn_k}{dt} = \frac{1}{3} n_k \left\langle v_k \right\rangle, \tag{6.37}$$

where n_k is the number density of particles of species k, and $\langle v_k \rangle$ is the mean velocity assuming a Maxwellian velocity distribution (Eq. 6.27). Multiplying by the momentum per particle, we obtain the pressure

$$P_k = m_k \left\langle v_k \right\rangle \frac{dn_k}{dt} = \frac{1}{3} n_k m_k \left\langle v_k^2 \right\rangle = \frac{2}{3} n_k \left\langle \mathrm{KE} \right\rangle\,. \tag{6.38}$$

Note that the gas pressure is proportional to the particle mean kinetic energy.

Applying Eq. 6.34, we have

$$P_k = n_k kT\,, \tag{6.39}$$

which is independent of m_k. Alternatively, applying Eqs. 6.30 and 6.33, we have

$$P_k = \frac{1}{3} n_k m_k \left\langle v_k^2 \right\rangle = (n_k m_k)\,\frac{kT}{m_k} = \frac{\rho_k}{m_k} kT \tag{6.40}$$

where $\rho_k = n_k m_k$ is the mass density [g cm^{-3}] of spceies k.

The quantity P_k is the partial pressure for particles of species k. The pressure from all atomic/nuclear particles is the sum of the partial pressures,

$$P_{\rm N} = \sum_k P_k = \left(\sum_k \frac{\rho_k}{m_k}\right) kT = \frac{k}{\mu_{\rm N} m_{\rm a}} \rho_{\rm N} T \tag{6.41}$$

where we have defined the "mean molecular weight" for the atoms/ions

$$\frac{1}{\mu_{\rm N}} = \frac{m_{\rm a}}{\rho_{\rm N}} \left(\sum_k \frac{\rho_k}{m_k}\right) \tag{6.42}$$

where $m_{\rm a}$ is the atomic mass unit, such that $m_k = A_k m_{\rm a}$. In terms of number densities, we have

$$P_{\rm N} = \left(\sum_k n_k\right) kT = n_{\rm N} kT \tag{6.43}$$

The same principle applies for the free electrons in the gas to obtain the electron pressure,

$$P_e = \frac{k}{\mu_e m_{\rm a}} \rho_{\rm N} T = n_e kT\,, \tag{6.44}$$

where we define μ_e, the mean molecular weight of electrons. Note that, as defined here, μ_e is in atomic mass units in proportion to the mass density of the nuclear/atomic particles, $\rho_{\rm N}$, yielding the relation $\rho_{\rm N}/(\mu_e m_{\rm a}) = n_e$.

The gas pressure is the sum of the partial pressures of the atoms/ions and the free electrons

$$P_g = \frac{k}{m_{\rm a}} \left(\frac{1}{\mu_{\rm N}} + \frac{1}{\mu_e}\right) \rho_{\rm N} T = \frac{k}{\mu m_{\rm a}} \rho_{\rm N} T \tag{6.45}$$

where we define the total mean molecular weight of the gas

$$\frac{1}{\mu} = \left(\frac{1}{\mu_{\rm N}} + \frac{1}{\mu_e}\right)\,. \tag{6.46}$$

In terms of number densities

$$P_g = (n_{\rm N} + n_e)\, kT = nkT\,. \tag{6.47}$$

To obtain the total pressure of a gas with radiation, we have

$$\boxed{P = P_g + P_r = \frac{k}{\mu m_{\rm a}}\rho_{\rm N} T + \frac{a}{3}aT^4 = nkT + \frac{a}{3}T^4} \tag{6.48}$$

Equation 6.48 is known as the equation of state. Note that this form assumes an ideal gas with radiation.

6.3.6 Mean Molecular Weights

As we have just outlined, writing the pressure in terms of mass densities must account for the mean mass of the particles, and this is quantitified in terms of the mean molecular weight.

6.3.6.1 Nuclear Particles, $\mu_{\rm N}$

Having defined the mean molecular weight for atomic/nuclear particles (Eq. 6.42),

$$\frac{1}{\mu_{\rm N}} = \frac{m_{\rm a}}{\rho_{\rm N}}\left(\sum_k \frac{\rho_k}{m_k}\right) , \tag{6.49}$$

we aim to express it independently of the mass densities of the individual species. From the definition of mass fraction, $x_k = \rho_k/\rho_{\rm N}$, and employing $m_k = A_k m_{\rm a}$, we have

$$\frac{\rho_k}{m_k} = \frac{\rho_{\rm N}}{m_{\rm a}}\frac{x_k}{A_k} \tag{6.50}$$

Substituting, we obtain

$$\boxed{\mu_{\rm N} = \left[\sum_k \left(\frac{x_k}{A_k}\right)\right]^{-1}} \tag{6.51}$$

Note that $\mu_{\rm N}$ depends only upon the mass fractions of the atomic/nuclear species and has no dependence on the ionization conditions of the gas.

6.3.6.2 Electrons, μ_e

From the definition of the electron pressure (Eq. 6.44),

$$P_e = \frac{k}{\mu_e m_{\rm a}}\rho_{\rm N} T = n_e kT , \tag{6.52}$$

we have

$$\mu_e = \frac{\rho_{\rm N}}{m_{\rm a}}\frac{1}{n_e} . \tag{6.53}$$

From charge density conservation (Eq. 6.20), we have

$$n_e = \sum_k n_k \sum_{j=1}^{k+1}(j-1) f_{jk} . \tag{6.54}$$

Employing Eq. 6.14, we invoke $n_k = (x_k/A_k)(m_{\rm a}/\rho_{\rm N})$, and obtain

$$\boxed{\mu_e = \left[\sum_k \left(\frac{x_k}{A_k}\right) \sum_{j=1}^{k+1} (j-1) f_{jk}\right]^{-1}} \tag{6.55}$$

Note that μ_e depends on both the mass fractions of the atomic/nuclear particles *and* the ionization balance of the gas via Eq. 6.22.

6.3.6.3 Total Gas, μ: Massless Electron Approximation

From Eq. 6.46, we immediately have

$$\frac{1}{\mu} = \left(\frac{1}{\mu_{\rm N}} + \frac{1}{\mu_e}\right) . \tag{6.56}$$

Note that when μ is inserted into Eq. 6.45 the total gas pressure is proportional to the mass density of the atomic/nuclear particles

$$P_g = \frac{k}{\mu m_{\rm a}} \rho_{\rm N} T \, . \tag{6.57}$$

However, the "massless electron approximation" is often implicitly used to write the gas pressure in terms of the total particle density, ρ. Consider

$$\frac{\rho}{\rho_{\rm N}} = \frac{\rho_{\rm N} + \rho_e}{\rho_{\rm N}} = \left(1 + \frac{\rho_e}{\rho_{\rm N}}\right) . \tag{6.58}$$

The magnitude of ρ_e is a maximum when the gas is fully ionized. Even in this extreme scenario, we find that $\rho_e/\rho_{\rm N} \ll 1$, which yields $\rho \simeq \rho_{\rm N}$ as an excellent approximation. For a fully ionized gas, all $f_{jk} = 0$, except for $f_{k+1,k} = 1$, i.e., there are no partially ionized atoms in the gas. Thus,

$$\rho_e = m_e n_e = m_e \left[\sum_k n_k \sum_{j=1}^{k+1} (j-1) f_{jk}\right] = m_e \sum_k k n_k \, . \tag{6.59}$$

For the atoms/nuclear particles,

$$\rho_{\rm N} = \sum_k m_k n_k = m_{\rm a} \sum_k A_k n_k \simeq 2 m_{\rm a} \sum_k k n_k \, , \tag{6.60}$$

where we have approximated $A_k \simeq 2k$, which is fairly accurate for all species except hydrogen. We have

$$\frac{\rho}{\rho_{\rm N}} = \left(1 + \frac{\rho_e}{\rho_{\rm N}}\right) \simeq \left(1 + \frac{m_e}{2 m_{\rm a}}\right) = (1 + 0.00028) \simeq 1 \, . \tag{6.61}$$

Therefore, even for the extreme scenario in which the gas is fully ionized, the electron mass density is no greater than 0.03% of the atomic/nuclear particle

mass density. Adopting the massless electron approximation, all pressures can be written to high accuracy in terms of the total mass density, i.e., $\rho \simeq \rho_{\rm N}$,

$$P_{\rm N} = \frac{k}{\mu_{\rm N} m_{\rm a}} \rho T \qquad P_e = \frac{k}{\mu_e m_{\rm a}} \rho T \qquad P_g = \frac{k}{\mu m_{\rm a}} \rho T \,. \tag{6.62}$$

Chapter 7

Radiative and Collisional Processes

In a gas with radiation blah blah blah.

Bound-bound refers to an excitation or a deexcitation of an atom or ion, A_{jk}.

7.1 Bound-Bound Processes

A bound-bound excitation is the process in which a bound electron in state i (where $i = 1$ is the ground state) absorbs energy either from the radiation field (photo-excitation) or from the particle field (collisional excitation) and is elevated to a less bound state i', where $i' > i$. A bound-bound de-excitation is the process in which a bound electron in excited state i' loses energy either to the radiation field (spontaneous emission) or to the particle field (collisional de-excitation) and transitions to a more bound state i, where $i < i'$, or to the ground state $i = 1$.

Note that in the case of bound-bound transitions, the energy exchange is between the internal energy of atoms/ions and either the radiation field or the electron pool. Also note that the energy exchange is discrete, being quantized by the difference in atomic excitation energies, $\chi_{i'jk} - \chi_{ijk}$, where $\chi_{i'jk} > \chi_{ijk}$.

7.1.1 Excitation

For photo-excitation, or absorption of a photon,

$$\mathrm{A}_{ijk} + \gamma \longrightarrow \mathrm{A}_{i'jk}\,. \tag{7.1}$$

In gas with relatively high density, collisional excitation, i.e., absorption of kinetic energy by a "colliding" free electron, becomes an important channel for excitation,

$$\mathrm{A}_{ijk} + e \longrightarrow \mathrm{A}_{i'jk} + e\,. \tag{7.2}$$

In both processes, the net internal energy increase of the atom/ion is $\chi_{i'jk} - \chi_{ijk}$, where $\chi_{i'jk} > \chi_{ijk}$. Recall that for the ground state, $i = 1$, the excitation energy is $\chi_{1jk} = 0$ eV. In the case of photo-absorption, the radiation field loses energy $h\nu = \chi_{i'jk} - \chi_{ijk}$. In the case of collisional excitation, the energy is taken from the electron pool, specifically from the kinetic energy of the colliding free electron, $\Delta E_e = m_e(v_\mathrm{i}^2 - v_\mathrm{f}^2)/2 = \chi_{i'jk} - \chi_{ijk}$, where v_i is the initial velocity of the free electron, and v_f is the final velocity.

7.1.2 De-excitation

For de-excitation, the electron transitions from an excited bound state to a less excited bound state or to the ground state. For spontaneous de-excitation,

$$\mathrm{A}_{i'jk} \longrightarrow \mathrm{A}_{ijk} + \gamma\,. \tag{7.3}$$

In a higher density gas, a colliding free electron can induce the de-excitation,

$$\mathrm{A}_{i'jk} + e \longrightarrow \mathrm{A}_{ijk} + e \tag{7.4}$$

The net internal energy of the atom/ion decreases by the amount $\chi_{i'jk} - \chi_{ijk}$. For spontaenous emission, this difference in the excitation energies is released to the radiation field, $h\nu = \chi_{i'jk} - \chi_{ijk}$. For collisionally induced de-excitation the energy is donated to the electron pool via an increase in the kinetic energy of the colliding free electron, $\Delta E_e = m_e(v_\mathrm{f}^2 - v_\mathrm{i}^2)/2 = \chi_{i'jk} - \chi_{ijk}$, where v_i is the initial velocity of the free electron, and v_f is the final velocity.

An additional process called stimulated emission,

$$\mathrm{A}_{i'jk} + \gamma \longrightarrow \mathrm{A}_{ijk} + 2\gamma\,. \tag{7.5}$$

can occur in which an incident photon with energy $h\nu = \chi_{i'jk} - \chi_{ijk}$ stimulates a de-excitation from state i' to i. Whereas collisional de-excitation is proportional to the product $n_e n_{i'jk}$, stimulated emission is proportional to $4\pi(J_\nu/h\nu)n_{i'jk}$. Thus, the relative contribution of stimulated emission increases when the mean intensity of the radiation field is relatively high.

7.2 Bound-Free Processes

Bound-free processes refer to ionization and recombination. Ionization, the removal of a bound electron from an atom/ion, can be induced either by a high energy photon (photo-ionization) or by a high energy free electron (collisional ionization). Recombination, the capture of a free electron by an atom/ion, is a collisional process.

The balance of ionizations and recombinations ultimately dictates the electron density and ionization conditions of the gas, most notably fixing the ionization fractions, $f_{j-1,k} = n_{j-1,k}/n_k$, $f_{jk} = n_{jk}/n_k$, and $f_{j+1,k} = n_{j+1,k}/n_k$, etc.

Effects on continuum opacity, govern shape of the stellar continuum.

7.2.1 Ionization

Ionization of an atom/ion can occur when a photon with energy greater than the binding energy of a bound electron is absorbed, following which the electron is ejected into the gas,

$$\mathrm{A}_{jk} + \gamma \longrightarrow \mathrm{A}_{j+1,k} + e\,. \tag{7.6}$$

Assuming that the bound electron is in the ground state, energy conservations gives $h\nu = \chi_{Ijk} + m_e v^2/2$, where the freed electron has an ejection velocity v, and where χ_{Ijk} is the ionization energy (negative of the binding energy). Energy is removed from the radiation field and transfered into the electron pool, less the binding energy.

Direct collisional ionization can occur when a free electron transfers enough of its kinetic energy to liberate a bound electron

$$\mathrm{A}_{jk} + e \longrightarrow \mathrm{A}_{j+1,k} + e + e\,. \tag{7.7}$$

Clearly, the incident electron must have $m_e v_\mathrm{i}^2/2 > \chi_{Ijk}$, assuming a ground state electron. The liberated electron has kinetic energy $E_e = m_e(v_\mathrm{i}^2 - v_\mathrm{f}^2)/2 - \chi_{Ijk}$, where v_i is the initial velocity of the free electron, and v_f is the final velocity.

7.2.2 Recombination

Recombination occurs when a free electron is captured by and becomes bound in an ion; neutral atoms do not typically capture a free electron since the atom is electrically neutral. The process is

$$\mathrm{A}_{j+1,k} + e \longrightarrow \mathrm{A}_{jk} + \gamma\,. \tag{7.8}$$

Energy is exchanged between the free electron pool, which decrements by the loss of the kinetic energy of the free electron, $\Delta E_e = m_e v_\mathrm{i}^2/2$, and the radiation field, which gains a new photon with energy $h\nu = \chi_{Ijk} + m_e v_\mathrm{i}^2/2$, where v_i is the initial velocity of the free electron and χ_{Ijk} is the ionization energy to the ground state.

Often, the electron does not recombine to the ground state. If the recombination is to an exited state $i > 1$ then the emitted photon energy is $h\nu = (\chi_{Ijk} - \chi_{ijk}) + m_e v_\mathrm{i}^2/2$. On a very short time scale, the excited electron will de-excite, either spontanesouly or by stimulated emission or collisional de-excitation. If the de-excitation process is spontaneous, the electron may radiatively "cascade" downward through several lower excited states until settling into the ground state. During the radiative cascade processes, a photon is released with each de-excitation; these are known as recombination photons.

Under certain physical conditions, a neutral atom will recombine with a free electron. In the stellar atomspheres of K, G, and F type stars in particular, the H^- ion can dominated the opacity of the optical continuum. The second electron is loosely bound, requiring only 0.755 eV to be liberated.

7.2.3 Other Branches

There are at least five other bound-free processes that are worth a mention. However, a deeper examination is beyond the scope of the present treatment.

The first is Auger ionization, which can have a non-negligible rate for multi-electron atoms. In the process of photo-ionization, if the incident photon has the required energy, a deep inner shell electron can be liberated and in the process some of its energy can be channelled into also liberating one or more of the less bound, higher shell electrons. Note that the ionization stage of the atom/ion will change by two or more (not adjacent stages).

The second is excitation-auto ionization, which occurs in ions with many inner filled shell electrons but few outer shell electrons. A collision with a free electron first excites the ion (collisional excitation). Then, during the internal de-excitation process (radiative cascade) the released energy can either channel into recombination emission lines or into liberating an outer shell electron, which is auto-ionization. As the name implies, excitation-auto ionization is a collisional excitation process (bound-bound) resulting in ionization (bound-free).

Recombination has several branches to follow. The above decription of recombination is known as radiative recombination; an electron is captured and a single photon is emitted, possibly followed by a series of recombination photons. There are three other non-negiglible branches: radiation-induced, three-body, and dielectronic.

Radiation-induced recombination is analogous to stimulated emission. In this process, a photon scattering off an electron in the proximity of an atom/ion induces the electron to be captured by the ion. Three-body Recombination is a process in which the capture of a free electron by the ion is accompanied by some energy and momentum transfer energy to a second free electron in the neighborhood of the ion. Dielectronic recombination, which often dominates over radiative recombination, is the process in which a high energy free electron first excites a bound deep inner shell electron prior to its capture in an elevated excited state of the ion. There are now two excited electrons and an unfilled state in an inner shell. Multiple channels of relaxation for the ion are now available, including radiative cascade or auto-ionization.

7.3 Free-Free Processes

7.4 Scattering

Line scattering

Bound-bound absorption followed by bound-bound emission between the same two excitatation levels. The incident photon energy is essentially[1] un-

[1]The energy can be slightly changed for two reasons. First, each of the energy levels in the atom/ion have a small energy spread, translating to a wavelength uncertainty of few $\times 10^{-4}$ Å. Second, and more importantly, the motion of the atom relative to the center of mass frame will Doppler shift the energy of absorption, and the scattered photon, being emitted in a

changed.

Complications of line scatteing
Electron scattering
Rayleigh Scattering

7.5 Detailed Balancing

Detailed balancing is an equlibrium condition imposed on the rates (per unit volume of gas) of the radiative and collisional processes that govern the excitation and ionization balance of the atomic/nuclear particles. The condition is that, for every atom/ion jk, the number of excitations, de-excitations, and recombinations *in* to excitation level i per unit time per unit volume equals the number of excitations, de-excitations, and ionizations *out* of excitation level i per unit time per unit volume. Detailed balancing does not imply thermodynamic equilibrium, it only implies that the ionization balance of the gas is steady state. That is, the condition of detailed balancing is also applicable when thermodynamic equilibrium does not hold.

If thermodynamic equilibrium, or even local thermodynamic equilbirium, does not hold, then the radiation field will not be coupled to the thermal properties of the particles. Thus, the photo-ionization rates will not correspond to the statistical equilibrium balance of collisional processes; we would be required to calculate the photo-ionization rates based upon a radiation field that is non-Planckian with respect to the temperature of the particle field (assuming the particles are themalized).

For the treatment of excitation and ionization balance, we will assume detailed balancing holds. We also will assume thermodynamic and/or local thermodynamic equilbrium holds. [This holds for $\tau > 0.1$.] The resulting treatment reduces to simple closed form expressions. In the case of excitation balance, we use the Boltzmann equation. In the case of ionization balance, we use the Saha equation. As we will elaborate later, the combination of the Boltzmann and Saha equations will be instrumental in computing the continuum and line opacities in stellar atmospheres.

7.6 Excitation in Equilibrium

Bound-bound photo-absorptions and collisional excitations elevate electrons to excited states, which transition to lower excitatation states and/or the ground state due to stimulated emission, and spontaneous and collisional de-excitation. In collisional equilibrium, the excitations into a given excitation state will equal the number of de-excitations out of the state.

The higher the equilibrium temperature, the greater is the average energy of the free electron pool, the greater the probability that higher energy excitation

different random direction will gain or lose energy due to the Doppler effect in proportion to the motion of the atom/ion relative to the photon propgagation direction.

states will be filled. Thus, the higher the temperature, the larger will be the equilibrium fraction of atoms/ions with electrons in excited states. For atomic species k of ionization stage j, this probablility scales as $\exp\{-\chi_{ijk}/kT\}$ for excitation state i, where χ_{ijk} is the excitation energy for the state (the energy of the level above the ground state, which has $\chi_{1jk} = 0$ eV).

We also must account for the fact that a given excitation level has several occupation states that are energy degenerate. The number of energy degenerate states is proportional to the number of angular momentum and spin states available in the level, the former being in proportion to the principle quantum number, n, and the latter being spin up and spin down states. The statistical weight g_{ijk} denotes this number. For hydrogenic atoms, $g_{ijk} = 2n^2$, where, for our notation, i is equivalent to n (this form of the statistical weight does not apply for multi-electron atoms). The probability of occupation of an excited state is then proportional to $g_{ijk}\exp\{-\chi_{ijk}/kT\}$ for excitation state i.

7.6.1 Relative Excited States

Under the assumption of thermal equilibrium of the radiation field and collisional equilibrium, Boltzmann derived the relation that provides the ratio of number densities for a given atom/ion jk in higher excited state i' to the number density in lower excited state i. His equation is

$$\frac{n_{i'jk}}{n_{ijk}} = \frac{g_{i'jk}}{g_{ijk}} \exp\left\{-\frac{\Delta E_{ijk}^{i'jk}}{kT}\right\} = \frac{g_{i'jk}}{g_{ijk}} \exp\left\{-\frac{(\chi_{i'jk} - \chi_{ijk})}{kT}\right\} . \tag{7.9}$$

where $\Delta E_{ijk}^{i'jk}$ is the energy difference of the two states. Since the ground state has $\chi_{1jk} = 0$ eV, the ratio of excited stage i to the ground state simplifies to

$$\frac{n_{ijk}}{n_{1jk}} = \frac{g_{ijk}}{g_{1jk}} \exp\left\{-\frac{\chi_{ijk}}{kT}\right\} . \tag{7.10}$$

7.6.2 Relative to the Ion

Using particle density conservation, the Boltzmann equation can be expanded to yield n_{ijk}/n_{jk}, the number density of atoms/ions of species k and ionization stage j in excited state i relative to the number density of atoms/ions of species k and ionization stage j in all excitations states [for example, the number density of neutral hydrogens ($k = 1, j = 1$) in the first excited state above ground level to the all neutral hydrogens].

Invoking particle conservation, $n_{jk} = \sum_i n_{ijk}$, we write

$$\frac{n_{ijk}}{n_{jk}} = \frac{(n_{ijk}/n_{1jk})}{\sum_i (n_{ijk}/n_{1jk})} = \frac{(g_{ijk}/g_{1jk}) \exp\left\{-\frac{\chi_{ijk}}{kT}\right\}}{\sum_i (g_{ijk}/g_{1jk}) \exp\left\{-\frac{\chi_{ijk}}{kT}\right\}} , \tag{7.11}$$

simplifying, we have

$$\frac{n_{ijk}}{n_{jk}} = \frac{g_{ijk} \exp\left\{-\dfrac{\chi_{ijk}}{kT}\right\}}{\displaystyle\sum_i g_{ijk} \exp\left\{-\frac{\chi_{ijk}}{kT}\right\}} \,. \tag{7.12}$$

The sum is known as the partition function,

$$U_{jk}(T) = \sum_i g_{ijk} \exp\left\{-\frac{\chi_{ijk}}{kT}\right\} \,. \tag{7.13}$$

Note that the partition function accounts for all excitation levels of the atom/ion; it can be interpreted as the total statistical weight at temperature T. In final form, we write

$$\boxed{\frac{n_{ijk}}{n_{jk}} = \frac{g_{ijk}}{U_{jk}(T)} \exp\left\{-\frac{\chi_{ijk}}{kT}\right\}} \tag{7.14}$$

Discuss divergence of $U_{jk}(T)$.

7.7 Ionization in Equilibrium

Under the assumptions of thermodynamic equilibrium (in which the radiation field is also in thermal equilibrium with the thermalized particles) and collisional equilibrium, Saha derived an equation (called the Saha equation) that provides the number density ratio of adjacent ionization stages, $n_{j+1,k}/n_{jk}$.

We will "derive" the Saha equation from the Boltzmann equation, which is not the manner in which Saha derived his equation, but is still illustrative. We will account for the general case in which the electron ejected from ionized atom/ion jk could be liberated from arbitrary excitation state i. We also allow for the resulting ion $j+1, k$ to have been excited to an aribitrary excitation state, i', during the ionization process. Note the connection here between the ratios of adjacent ionization stages, their excitation states, and the velocity of free electrons entering the gas.

Starting with Eq. 7.9 and including the liberated electron,

$$\frac{n_{i',j+1,k}\, n_e(v)dv}{n_{ijk}} = \frac{g_{i',j+1,k}\, g_e(v)dv}{g_{ijk}} \exp\left\{-\frac{\Delta E_{ijk}^{i',j+1,k}}{kT}\right\} \,, \tag{7.15}$$

where $n_e(v)dv$ is the number density and $g_e(v)dv$ is the statistical weight of free electrons with velocity in the interval $v \to v + dv$. The energy difference between the initial state (atom/ion ijk prior to ionization) and the final state (ion $i', j+1, k$ and the free electron, both resulting from the ionization process) is

$$\Delta E_{ijk}^{i',j+1,k} = \left(\chi_{Ijk} - \chi_{ijk} + \frac{1}{2} m_e v^2\right) + \chi_{i',j+1,k} \tag{7.16}$$

where $\chi_{Ijk} - \chi_{ijk}$ is the binding energy of the liberated electron, which has kinetic energy $m_e v^2/2$, and where the excitation energy in the resulting ion is $\chi_{i',j+1,k}$. Inserting into Eq. 7.15,

$$\frac{n_{i',j+1,k}\, n_e(v)dv}{n_{ijk}} = G_{ijk}^{i',j+1,k}(T) \cdot \exp\left\{-\frac{m_e v^2}{2kT}\right\} g_e(v)dv\,, \tag{7.17}$$

where we define

$$G_{ijk}^{i',j+1,k}(T) = \frac{g_{i',j+1,k}\exp\left\{-\dfrac{\chi_{i',j+1,k}}{kT}\right\}}{g_{ijk}\exp\left\{-\dfrac{\chi_{ijk}}{kT}\right\}} \exp\left\{-\frac{\chi_{Ijk}}{kT}\right\}\,. \tag{7.18}$$

in order to separate the variables T and v.

For a free electron in the velocity interval $v \to v + dv$, the statistical weight is $g_e(v)dv = (2/h^3)dp_x dp_y dp_z$, which provides the number of momentum continuum phase space elements that can be occupied by the electron (the factor of two accounting for the two spin states). Writing the momentum elements in terms of the electron velocity, $dp_x dp_y dp_z = 4\pi p^2 dp = 4\pi m_e^3 v^2 dv$, we have

$$g_e(v)dv = \frac{8\pi}{h^3} m_e^3 v^2 dv\,, \tag{7.19}$$

which results in

$$\frac{n_{i',j+1,k}\, n_e(v)dv}{n_{ijk}} = \frac{8\pi m_e^3}{h^3}\, G_{ijk}^{i',j+1,k}(T) \cdot \exp\left\{-\frac{m_e v^2}{2kT}\right\} v^2 dv\,. \tag{7.20}$$

We now integrate over all electron velocities

$$\frac{n_{i,j+1,k}\, n_e}{n_{ijk}} = \frac{8\pi m_e^3}{h^3}\, G_{ijk}^{i',j+1,k}(T) \int_0^\infty \exp\left\{-\frac{m_e v^2}{2kT}\right\} v^2 dv\,, \tag{7.21}$$

where the left hand side follows directly from

$$\int_0^\infty n_e(v)dv = \int_0^\infty n_e f_e(v)dv = n_e\,, \tag{7.22}$$

where $f_e(v)$ is the Maxwell-Boltzmann distribution (Eq. 6.27) for thermalized electrons. Employing the substitution $x^2 = m_e v^2/2kT$, the integral on the right hand side of Eq. 7.21 simplifies to

$$\int_0^\infty \exp\left\{-x^2\right\} x^2 dx = \frac{\sqrt{\pi}}{4}\,, \tag{7.23}$$

and we obtain

$$\frac{n_{i',j+1,k}}{n_{ijk}} = \frac{2}{n_e}\left(\frac{2\pi m_e kT}{h^2}\right)^{3/2} G_{ijk}^{i',j+1,k}(T)\,. \tag{7.24}$$

This form of the Saha equation accounts for ionization of the atom/ion in state ijk to the upward ion in state $i', j+1, k$. As such, it describes the ratio of two adjacent ionization stages in arbitrary excitation states.

To obtain the ionization fraction, $f_{jk} = n_{jk}/n_k$, we require a form of the Saha equation that provides the ratio of the two adjacent ionization stages taken over all excitation states, $n_{j+1,k}/n_{jk}$. To simplify notation, we gather the physical constants and define

$$C_\Phi = 2\left(\frac{2\pi m_e k}{h^2}\right)^{3/2} = 4.83 \times 10^{15}\,, \tag{7.25}$$

which has units [cm^{-3} K$^{-3/2}$]. Substituting Eqs. 7.18 and 7.25 into Eq. 7.24, we have

$$\frac{n_{i',j+1,k}}{n_{ijk}} = C_\Phi \frac{T^{3/2}}{n_e} \cdot \frac{g_{i',j+1,k} \exp\left\{-\dfrac{\chi_{i',j+1,k}}{kT}\right\}}{g_{ijk} \exp\left\{-\dfrac{\chi_{ijk}}{kT}\right\}} \exp\left\{-\frac{\chi_{Ijk}}{kT}\right\}\,. \tag{7.26}$$

To obtain $n_{j+1,k}/n_{jk}$, we invoke Eq. 7.14, which we write

$$\begin{aligned} n_{ijk} &= n_{jk} \frac{g_{ijk}}{U_{jk}(T)} \exp\left\{-\frac{\chi_{ijk}}{kT}\right\} \\ n_{i',j+1,k} &= n_{j+1,k} \frac{g_{i',j+1,k}}{U_{j+1,k}(T)} \exp\left\{-\frac{\chi_{i',j+1,k}}{kT}\right\} \end{aligned} \tag{7.27}$$

Substituting for $n_{i',j+1,k}$ and n_{ijk} on the left hand side of Eq. 7.26, and rearranging, we arrive at the Saha equation

$$\boxed{\begin{aligned} \frac{n_{j+1,k}}{n_{jk}} &= n_e^{-1} \Phi_{jk}(T) \\ \Phi_{jk}(T) &= C_\Phi T^{3/2} \frac{U_{j+1,k}(T)}{U_{jk}(T)} \exp\left\{-\frac{\chi_{Ijk}}{kT}\right\} \end{aligned}} \tag{7.28}$$

Note that the ratio $n_{j+1,k}/n_{jk}$ is proportional to temperature and the ratio of partition functions of the upper to the lower adjacent ionization stages, but inversely proportional to electron density. The ratio also scales inverse exponentially with the ratio of the ground state ionization potential of the lower ionization stage (i.e., the negative of the binding energy of the ground state of the initial atom/ion prior ionization) to the mean kinetic energy per particle in the gas.

Interpreting Eq. 7.28, the number density of the upper ionization stage decreases relative to the lower ionization stage with increasing electron density. This is because, in a higher density electron pool, the number of recombinations increase more rapidly for ion $j+1, k$ than for ion jk due to the greater electron (charge) affinity of the higher ion.

7.8 Ionization Fractions

The Saha equation provides only the ratio of densities for adjacent ionization stages, $n_{j+1,k}/n_{jk}$. In order to fully characterize the gas ionization conditions and evaulate the equation of state, we require the ionization fractions,

$$f_{jk} = \frac{n_{jk}}{n_k} \quad \text{where} \quad n_k = \sum_{j=1}^{k+1} n_{jk}\,. \tag{7.29}$$

How is the Saha equation applied to obtain the ionization fractions?

We simplify the notation of the Saha equation by defining

$$\boxed{Y_{jk}(n_e, T) = \frac{n_{j+1,k}}{n_{jk}} = n_e^{-1}\Phi_{jk}(T)} \tag{7.30}$$

Consider the ionization of hydrogen ($k = 1$), which has two ionization stages, where the number density of the neutral stage is denoted n_{11} and the that of the ionized stage is denoted n_{21}. The ionization fraction of neutral hydrogen, f_{11}, is

$$f_{11} = \frac{n_{11}}{n_1} = \frac{n_{11}}{n_{11} + n_{21}} = \frac{1}{1 + (n_{21}/n_{11})} = \frac{1}{1 + Y_{11}} \tag{7.31}$$

where $Y_{11} = n_e^{-1}\Phi_{11}(T)$. Similarly, for ionized hydrogen,

$$f_{21} = \frac{n_{21}}{n_1} = \frac{(n_{21}/n_{11})}{1 + (n_{21}/n_{11})} = \frac{Y_{11}}{1 + Y_{11}} = f_{11}Y_{11} \tag{7.32}$$

For helium ($k = 2$), for which we have n_{12}, n_{22}, and n_{32} for the neutral, once ionized, and fully ionized number densities,

$$\begin{aligned} f_{12} &= \frac{n_{12}}{n_{12} + n_{22} + n_{32}} \\ &= \frac{1}{1 + (n_{22}/n_{12}) + (n_{32}/n_{12})} \\ &= \frac{1}{1 + (n_{22}/n_{12}) + (n_{32}/n_{22})(n_{22}/n_{12})} \\ &= \frac{1}{1 + Y_{12} + Y_{22}Y_{12}} \end{aligned} \tag{7.33}$$

$$\begin{aligned} f_{22} &= \frac{n_{22}}{n_{12} + n_{22} + n_{32}} \\ &= \frac{(n_{22}/n_{12})}{1 + (n_{22}/n_{12}) + (n_{32}/n_{22})(n_{22}/n_{12})} \\ &= \frac{Y_{12}}{1 + Y_{12} + Y_{22}Y_{12}} \\ &= f_{12}Y_{12} \end{aligned} \tag{7.34}$$

$$\begin{aligned} f_{32} &= \frac{n_{32}}{n_{12}+n_{22}+n_{32}} \\ &= \frac{(n_{32}/n_{22})(n_{22}/n_{12})}{1+(n_{22}/n_{12})+(n_{32}/n_{22})(n_{22}/n_{12})} \\ &= \frac{Y_{22}Y_{12}}{1+Y_{12}+Y_{22}Y_{12}} \\ &= f_{22}Y_{22} \end{aligned} \tag{7.35}$$

7.8.1 Recursive Saha

A pattern of recursion is apparent when computing ionization fractions. We define the recursion formulea

$$\boxed{\begin{aligned} P_{jk} &= P_{j-1,k}Y_{j-1,k} \quad \text{where} \quad P_{1k}=1 \\ S_k &= \sum_{j=1}^{k+1} P_{jk} \\ f_{jk} &= f_{j-1,k}Y_{j-1,k} \quad \text{where} \quad f_{1k}=\frac{1}{S_k} \end{aligned}} \tag{7.36}$$

Applying the recursive formulae for lithium ($k=3$), we obtain

$$P_{13}=1 \qquad P_{23}=Y_{13} \qquad P_{33}=Y_{13}Y_{23} \qquad P_{43}=Y_{13}Y_{23}Y_{33} \tag{7.37}$$

and

$$S_3 = 1+Y_{13}+Y_{13}Y_{23}+Y_{13}Y_{23}Y_{33} \tag{7.38}$$

yeilding

$$\begin{aligned} f_{13} &= \frac{1}{1+Y_{13}+Y_{13}Y_{23}+Y_{13}Y_{23}Y_{33}} \\ f_{23} &= f_{13}Y_{13} \\ f_{33} &= f_{23}Y_{23} \\ f_{43} &= f_{33}Y_{33} \end{aligned} \tag{7.39}$$

7.9 Excitation Fractions

Obtaining the the number density of an atom/ion jk in excitation state i relative to the number density of all ions of the same species, n_{ijk}/n_k is often required. For example, the Balmer series lines in stellar spectra originate from bound-bound absorption by excited netural hydrogen atoms with the excited electron in the $n=2$ level. The strength of the Balmer decrement is in proportion to the rate of ionizations of these same excited netural hydrogen atoms.

In general,

$$\frac{n_{ijk}}{n_k} = \frac{n_{ijk}}{n_{jk}}\frac{n_{jk}}{n_k} = \frac{n_{ijk}}{n_{jk}} f_{jk} \tag{7.40}$$

where f_{jk} is the ionization fraction (Eqs. 7.29 and 7.36), and n_{ijk}/n_{jk} is the ratio of atoms/ions jk in excitation state i to all atoms/ions of the species k in ionization stage j, given by the Boltzmann equation (Eq. 7.14). Writing out the Boltzmann portion, we have

$$\boxed{\frac{n_{ijk}}{n_k} = f_{jk}\frac{g_{ijk}}{U_{jk}(T)}\exp\left\{-\frac{\chi_{ijk}}{kT}\right\}} \tag{7.41}$$

Expressing this relation explicitly for Balmer absorbing neutral hydrogen atoms ($i = 2, j = 1, k = 1$), $g_{211} = 2n^2$ and $\chi_{211} = R_1(1 - 1/n^2)$, where $n = 2$ and $R_1 = 13.598$ is the Rydberg constant for hydrogen. We have

$$\frac{n_{211}}{n_1} = \frac{2n^2 \exp\left\{-R_1(1 - 1/n^2)/kT\right\}}{(1 + Y_{11})U_{11}(T)}\,. \tag{7.42}$$

If it is desired to know the ratio relative to all atomic/nuclear particles, we invoke $n_k = \alpha_k n_{\rm N}$, yielding

$$\boxed{\frac{n_{ijk}}{n_{\rm N}} = \alpha_k f_{jk}\frac{g_{ijk}}{U_{jk}(T)}\exp\left\{-\frac{\chi_{ijk}}{kT}\right\}} \tag{7.43}$$

Similarly, if it is desired to know the ratio relative to *all* hydrogen, we invoke $n_k = \alpha_k n_{\rm N} = (\alpha_k/\alpha_{\rm H})n_{\rm H}$, yielding

$$\boxed{\frac{n_{ijk}}{n_{\rm H}} = \frac{\alpha_k}{\alpha_{\rm H}} f_{jk}\frac{g_{ijk}}{U_{jk}(T)}\exp\left\{-\frac{\chi_{ijk}}{kT}\right\}} \tag{7.44}$$

where we have explicitly written $n_{\rm H}$ for n_1. Clearly, Eq. 7.44 reduces to Eq. 7.41 for $k = 1$. Eqs. 7.41, 7.43, and 7.44 are very useful when computing the continuum and line opacities from various atoms/ions in certain excitation states.

Chapter 8

Thermodynamics and Atmosphere Gradients

Having outlined the principles of particle and charge conservation, and having presented the formalism for determining the ionization balance of all atomic species and solving for the the number and mass densities of all particles under the conditions of local thermal equilibrium, we now present the thermodynamics of an ideal gas with radiation for a stellar atmosphere in hydrostatic equilibrium.

We first provide the differential form of the equation of state, which quantifies incremental changes in the mass density for incremental changes in the pressure, temperature, and/or the mean molecular weight. We also require a formalism for understanding how the energy content of the gas responds to such changes. We then introduce the energy transport mechanisms (radiative, convective, superadiabatic), from which we determine the temperature gradient of the atmosphere.

8.1 The Equation of State

We remind the reader that the total pressure of an ideal gas with radiation is

$$P = P_g + P_r = (P_{\rm N} + P_e) + P_r \tag{8.1}$$

where P_g is the gas pressure, $P_{\rm N}$ is the partial pressure from nuclear particles (atoms and ions), P_e is the partial pressure from free electrons, and where $P_r = (a/3)T^4$ for a Blackbody Planck function.

In terms of number densities,

$$\begin{aligned} P_{\rm N} &= n_{\rm N} kT \\ P_e &= n_e kT \\ P &= (n_{\rm N} + n_e)kT + \frac{a}{3}T^4 = nkT + \frac{a}{3}T^4 \end{aligned} \tag{8.2}$$

In terms of mass densities

$$\begin{aligned} P_{\rm N} &= \frac{k}{\mu_{\rm N} m_{\rm a}} \rho T \\ P_e &= \frac{k}{\mu_e m_{\rm a}} \rho T \\ P &= \frac{k}{\mu m_{\rm a}} \rho T + \frac{a}{3} T^4 \,, \end{aligned} \tag{8.3}$$

where we have adopted the massless electron approximation (§ 6.3.6.3), $\rho \simeq \rho_{\rm N}$.

We can write the equation of state as $\rho = \rho(P, T, \mu)$. We further define

$$\beta = \frac{P_g}{P} \qquad 1 - \beta = \frac{P_r}{P}, \tag{8.4}$$

then

$$\boxed{\rho(P, T, \mu) = \frac{\mu m_{\rm a}}{kT} \left(P - \frac{a}{3} T^4 \right) = \frac{\mu m_{\rm a}}{kT} \beta P.} \tag{8.5}$$

A highly useful differential relation is

$$\boxed{\frac{d\rho}{\rho} = \left(\frac{\partial \ln \rho}{\partial \ln P} \right) \frac{dP}{P} + \left(\frac{\partial \ln \rho}{\partial \ln T} \right) \frac{dT}{T} + \left(\frac{\partial \ln \rho}{\partial \ln \mu} \right) \frac{d\mu}{\mu}} \tag{8.6}$$

The equation allows us to examine a fractional change in the mass density in terms of fraction changes in the pressure, temperature, and/or mean molecular weight. We define the coefficients

$$\begin{aligned} \alpha &= \frac{\partial \ln \rho}{\partial \ln P} = \frac{d\rho}{\rho} \frac{P}{dP} = \frac{1}{\beta} \\ \delta &= -\frac{\partial \ln \rho}{\partial \ln T} = -\frac{d\rho}{\rho} \frac{T}{dT} = \frac{4 - 3\beta}{\beta} \\ \phi &= \frac{\partial \ln \rho}{\partial \ln \mu} = \frac{d\rho}{\rho} \frac{\mu}{d\mu} = 1, \end{aligned} \tag{8.7}$$

which yields

$$\boxed{\frac{d\rho}{\rho} = \alpha \frac{dP}{P} - \delta \frac{dT}{T} + \phi \frac{d\mu}{\mu} = \frac{1}{\beta} \frac{dP}{P} - \left(\frac{4 - 3\beta}{\beta} \right) \frac{dT}{T} + \frac{d\mu}{\mu}} \tag{8.8}$$

This relation will be used often. Note that in a gas with no radiation, $\beta = 1$, and we have $\alpha = \delta = 1$.

8.2 Thermodynamics

The differential form of the equation of state, Eq. 8.8, provides the relationship between changes in state variables. To fully model the gas, we also require a

differential relation between the state variables and the energy content of the gas. From the first law of thermodynamics, we have

$$\boxed{dQ = dU + PdV} \tag{8.9}$$

where

$$\begin{array}{lll} Q = & \text{the "heat" per unit mass} & [\text{erg}^3\ \text{g}^{-1}] \\ U = & \text{specific energy, the energy per unit mass} & [\text{erg}^3\ \text{g}^{-1}] \\ P = & \text{pressure} & [\text{dyne cm}^{-2}] \\ V = & \text{specific volume} = 1/\rho & [\text{cm}^3\ \text{g}^{-1}] \end{array} \tag{8.10}$$

Note that

$$dV = -\frac{d\rho}{\rho^2}\,. \tag{8.11}$$

The term $PdV = -Pd\rho/\rho^2$ is the incremental work done on or by the gas corresponding to an incremental density change $d\rho$. The term dU is the incremental change in the specific energy. We will continue to assume an ideal gas with radiation (which means we ignore the internal energy stored in excited atoms and ions). The increment in the heat, dQ, quantifies the total energy per unit mass, i.e, the gas plus radiation specific energy and the potential energy of the gas to do work.

For gas with radiation, the specific energy [erg g^{-1}] is

$$U = \frac{3}{2}\frac{nkT}{\rho} + U_r = \frac{3}{2}\frac{nkT}{\rho} + \frac{aT^4}{\rho}, \tag{8.12}$$

In terms of $\beta = P_g/P$, we have

$$\boxed{U = \frac{kT}{\mu m_{\rm a}}\left[\frac{3}{2} + \frac{3(1-\beta)}{\beta}\right]} \tag{8.13}$$

8.2.1 Specific Heats

In order to quantify how heat-energy content changes with a change of temperature or work done on or by the gas, we define the specific heat. We assume changes, dQ, occur either under the condition of constant pressure, $dP = 0$, or constant volume (density), $dV = 0$. For constant pressure processes

$$C_{\rm P} = \left(\frac{dQ}{dT}\right)_{\rm P} = \left(\frac{dU}{dT}\right)_{\rm P} + P\left(\frac{dV}{dT}\right)_{\rm P}\,. \tag{8.14}$$

Carrying our the differentiation

$$\begin{aligned} \left(\frac{dU}{dT}\right)_{\rm P} &= \frac{k}{\mu m_{\rm a}}\left[\frac{3}{2} + \frac{3(4+\beta)(1-\beta)}{\beta^2}\right] \\ P\left(\frac{dV}{dT}\right)_{\rm P} &= -\frac{P}{\rho^2}\left(\frac{d\rho}{dT}\right)_{\rm P} = -\frac{k}{\mu m_{\rm a}}\left[\frac{3\beta - 4}{\beta^2}\right] \end{aligned} \tag{8.15}$$

which yields

$$\boxed{C_{\rm P} = \frac{k}{\mu m_{\rm a}} \left[\frac{3}{2} + \frac{3(4+\beta)(1-\beta) + (4-3\beta)}{\beta^2} \right]} \tag{8.16}$$

The spcific heat, $C_{\rm P}$, is defined as the change in heat, dQ, that occurs when the temperature changes by 1° celsius.

The specific heat at constant volume (density) is related through

$$C_{\rm V} = \left(\frac{dQ}{dT} \right)_{\rm V} = C_{\rm P} - \frac{k}{\mu m_{\rm a}}, \tag{8.17}$$

which gives

$$\boxed{C_{\rm V} = \frac{k}{\mu m_{\rm a}} \left[\frac{1}{2} + \frac{3(4+\beta)(1-\beta) + (4-3\beta)}{\beta^2} \right]} \tag{8.18}$$

For a radiationless gas, $P_r = 0$, we have $\beta = 1$, which yields

$$C_{\rm P} = \frac{5}{2} \frac{k}{\mu m_{\rm a}} \qquad C_{\rm V} = \frac{3}{2} \frac{k}{\mu m_{\rm a}} \tag{8.19}$$

Defining the adiabatic index, γ, for an ideal gas with no radiation, we have

$$\gamma = \frac{C_{\rm P}}{C_{\rm V}} = \frac{5}{3} \, . \tag{8.20}$$

8.2.2 Energy Density

The incremental total energy per unit volume [erg cm^{-3}] is obtained by multiplying Eq. 8.9 by the total gas mass density

$$d\mathcal{E} = \rho dQ = \rho dU + \rho P dV = dE + \rho P dV \tag{8.21}$$

for which the gas energy density [erg cm^{-3}] is

$$\boxed{E = \rho U = \frac{\rho k T}{\mu m_{\rm a}} \left[\frac{3}{2} + \frac{3(1-\beta)}{\beta} \right]} \tag{8.22}$$

In terms of specific heats,

$$\left(\frac{d\mathcal{E}}{dT} \right)_{\rm P} = \rho \left(\frac{dQ}{dT} \right)_{\rm P} = \rho \, C_{\rm P} \tag{8.23}$$

$$\left(\frac{d\mathcal{E}}{dT} \right)_{\rm V} = \rho \left(\frac{dQ}{dT} \right)_{\rm V} = \rho \, C_{\rm V} \, . \tag{8.24}$$

This yields

$$\boxed{d\mathcal{E} = \rho C_{\rm P} dT} \tag{8.25}$$

and important relation that we will use often when working out the details of energy transport for convection.

8.2.3 Adiabatic Processes

An adiabatic process is one in which pressure, density, volume, temperature, and specific energy can change, but there is no heat loss or gain, i.e., $dQ = 0$. This means $dU = -PdV$, that the change in the specific energy is the negative of the increment of work, PdV, done by the gas. The gas does work ($dV > 0$), the specific energy declines; work is done on the gas ($dV < 0$), the specific energy increases. This is a constant entropy process,

$$dS = \frac{dQ}{T} = 0, \tag{8.26}$$

where entropy is defined as

$$S = \int_a^b \frac{dQ}{T} + S_0(T), \tag{8.27}$$

where $S_0(T) = 0$ at $T = 0°$ K (Nerst's Theorem), and where a and b denote the intial and final states of the gas. As we will discuss below, the adiabatic process is an ideal process. Normally, $dQ = 0$ does not hold.

8.3 Radial Gradients in Stars

8.3.1 Pressure Gradient

Assuming hydrostatic equilibrium, the pressure gradient in a stellar atmosphere is

$$\boxed{\frac{dp}{dr} = -g\rho} \tag{8.28}$$

where the gravitational acceleration is

$$g = \frac{GM(r)}{r^2} \tag{8.29}$$

where $M(r)$ is the mass inside radius r. For practical purposes, the atmosphere is thin compared to the stellar radius, and we can approximate $g = GM_*/R_*^2$.

The presure scale height is defined

$$\boxed{H = -\frac{dr}{d\ln P} = -P\frac{dr}{dP} = \frac{P}{g\rho}} \tag{8.30}$$

8.3.2 Defining the Temperature Gradient

The temperature gradient depends upon the energy transport mechanism, which is often one of the following

1. *radiative* – energy is transported via radiation

2. *adiabatic* – energy carried along in bulk motion of gas elements with no radiation losses; a contant entropy process, i.e., $dQ = 0$.

3. *superadiabatic* – some energy loss due to radiative losses during translation of elements.

The adiabatic process is an ideal process. In reality, a gas element moving through an atmospheric strata will lose *some* of its energy to radiation if it is hotter than its surroundings.

We examine each of these temperature gradients. First, we define the generalized quantity, ∇, simply refered to as "the gradient".

$$\nabla = \frac{d\ln P}{d\ln T} = \frac{dT}{T}\frac{P}{dP} = \frac{P}{T}\frac{dT}{dr}\frac{dr}{dP} = \frac{1}{T}\left(P\frac{dr}{dP}\right)\frac{dT}{dr} = -\frac{H}{T}\frac{dT}{dr}\,, \tag{8.31}$$

where the last step following from $P(dr/dP) = -P/g\rho = -H$, from which we solve

$$\boxed{\frac{dT}{dr} = -\frac{T}{H}\nabla} \tag{8.32}$$

This form assumes only that there is a well defined scale height at each location r in the atmosphere.

Under the conditions of hydrostatic equilibrium, we can write the temperature gradient in more explicit terms. Noting that

$$\frac{T}{H} = g\rho\frac{T}{P} \tag{8.33}$$

and invoking the equation of state

$$\rho = \frac{\mu m_{\rm a}}{kT}\beta P \qquad \rightarrow \qquad \frac{T}{P} = \frac{\mu m_{\rm a}}{k}\frac{\beta}{\rho} \tag{8.34}$$

we obtain

$$\boxed{\left(\frac{dT}{dr}\right)_x = -\left(\frac{g\mu m_{\rm a}\beta}{k}\right)\nabla_x} \tag{8.35}$$

where ∇_x depends upon the energy transport mechanism, denoted by x (radiative, adiabatic, or superadiabatic).

8.3.3 Adiabatic Temperature Gradient

Consider adiabatic energy transport. This corresponds to convection with no radiative losses from the rising gas elements. The energy carried by the element is finally released into the atmosphere when the element "dissolves" into the surrounding medium. The adiabatic gradient is defined

$$\nabla_{\rm ad} = \left(\frac{d\ln T}{d\ln P}\right)_s = \frac{P}{T}\left(\frac{dT}{dP}\right)_s \tag{8.36}$$

where the subscript s denotes constant entropy, $dQ = 0$. We obtain

$$\boxed{\nabla_{\rm ad} = \frac{1 + \frac{1}{\beta^2}\,(1-\beta)\,(4+\beta)}{\frac{5}{2} + \frac{4}{\beta^2}\,(1-\beta)\,(4+\beta)}} \tag{8.37}$$

with

$$\left(\frac{dT}{dr}\right)_{\rm ad} = -\left(\frac{g\mu m_{\rm a}\beta}{k}\right)\nabla_{\rm ad} \tag{8.38}$$

Note that if $\beta = 1$ (a radiationless ideal gas), then $\nabla_{\rm ad} = (\gamma - 1)/\gamma = 2/5$, yielding

$$\left(\frac{dT}{dr}\right)_{\rm ad} = -\left(\frac{g\mu m_{\rm a}}{k}\right)\frac{\gamma - 1}{\gamma} = -\frac{2}{5}\frac{g\mu m_{\rm a}}{k}\,. \tag{8.39}$$

8.3.4 Radiative Temperature Gradient

We assume the "diffusion approximation", in which the mean free path of the photons, $\ell_{\rm ph}$, are short compared to changes in the state variables of the gas (P, T, ρ, μ). This is pretty equivalent to saying that the average photon mean free path is much shorter than the pressure scale height, $\ell_{\rm ph} \ll H$. This is the optically thick regime, $\tau \geq 1$.

The mean free path of a photon of wavelength λ is the inverse of the opacity, χ_λ [cm^{-1}]. We write the opacity in terms of the mass absorption coefficient, κ_λ [cm^2 g^{-1}] , which yields

$$\ell_{\rm ph}(\lambda) = \frac{1}{\chi_\lambda} = \frac{1}{\rho\kappa_\lambda}\,. \tag{8.40}$$

The mass absorption coefficient is effectively the cross section for absorption and/or scattering per unit mass.

We desire the mean of the photon mean free path, which requires we obtain the mean mass absorption coefficient,

$$\frac{1}{\kappa} = \frac{\int_0^\infty \frac{1}{\kappa_\lambda}\frac{dB_\lambda(T)}{dT}d\lambda}{\int_0^\infty \frac{dB_\lambda(T)}{dT}d\lambda} \tag{8.41}$$

where $B_\lambda(T)$ is blackbody Planck curve (assuming LTE). Following evaluation of the integrals, the mean photon mean free path is $\ell_{\rm ph} = 1/\rho\kappa$.

To obtain the radiative gradient, we assume the diffusion approximation to obtain the radiative flux at aribitrary depth, $F_r(r)$,

$$F_r(r) = -\frac{1}{3}c\ell_{\rm ph}\frac{du_r}{dr} = -\frac{4ac}{3}\frac{T^3}{\rho\kappa}\frac{dT}{dr} \tag{8.42}$$

where we have used $u_r = aT^4$ (blackbody), for which $du_r/dT = 4aT^3$, and where we have applied the chain rule, $du_r/dr = (du_r/dT)(dT/dr)$. Rearranging, we obtain

$$\frac{dT}{dr} = -\frac{3\rho\kappa}{4ac}\frac{F_r(r)}{T^3} \tag{8.43}$$

Since there are no sources or sinks of flux in the stellar atmosphere, the total flux at aribitrary r must be equal to the flux emitted from the photosphere,

$$F_r(r) = \sigma T_{\rm eff}^4 \,, \tag{8.44}$$

where $T_{\rm eff}^4$ is the "effective temperature" of the stellar surface (taken at $\tau = 2/3$). In this case, we have assumed all the flux is carried by radiation. We thus have

$$\frac{dT}{dr} = -\frac{3\rho\kappa}{4ac}\frac{\sigma T_{\rm eff}^4}{T^3} \,. \tag{8.45}$$

Invoking $\rho = (\mu m_{\rm a}/kT)\beta P$, we eliminate ρ to obtain

$$\frac{dT}{dr} = -\frac{\mu m_{\rm a}}{k}\frac{3\kappa\beta P}{16}\left[\frac{T_{\rm eff}}{T}\right]^4 \,, \tag{8.46}$$

where we have also utilized the fact that $a = 4\sigma/c$. Comparing to the general form, Eq. 8.35, we have

$$\left(\frac{dT}{dr}\right)_r = -\left(\frac{g\mu m_{\rm a}\beta}{k}\right)\nabla_r \tag{8.47}$$

where the radiative gradient is

$$\boxed{\nabla_r = \frac{3}{16}\frac{\kappa P}{g}\left[\frac{T_{\rm eff}}{T^3}\right]^4} \tag{8.48}$$

As the optical depth drops below $\tau \simeq 0.5$, the diffusion approximation breaks down. This is in part due to the loss of isotropy in the mean free path of the photons. In this regime of optical depth, the escape probability of photons becomes high enough that some photons actually escape the atmosphere into space, while others have $\ell_{\rm ph} > H$. Consequently, the temperature gradient steepens.

Recall that the optical depth is an integrated quantity, which is interpreted as the number of mean free paths over a path length $r \to r + \Delta r$

$$\tau = \int_r^{r+\Delta r} \kappa\rho\, dr \qquad d\tau = \kappa\rho dr \tag{8.49}$$

In the practice of modeling stellar atmospheres, the radiative gradient, ∇_r, is multiplied by a correction factor, r_d,

$$\boxed{\nabla_r \to r_d \nabla_r,} \tag{8.50}$$

where

$$r_d = \frac{4}{3}\frac{1}{T_{\rm eff}^4}\frac{dT^4}{d\tau} \,. \tag{8.51}$$

In the grey atmosphere model, per Eddington's approximations,

$$T^4(\tau) = \frac{3}{4} T_{\rm eff}^4 \left[\tau + q(\tau)\right] , \tag{8.52}$$

where $q(\tau)$ is known as the Hopf function, which accounts for the break down of isotropy in the photon field. We have

$$\frac{dT^4}{d\tau} = \frac{3}{4} T_{\rm eff}^4 \left[1 + \frac{dq(\tau)}{d\tau}\right] , \tag{8.53}$$

yielding

$$r_d = 1 + \frac{dq(\tau)}{d\tau} \quad \begin{cases} r_d = 1 & \tau > 0.5 \\ r_d > 1 & \tau < 0.5 \end{cases} \tag{8.54}$$

Since r_d increases with decreasing optical depth, the temperature gradient steepens in the optically thin regime,

$$\left(\frac{dT}{dr}\right)_r = -\frac{g\mu m_{\rm a}\beta}{k} \left(r_d \nabla_r\right) \tag{8.55}$$

8.3.5 The Superadiabatic Gradient

Having derived the adiabatic and radiative gradients, we can model the temperature gradient for purely adaiabatic convection, using $\nabla_{\rm ad}$, and for purely radiative energy transport, using ∇_r.

However, we have yet to establish the physical condition for the onset of convection. We do this in the next section. As previously stated, adiabatic convection is an ideal scenario. In reality, *some* of the energy in the rising gas elements will be lost to radiation. Thus, when convection occurs, the actual gradient will not be strictly adiabatic, nor strictly radiative.

This combination of part adiabatic and part radiative physical process, is known as superadiabatic. As such, we must determine the "true" gradient of the stellar atmosphere in convective regions. This will be the topic of the next Chapter. In the following, we examine the conditions under which the atmosphere is unstable to convection.

8.4 Conditions for Convection

To establish the criterion for the onset of convection, we examine the bouyancy force, F_b, on an element of gas that is hotter than its immediate surroundings at the same r. We assume pressure balance of the element and surrounding atmosphere during the lifetime of the element. Thus, the initially hotter element will therefore be less dense than its immediate surroundings.

The bouyance force, taken over a incremental displacements Δr, can be written

$$F_b(\Delta r) d(\Delta r) = -g \left[\left(\frac{d\rho}{dr}\right)_e \Delta r - \left(\frac{d\rho}{dr}\right)_s \Delta r\right] d(\Delta r) , \tag{8.56}$$

where $(d\rho/dr)_e$ is the density change in the element over the depth range $r \rightarrow r + \Delta r$, and $(d\rho/dr)_s$ is the corresponding density change in the surrounding atmosphere. We obtain $\Delta\rho$ from Eq. 8.8. Dividing this equation by dr, we obtain

$$\frac{1}{\rho}\frac{d\rho}{dr} = \frac{\alpha}{P}\frac{dP}{dr} - \frac{\delta}{T}\frac{dT}{dr} + \frac{\phi}{\mu}\frac{d\mu}{dr} \tag{8.57}$$

where we remind the reader that $\alpha = 1/\beta$, $\delta = (4-3\beta)/\beta$, and $\phi = 1$. We have

$$\begin{aligned}
\left(\frac{d\rho}{dr}\right)_e &= \rho\left[\frac{\alpha}{P}\left(\frac{dP}{dr}\right)_e - \frac{\delta}{T}\left(\frac{dT}{dr}\right)_e + \frac{\phi}{\mu}\left(\frac{d\mu}{dr}\right)_e\right] \\
\left(\frac{d\rho}{dr}\right)_s &= \rho\left[\frac{\alpha}{P}\left(\frac{dP}{dr}\right)_s - \frac{\delta}{T}\left(\frac{dT}{dr}\right)_s + \frac{\phi}{\mu}\left(\frac{d\mu}{dr}\right)_s\right]
\end{aligned} \tag{8.58}$$

for the element and the surroundings, respectively. Re-writing in terms of the (yet to be determined) gradients within the element and in the surrounding atmosphere, we invoke $\nabla = -(H/T)(dT/dr)$, which yields the substitution $(\delta/T)(dT/dr) = -(\delta/H)\nabla$, and introduced the gradient of the mean molecular weight

$$\nabla_\mu = \frac{d\ln\mu}{d\ln P} = \frac{d\mu}{\mu}\frac{P}{dP} = \frac{P}{\mu}\frac{d\mu}{dr}\frac{dr}{dP} = -\frac{H}{\mu}\frac{d\mu}{dr}\,, \tag{8.59}$$

which yields the subsitution $(\phi/\mu)(d\mu/dr) = -(\phi/H)\nabla_\mu$. Carrying the manipulations through Eq. 8.56, the bouyancey force is written

$$F_b(\Delta r) = -\frac{g\rho}{H}\Big[\delta\left\{\nabla_e - \nabla_s\right\} - \phi\left\{\nabla_{\mu,e} - \nabla_{\mu,s}\right\}\Big]\Delta r\,, \tag{8.60}$$

where we have applied pressure balance between the element and surroundings, i.e., $(\alpha/P)[(dP/dr)_e - (dP/dr)_s] = 0$,

Dynamical instability to convection occurs when the bouyancy force on the element is positive upward, i.e., $F_b(\Delta r) > 0$ for $\Delta r > 0$. This condition forces the element upward relative to its surroundings.

8.4.1 Dynamical Instability

For the ideal scenario in which the elements are adiabatic ($\nabla_e \rightarrow \nabla_{\rm ad}$), and the surrounding atmosphere is fully radiative ($\nabla_s \rightarrow r_d\nabla_r$), then the condition $F_b(\Delta r) > 0$ for $\Delta r > 0$ dictates

$$\delta\left(\nabla_{\rm ad} - r_d\nabla_r\right) - \phi\left(\nabla_{\mu,e} - \nabla_{\mu,s}\right) < 0 \tag{8.61}$$

as the criterion in which the atmosphere is unstable to adiabatic convection (convection will occur).

First, consider the quantity $\nabla_{\mu,e} - \nabla_{\mu,s}$, which could be nonzero if the chemical composition varies with Δr in either the element or the atmosphere, or the ionization conditions change with Δr (which changes the mean molecular

weight of the electrons). In a stellar atmosphere, the former is unlikely, and any *difference* in the gradients of the mean molecular weights of the convecting element and atmosphere are likely to be negligible. Thus, if $\nabla_{\mu,e} - \nabla_{\mu,s} = 0$, we obtain $\delta\left(\nabla_{\rm ad} - r_d\nabla_r\right) < 0$ as the condition under which convection will occur. Then,

$$\begin{aligned} &\boxed{\nabla_{\rm ad} < r_d\nabla_r} \quad \text{dynamically unstable to convection} \\ &\boxed{\nabla_{\rm ad} > r_d\nabla_r} \quad \text{dynamically stable against convection} \end{aligned} \tag{8.62}$$

The latter conditions is known as the *Schwarzchild Criterion*.

A second criterion, known as the *Ledoux Criterion*, allows for nonzero $\nabla_{\mu,s}$. That is the element carries its chemical content and ionization conditions unaltered, $\nabla_{\mu,e} = 0$, whereas a gradient in the mean molecular weight of the surrounding atmosphere is not ruled out. For the *Ledoux Criterion*, it is not assumed that the convective element is adiabatic and the surrounding is radiative, as was assumed for the *Schwarzchild Criterion*. Then, $F_b > 0$ for $\Delta r > 0$ gives

$$\delta\left(\nabla_e - \nabla_s\right) + \phi\nabla_{\mu,s} < 0, \tag{8.63}$$

which can be written

$$\begin{aligned} &\boxed{\nabla_e < \nabla_s - \frac{\phi}{\delta}\nabla_{\mu,s}} \quad \text{dynamically unstable to convection} \\ &\boxed{\nabla_e > \nabla_s - \frac{\phi}{\delta}\nabla_{\mu,s}} \quad \text{dynamically stable against convection} \end{aligned} \tag{8.64}$$

Note that the *Ledoux Criterion* is in terms of the yet-to-be determined superadiabatic gradients of the element, ∇_e and the surrounding atmosphere, ∇_s, which carries the remaining energy density (or flux) not transported by the convecting element. The mathematical model for determining these quantities is known as the *mixing length model*. As we will see. evaluation of the *Ledoux Criterion* is substantially more computationally intensive than evaluation of the *Schwarzchild Criterion*.

Chapter 9

The Mixing Length Model

A convective element will radiate *some* of its energy into the surrounding atmosphere. Therefore, some of the flux energy will be transported (literally carried) by convection and some will be transported by radiation. This results in a gradient that is somewhat shallower than the radiative gradient, $r_d \nabla_r$, yet steeper than the gradient of the convective elements, ∇_e, which is steeper than the adiabatic gradient, $\nabla_{\rm ad}$.

We will call this the "true" gradient, ∇, and denote it by having no subscript. In regions where convection operate, this true gradient will dictate the temperature gradient in the atmosphere.

We use the mixing length model, which is a one-dimensional treatment in which convective elements rise over some characteristic distance, called the mixing length, $\ell_{\rm mix}$, and then dissolve (dissipate their remaining excess energy) into the surrounding atmosphere. The mixing length is a free parameter, usually taken to be on the order of the pressure scale height, H. We define the unitless mixing length parameter

$$\alpha_{\rm mix} = \frac{\ell_{\rm mix}}{H} = \frac{g\rho}{P}\ell_{\rm mix} \tag{9.1}$$

This is the main parameter of the mixing length model. Typical values are $1 \leq \alpha_{\rm mix} \leq 1.5$.

The model is crude, incomplete, and frought with approximations and assumption. The strengths of the mixing length model is that it can treat the complexity of convection using only local variables. A weakness of the mixing length model is that it can treat the complexity of convection using only local variables!

Among the uncertainties, all convective elements are treated identically; there is no inclusion of different element geometries, sizes, velocities, excess energies, or mixing lengths. These quantities are all treated as some "average". In summary, the uncertainties include

- the mixing length, which dictates the lifetime of the element.

- element geometry, which dictates the ratio of volume to surface area, where volume regulates the energy content of the element and surface area regulates the rate of radiative losses (flux).
- optical depth of the element, which governs the radiative loss rate.
- how work is done on the element, which includes energy loss due to friction or viscocity, and compression (volume density adjustment). All depend upon the element geometrey and velocity.

9.1 Constraint Equations

The mixing length model is based upon two primary constraint equations that are coupled. The first is conservation of flux. Denoting the total flux as F, the radiative flux as F_r, and the convective flux as F_c, we have

$$\boxed{\pi F = \pi F_r + \pi F_c} \tag{9.2}$$

at all locations or "layers" of the atmosphere. The second constraint equation is the efficiency parameter, γ, which is defined as

$$\boxed{\gamma = \frac{\text{excess energy density content at dissolution}}{\text{energy density lost by radiation}}} \tag{9.3}$$

Both constraint equations are written in terms of local variables, (P, ρ, T, μ, and β) and in terms of the gradients ($\nabla, \nabla_r, \nabla_e$, and $\nabla_{\rm ad}$). When the two constrain equations are coupled, a third order polynomial will result that once root solved, provides the gradients in terms of local variables via back subsitution of other relationships.

9.1.1 Conservation of Flux

We wish to express the total flux, F, radiative flux, F_r, and convective flux, F_c, in Eq. 9.2 in terms of local variables and gradients. The flux is conserved throughout the atmosphere, so the total flux at all layers is

$$F = \sigma T_{\rm eff}^4 \,. \tag{9.4}$$

9.1.1.1 The Total Flux, F

In radiative zones, the total flux is carried by radiation. Since flux is conserved at all layers in the atmosphere, the total flux in the convective regions is equal to what the radiative flux would be in the absence of convection. From Eq. 8.42, we have

$$F = -\frac{4ac}{3}\frac{T^3}{\rho\kappa}\left(\frac{dT}{dr}\right)_r \qquad \left(\frac{dT}{dr}\right)_r = -\frac{T}{H}\left(r_d \nabla_r\right) \tag{9.5}$$

which is expressed

$$\boxed{F = \frac{16}{3}\frac{\sigma T^4}{\rho\kappa H}\left(r_d\nabla_r\right)} \tag{9.6}$$

by invoking $a = 4\sigma/c$.

9.1.1.2 The Radiative Flux, F_r

In regions of convection, the portion of the flux carried by radiation is

$$F_r = -\frac{4ac}{3}\frac{T^3}{\rho\kappa}\left(\frac{dT}{dr}\right) \qquad \left(\frac{dT}{dr}\right) = -\frac{T}{H}\nabla \tag{9.7}$$

where ∇ is the "true" gradient. Invoking $a = 4\sigma/c$, we have

$$\boxed{F_r = \frac{16}{3}\frac{\sigma T^4}{\rho\kappa H}\nabla} \tag{9.8}$$

Recall that $\nabla < r_d\nabla_r$, which yields $F_r < F$.

9.1.1.3 The Convective Flux, F_c

The convective flux is the product of velocity and the energy density crossing a unit area. In this case, the velocity is the mean velocity of the convective element, $\bar{v}_e$, and the energy density is the excess released by the element at dissolution, $\Delta\mathcal{E}_{\rm ex}$. Thus,

$$F_c = \bar{v}_e\Delta\mathcal{E}_{\rm ex} = \bar{v}_e\rho C_{\rm P}\Delta T_{\rm ex}\,, \tag{9.9}$$

where $\Delta\mathcal{E}_{\rm ex}$ follows from Eq. 8.25, where $\Delta T_{\rm ex}$ is the excess temperature of the convective element at dissolution. We write

$$\Delta T_{\rm ex} = \left[\left(\frac{dT}{dr}\right)_e - \left(\frac{dT}{dr}\right)\right]\Delta r = \frac{T}{H}\left(\nabla - \nabla_e\right)\Delta r\,, \tag{9.10}$$

We assume Δr is an average displacement taken over many convective elements and parameterize this as $\Delta r = f_\ell\ell_{\rm mix}$. Almost universally, $f_\ell = 1/2$ is assumed.

Invoking the mixing length parameter (Eq. 9.1), we obtain

$$F_c = \bar{v}_e\Delta\mathcal{E}_{\rm ex} = \bar{v}_e\rho C_{\rm P}T\left(\nabla - \nabla_e\right)f_\ell\alpha_{\rm mix} \tag{9.11}$$

To estimate the average velocity of the element, we equate the average kinetic energy density of the element over its path, $\rho\bar{v}_e^2/2$, to the work, W, done on the element by the surrounding atmosphere as it rises,

$$\frac{\rho}{2}\bar{v}_e^2 = W = \int_0^\ell f(v)F_b(\Delta r)\,d(\Delta r)\,. \tag{9.12}$$

where the W is the integral of the net force over the path length, ℓ, over which the force acts. The net force is the difference between the upward bouyancy

force, $F_b(\Delta r)$, and the downward viscous/friction force, which is velocity dependent. There is a great deal of uncertainty in estimating this friction force, such as the relationship between the assumed geometry of the convective elements and the velocity dependence of the force. This complexity can be grossly simplified by scaling the bouyancy force by a velocity dependent correction factor, $f(v)$. The functional form for $f(v)$ is so uncertain, that it is taken as an "averaged" constant, $f_{\rm v} = f(v)$, with $0 \leq f_{\rm v} \leq 1$.

Substituting the bouyancy force (Eq. 8.60) into the integral and carrying out the integration, we obtain

$$W = -f_{\rm v}\frac{g\rho\delta}{H}\left(\nabla_e - \nabla\right)\int_0^{f_{\rm W}\ell_{\rm mix}} \Delta r\, d(\Delta r) = f_{\rm v}\frac{g\rho\delta}{H}\left(\nabla - \nabla_e\right)\frac{\left(f_{\rm W}\ell_{\rm mix}\right)^2}{2}\,, \quad (9.13)$$

where we have ignored the term $(\nabla_{\mu,e} - \nabla_\mu)$. We parameterize the average path length over which work is done on the convective elements as a fraction, $f_{\rm W}$, of the mixing length, $\Delta r = f_{\rm W}\ell_{\rm mix} = f_{\rm W}H\alpha_{\rm mix}$. We have

$$W = \frac{1}{2}f_{\rm v}f_{\rm W}^2 g\rho H\delta\left(\nabla - \nabla_e\right)\alpha_{\rm mix}^2\,. \quad (9.14)$$

Defining $f_{\rm v}f_{\rm W}^2 = (1/\nu)^{1/2}$, and invoking Eq. 9.12, we solve for

$$\boxed{\bar{v}_e = \left\{\frac{gH\delta}{\nu}\right\}^{1/2}\left(\nabla - \nabla_e\right)^{1/2}\alpha_{\rm mix}} \quad (9.15)$$

Typically, $f_{\rm v} = f_{\rm W} = 1/2$ is explicitly assumed in the derivation of $\bar{v}_e$, which yields $\nu = 8$. Substituting Eq. 9.15 into Eq. 9.11, we obtain

$$\boxed{F_c = \left\{\frac{gH\delta}{\nu}\right\}^{1/2}\rho C_{\rm P}T\left(\nabla - \nabla_e\right)^{3/2} f_\ell\alpha_{\rm mix}^2} \quad (9.16)$$

As previously mentioned, in most treatments, $f_{\rm v} = f_{\rm W} = 1/2$ is explicitly assumed in the derivation of $\bar{v}_e$ (Eq. 9.15), and $f_\ell = 1/2$ is explicitly assumed in the derivation of F_c (Eq. 9.11). For such derivations, these "free parameters" are combined resulting in $F_c = \{gH\delta/32\}^{1/2}\rho C_{\rm P}T\left(\nabla - \nabla_e\right)^{3/2}\alpha_{\rm mix}^2$.

9.1.1.4 First Constraint Equation

Dividing Eq. 9.2 by the total flux, F,

$$\frac{F_r}{F} + \frac{F_c}{F} = 1 \quad (9.17)$$

From Eq. 9.6 and Eq. 9.8, we have the ratio

$$\frac{F_r}{F} = \frac{\nabla}{r_d\nabla_r}\,.. \quad (9.18)$$

Invoking $F = \sigma T_{\rm eff}^4$ and substituting Eq. 9.16 for F_c, we obtain

$$\frac{\nabla}{r_d \nabla_r} + \frac{A' \left(\nabla - \nabla_e\right)^{3/2}}{\sigma T_{\rm eff}^4} = 1 \,, \tag{9.19}$$

where

$$A' = \left\{ \frac{gH\delta}{\nu} \right\}^{1/2} \rho C_{\rm P} T f_\ell \alpha_{\rm mix}^2 \,, \tag{9.20}$$

combines the local variables appearing in the convective flux (Eq. 9.16). Rearranging, we obtain the first constraint equation in terms of local variables and gradients,

$$\boxed{A \left(\nabla - \nabla_e\right)^{3/2} = r_d \nabla_r - \nabla} \tag{9.21}$$

where

$$A = A' \frac{r_d \nabla_r}{\sigma T_{\rm eff}^4} \tag{9.22}$$

with ∇_r obtained from Eq. 8.48 and where ∇ and ∇_e remain to be determined.

9.1.2 Efficiency of Convection

Following Unsöld, we define the efficiency of convection using the parameter, γ, which is defined

$$\gamma = \frac{\text{excess energy density content at dissolution}}{\text{energy density lost by radiation}} = \frac{\Delta\mathcal{E}_{\rm ex}}{\Delta\dot{\mathcal{E}}_r \Delta t} \,, \tag{9.23}$$

where

$$\begin{aligned} \Delta\mathcal{E}_{\rm ex} &= \text{remaining energy density in element at dissolution [erg cm}^{-3}\text{]} \\ \Delta\dot{\mathcal{E}}_r &= \text{loss rate of radiative energy density [erg s}^{-1}\text{ cm}^{-3}\text{]} \\ \Delta t &= \text{life time of element} \end{aligned}$$

Alternatively, the energy lost by radiation over the life time of the element can be expressed as the difference between the energy density a convective element would have had at dissolution with no radiation losses, which is an adiabatic process, $\Delta\mathcal{E}_{\rm ad}$, and the energy density that remains within a radiating element at dissolution, $\Delta\mathcal{E}_{\rm ex}$, i.e.,

$$\dot{\mathcal{E}}_r \Delta t = \Delta\mathcal{E}_{\rm ad} - \Delta\mathcal{E}_{\rm ex} \,. \tag{9.24}$$

Following the logic of Eqs. 9.9 and 9.10, to derive Eq. 9.11, we have

$$\Delta\mathcal{E}_{\rm ex} = \rho C_{\rm P} \Delta T_{\rm ex} = \rho C_{\rm P} T \left(\nabla - \nabla_e\right) f_\ell \alpha_{\rm mix} \tag{9.25}$$

which follows from application of Eq. 8.25. Using the identical principles used to obtain $\Delta\mathcal{E}_{\rm ex}$, it is trivial to derive

$$\Delta\mathcal{E}_{\rm ad} = \rho C_{\rm P} T \left(\nabla - \nabla_{\rm ad}\right) f_\ell \alpha_{\rm mix} \,, \tag{9.26}$$

which follows by applying the adiabatic gradient, $\nabla_{\rm ad}$, in place of the gradient of a radiating convective element, ∇_e. We have

$$\gamma = \frac{\Delta\mathcal{E}_{\rm ex}}{\Delta\mathcal{E}_{\rm ad} - \Delta\mathcal{E}_{\rm ex}} = \frac{(\nabla - \nabla_e)}{(\nabla - \nabla_{\rm ad}) - (\nabla - \nabla_e)} \tag{9.27}$$

which simplifies to

$$\boxed{\gamma = \frac{\nabla - \nabla_e}{\nabla_e - \nabla_{\rm ad}}} \tag{9.28}$$

This expression for the efficiency in terms of gradients is not complete, for it provides no physical insight from the local variables. We thus must derive an alternative form of γ in terms of local variables, which we then equate to the right hand side of Eq. 9.28 to obtain our second constraint equation for the mixing length model.

Deriving γ in terms of local variables includes the additional challenge of accounting for whether the convective elements are optically thick or optically thin. Clearly, the efficiency of convection will be much lower for optically thin elements than for optically thick elements, since the former will have experienced larger radiative losses by the time of dissolution. We consider each regime separately.

9.1.2.1 Optically Thick Elements

In the optically thick regime, where the diffusion approximation applies, the energy density radiative loss rate [erg s^{-1} cm^{-3}] from a convective element can be expressed as

$$\Delta\dot{\mathcal{E}}_r = \frac{F_r \cdot A_e}{V_e}\,, \tag{9.29}$$

where A_e and V_e are the surface area and volume of the element (on average). Adopting the diffusion approximation, the radiative flux from a convective element will be

$$F_r = \frac{1}{3}\frac{c}{\rho\kappa}\left(\frac{du_r}{dr}\right)_e\,, \tag{9.30}$$

where, $(du_r/dr)_e = (du_r/dT)_e(dT/dr)_e$ is the upward gradient from the base of the convective element, and, as before, we assume $u_r = aT^4$.

Noting that, in general, $d\tau = \rho\kappa dr$, we can approximate the optical depth of the convective element as

$$\tau_e = \rho\kappa\ell_e \simeq \alpha_{\rm mix} H\rho\kappa, \tag{9.31}$$

where ℓ_e a characteristic length scale of the element, which we approximates as $\ell_e = \ell_{\rm mix}$. We obtain

$$F_r = \frac{4acT^3}{3}\frac{\ell_e}{\tau_e}\left(\frac{dT}{dr}\right)_e\,, \tag{9.32}$$

which yields

$$\Delta\dot{\mathcal{E}}_r = 16\sigma T^3 \left(\frac{\ell_e A_e}{3V_e}\right) \frac{1}{\tau_e} \left(\frac{dT}{dr}\right)_e , \tag{9.33}$$

where we invoked $a = 4\sigma/c$.

Clearly, we see that the energy density radiative loss rate is dependent upon the geometry of the convective element. We parameterize the geometry as $R_{\rm g} = (\ell_e A_e/3V_e)$. For a sphere, $R_{\rm g} = 1$, and for a cylinder, $R_{\rm g} = 2(1+x)/3x$, where $x = h/r$, the ratio of the cyclinder height to its radius. Interestingly, for a cyclinder in which its height is equal to twice its radius (i.e., diameter, $x = 2$), we recover $R_{\rm g} = 1$.

To estimate $(dT/dr)_e$, we adopt the time average excess temperature distribution, $f_t \Delta T_{\rm ex}$, where f_t estimates the mean excess over the life time of the element (usually assumed to be $f_t = 1/2$). We also allow for a nonuniform temperature distribution within the convective element averaged over the mixing length, and write

$$\left(\frac{dT}{dr}\right)_e = \frac{1}{y}\left(\frac{f_t \Delta T_{\rm ex}}{\ell_{\rm mix}}\right) , \tag{9.34}$$

where y is a constant resulting from integration across the temperature distribution. For a linear distribution, $y = 0.5$, for a parabolic distribution, $y = 1/20 = 0.05$, and for a truncated sinusoidal distribution, $\propto (\sin ar)/ar$ where a is a scale length, $y = 3/4\pi^2 \simeq 0.076$. We have

$$\Delta\dot{\mathcal{E}}_r = 16\sigma T^3 \frac{f_t \Delta T_{\rm ex}}{\ell_{\rm mix}} \frac{R_{\rm g}}{y} \frac{1}{\tau_e} . \tag{9.35}$$

Finally, we obtain the energy density lost to radiation over the average life time of a convective element, $\Delta t = \ell_{\rm mix}/\bar{v}_e$,

$$\Delta\dot{\mathcal{E}}_r \Delta t = 16\sigma T^3 \frac{f_t \Delta T_{\rm ex}}{\bar{v}_e} \frac{R_{\rm g}}{y} \frac{1}{\tau_e} . \tag{9.36}$$

Applying $\Delta\mathcal{E}_{\rm ex} = \rho C_{\rm P} \Delta T_{\rm ex}$, the efficiency in the optically thick regime is

$$\gamma_{\rm thick} = \frac{\Delta\mathcal{E}_{\rm ex}}{\Delta\dot{\mathcal{E}}_r \Delta t} = \frac{\rho C_{\rm P} \bar{v}_e}{16 f_t \sigma T^3} \frac{y}{R_{\rm g}} \tau_e \tag{9.37}$$

9.1.2.2 Optically Thin Elements

In the optically thick regime, we write

$$\Delta\dot{\mathcal{E}}_r = c\tau_e \left(\frac{du_r}{dr}\right)_e = c\tau_e \left(\frac{du_r}{dT}\frac{dT}{dr}\right)_e = 4acT^3\,\tau_e \left(\frac{dT}{dr}\right)_e \tag{9.38}$$

where $\tau_e = \rho\kappa\ell_e = \alpha_{\rm mix} H \rho\kappa$ is given by Eq. 9.31, though $\rho\kappa$ will be small. For an optically thin element, the temperature distribution throughout the element will be constant ($y = 1$), yielding $(dT/dr)_e = f_t \Delta T_{\rm ex}/\ell_{\rm mix}$. We obtain,

$$\Delta\dot{\mathcal{E}}_r = 4acT^3 \frac{f_t \Delta T_{\rm ex}}{\ell_{\rm mix}} \tau_e = 16\sigma T^3 \frac{f_t \Delta T_{\rm ex}}{\ell_{\rm mix}} \tau_e \tag{9.39}$$

where the last step uses $a = 4\sigma/c$. Multiplying by the life time, $\ell_{\rm mix}/\bar{v}_e$, of the element

$$\Delta\dot{\mathcal{E}}_r \Delta t = 16\sigma T^3 \frac{f_t \Delta T_{\rm ex}}{\bar{v}_e}\tau_e \tag{9.40}$$

Applying $\Delta\mathcal{E}_{\rm ex} = \rho C_{\rm P}\Delta T_{\rm ex}$, the efficiency in the optically thin regime is

$$\gamma_{\rm thin} = \frac{\Delta\mathcal{E}_{\rm ex}}{\Delta\dot{\mathcal{E}}_r\Delta t} = \frac{\rho C_{\rm P}\bar{v}_e}{16 f_t \sigma T^3}\frac{1}{\tau_e} \tag{9.41}$$

9.1.2.3 The Second Constraint Equation

Since the efficiency of convection is depends upon optical depth, and a range of optical depths for an ensemble of convective elements is expected, the mean efficiency is obtained by "interpolating" between the optically thick and optically thin cases,

$$\gamma = \gamma_{\rm thick} + \gamma_{\rm thin} = \frac{\rho C_{\rm P}\bar{v}_e}{16 f_t \sigma T^3\,\tau_e}\left[1 + \frac{y}{R_{\rm g}}\tau_e^2\right] . \tag{9.42}$$

Substituting $\bar{v}_e$ (Eq. 9.15),

$$\gamma = \frac{\rho C_{\rm P}\alpha_{\rm mix}}{16 f_t \sigma T^3\,\tau_e}\left\{\frac{gH\delta}{\nu}\right\}^{1/2}\left[1 + \frac{y}{R_{\rm g}}\tau_e^2\right](\nabla - \nabla_e)^{1/2} . \tag{9.43}$$

Equating to Eq. 9.28,

$$\frac{\nabla - \nabla_e}{\nabla_e - \nabla_{\rm ad}} = \frac{\rho C_{\rm P}\alpha_{\rm mix}}{16 f_t \sigma T^3\,\tau_e}\left\{\frac{gH\delta}{\nu}\right\}^{1/2}\left[1 + \frac{y}{R_{\rm g}}\tau_e^2\right](\nabla - \nabla_e)^{1/2} , \tag{9.44}$$

from which we obtain the second constraint equation,

$$\boxed{B\,(\nabla - \nabla_e)^{1/2} = \nabla_e - \nabla_{\rm ad}} \tag{9.45}$$

where

$$B = \frac{16 f_t \sigma T^3}{\rho C_{\rm P}\alpha_{\rm mix}\,(gH\delta/\nu)^{1/2}}\left(\frac{\varphi}{\alpha_{\rm mix}H\rho\kappa}\right) \tag{9.46}$$

and where

$$\varphi = \frac{\tau_e^2}{1 + (y/R_{\rm g})\,\tau_e^2} = \frac{(\alpha_{\rm mix}H\rho\kappa)^2}{1 + (y/R_{\rm g})\,(\alpha_{\rm mix}H\rho\kappa)^2} . \tag{9.47}$$

9.2 Solution to the Mixing Length Model

Our two constraint equations (Eqs. 9.21 and 9.45) are

$$\boxed{\begin{aligned} A\,(\nabla - \nabla_e)^{3/2} &= r_d\nabla_r - \nabla \\ B\,(\nabla - \nabla_e)^{1/2} &= \nabla_e - \nabla_{\rm ad} \end{aligned}} \tag{9.48}$$

where the first equation follows from flux conservation, and the second equation expresses the efficiency of convection. The local variables are combined in the parameters A (Eq. 9.22) and B (Eq. 9.46) and the gradients $r_d\nabla_r$ and $\nabla_{\rm ad}$. We now couple these equations.

Adding $(\nabla - \nabla_e) - (\nabla_e - \nabla_{\rm ad})$ to both sides of the first constraint equation, we obtain

$$A\left(\nabla - \nabla_e\right)^{3/2} + (\nabla - \nabla_e) + (\nabla_e - \nabla_{\rm ad}) = r_d\nabla_r - \nabla_{\rm ad}\,. \tag{9.49}$$

From the second constraint equation, we have $(\nabla_e - \nabla_{\rm ad}) = B(\nabla - \nabla_e)^{1/2}$. Substituting for the last term on the left hand side of Eq. 9.49, and defining $\xi = (\nabla - \nabla_e)^{1/2}$, we obtain the cubic equation

$$\boxed{A\xi^3 + \xi^2 + B\xi - (r_d\nabla_r - \nabla_{\rm ad}) = 0\,,} \tag{9.50}$$

which is solved for the root ξ_0.

Through the definition of ξ, we express $\nabla_e = \nabla - \xi_0^2$, which we back substitute into the second constraint equation to obtain

$$B\xi_0 = \left(\nabla - \xi_0^2\right) - \nabla_{\rm ad} \tag{9.51}$$

which provides the solution

$$\boxed{\begin{aligned} \nabla &= \nabla_{\rm ad} + B\xi_0 + \xi_0^2 \\ \nabla_e &= \nabla_{\rm ad} + B\xi_0 \end{aligned}} \tag{9.52}$$

Recall that in regions where the atmosphere is unstable to convection, the Schwarzchild criterion dictates $r_d\nabla_r > \nabla_{\rm ad}$. Flux conservation and a less than 100% efficiency in the convective transport of the energy (i.e., radiative losses) must always yield

$$r_d\nabla_r > \nabla > \nabla_e > \nabla_{\rm ad}\,. \tag{9.53}$$

The real root ξ_0 is obtained from

$$\xi_0 = \frac{1}{3A}\left[\frac{(3AB-2)}{C} - 1\right]\,, \tag{9.54}$$

where

$$\begin{aligned} C &= \left\{\tfrac{1}{2}\left(\left[\alpha^2 - 4\beta^3\right]^{1/2} + \alpha\right)\right\}^{3/2} \\ \alpha &= 2 - 9AB - 27A^2\left(r_d\nabla_r - \nabla_{\rm ad}\right) \\ \beta &= 1 + 3AB \end{aligned} \tag{9.55}$$

Chapter 10

Stellar Atmospheres

10.1 Plane-Parallel Geometry

Discuss the plane-parallel assumption including angles etc.

10.1.1 Solution to Transfer Equation

Under the plane-parallel assumption.

$$\frac{1}{w}\frac{dI_\lambda(\tau_\lambda,\theta)}{d\tau_\lambda} = I_\lambda(\tau_\lambda,\theta) - S_\lambda(\tau_\lambda)\,, \tag{10.1}$$

where $w = 1/\cos\theta = \sec\theta$. To solve this first order differential equation, we assume the form $I_\lambda = f_\lambda \exp\{k\tau_\lambda\}$, where $\exp\{k\tau_\lambda\}$ is the standard integrating factor. Carrying out the differentiation on the left hand side, we obtain

$$\frac{1}{w}\frac{dI_\lambda}{d\tau_\lambda} = \frac{1}{w}\left[\frac{df_\lambda}{d\tau_\lambda}\exp\{k\tau_\lambda\} + kf_\lambda\exp\{k\tau_\lambda\}\right]. \tag{10.2}$$

Equating the right hand sides of Eqs.10.1 and 10.2, we have

$$\begin{aligned} I_\lambda &= \frac{k}{w}f_\lambda\exp\{k\tau_\lambda\} \\ S_\lambda &= -\frac{1}{w}\frac{df_\lambda}{d\tau_\lambda}\exp\{k\tau_\lambda\} \end{aligned} \tag{10.3}$$

To recover $I_\lambda = f_\lambda\exp\{k\tau_\lambda\}$, we immediately find $k = w$. To obtain f_λ, we rearrange the expression for S_λ and integrate from τ_1 to τ_2,

$$f_\lambda = -w\int_{\tau_1}^{\tau_2} S_\lambda \exp\{-wt_\lambda\}\,dt_\lambda + C\,, \tag{10.4}$$

where C is a constant depending upon the boundary conditions. We have

$$I_\lambda(\tau_\lambda,\theta) = \exp\{w\tau_\lambda\}\left[-w\int_{\tau_1}^{\tau_2} S_\lambda(t_\lambda)\exp\{-wt_\lambda\}\,dt_\lambda + C\right] \tag{10.5}$$

Integrating from $\tau_1 = \tau'_\lambda$ to $\tau_2 = \tau_\lambda$, where $\tau'_\lambda > \tau_\lambda$ and the incident specific intensity at τ'_λ is $I_\lambda(\tau'_\lambda, \theta)$, we obtain the solution

$$\boxed{\begin{aligned} I_\lambda(\tau_\lambda, \theta) &= I_\lambda(\tau'_\lambda, \theta) \exp\left\{-w(\tau'_\lambda - \tau_\lambda)\right\} \\ &\quad + w \int_{\tau_\lambda}^{\tau'_\lambda} S_\lambda(t_\lambda) \exp\left\{-w\left(t_\lambda - \tau_\lambda\right)\right\} dt_\lambda \end{aligned}} \tag{10.6}$$

which is valid for $0 \leq \theta \leq \pi/2$ corresponding to the directions toward lower optical depths higher in the atmosphere.

10.1.2 The Diffusion Approximation

$$S_\lambda(\tau_\lambda) = \sum_{n=0}^{\infty} \frac{d^n S_\lambda(\tau_\lambda)}{d\tau_\lambda^n} \frac{\left(t_\lambda - \tau_\lambda\right)^n}{n!} \tag{10.7}$$

Substituting into $I_\lambda^{\rm out}(\tau_\lambda, \theta)$ (Eq. 10.16),

$$\begin{aligned} I_\lambda^{\rm out}(\tau_\lambda, \theta) &= \int_{\tau_\lambda}^{\infty} \sum_{n=0}^{\infty} \frac{d^n S_\lambda(\tau_\lambda)}{d\tau_\lambda^n} \frac{\left(t_\lambda - \tau_\lambda\right)^n}{n!} \exp\left\{-w\left(t_\lambda - \tau_\lambda\right)\right\} w\, dt_\lambda \\ &= \sum_{n=0}^{\infty} \frac{d^n S_\lambda(\tau_\lambda)}{d\tau_\lambda^n} \frac{1}{n!} \int_{\tau_\lambda}^{\infty} \left(t_\lambda - \tau_\lambda\right)^n \exp\left\{-w\left(t_\lambda - \tau_\lambda\right)\right\} w\, dt_\lambda \\ &= \sum_{n=0}^{\infty} \frac{d^n S_\lambda(\tau_\lambda)}{d\tau_\lambda^n} \frac{1}{w^n n!} \int_{\tau_\lambda}^{\infty} x^n \exp\{-x\}\, dx\,, \end{aligned} \tag{10.8}$$

where the last step follows from the substution $x = w(t_\lambda - \tau_\lambda)$. Since the integral evaluates to $\int_0^\infty x^n e^{-x} dx = n!$, we have

$$I_\lambda^{\rm out}(\tau_\lambda, \theta) = \sum_{n=0}^{\infty} \frac{1}{w^n} \frac{d^n S_\lambda(\tau_\lambda)}{d\tau_\lambda^n}\,, \tag{10.9}$$

which written out to the first few terms is

$$I_\lambda^{\rm out}(\tau_\lambda, \theta) = S_\lambda(\tau_\lambda) + \frac{1}{w} \frac{dS_\lambda(\tau_\lambda)}{d\tau_\lambda} + \frac{1}{w^2} \frac{d^2 S_\lambda(\tau_\lambda)}{d\tau_\lambda^2} + \cdots\,. \tag{10.10}$$

Following the same proceedure for $J_\lambda^{\rm out}(\tau_\lambda)$, $H_\lambda^{\rm out}(\tau_\lambda)$ and $K_\lambda^{\rm out}(\tau_\lambda)$ by substituting Eq. 10.7 into Eqs. 10.24, 10.27, and 10.28, we obtain

$$\begin{aligned} J_\lambda^{\rm out}(\tau_\lambda) &= \sum_{n=0}^{\infty} \frac{1}{2n+1} \frac{d^{2n} S_\lambda(\tau_\lambda)}{d\tau_\lambda^{2n}} \\ &= S_\lambda(\tau_\lambda) + \frac{1}{3} \frac{d^2 S_\lambda(\tau_\lambda)}{d\tau_\lambda^2} + \frac{1}{5} \frac{d^4 S_\lambda(\tau_\lambda)}{d\tau_\lambda^4} + \cdots\,, \end{aligned} \tag{10.11}$$

and,

$$\begin{aligned} H_\lambda^{\rm out}(\tau_\lambda) &= \sum_{n=0}^{\infty} \frac{1}{2n+3} \frac{d^{2n+1} S_\lambda(\tau_\lambda)}{d\tau_\lambda^{2n+1}} \\ &= \frac{1}{3}\frac{dS_\lambda(\tau_\lambda)}{d\tau_\lambda} + \frac{1}{5}\frac{d^3 S_\lambda(\tau_\lambda)}{d\tau_\lambda^3} + \cdots . \end{aligned} \tag{10.12}$$

and,

$$\begin{aligned} K_\lambda^{\rm out}(\tau_\lambda) &= \sum_{n=0}^{\infty} \frac{1}{2n+3} \frac{d^{2n} S_\lambda(\tau_\lambda)}{d\tau_\lambda^{2n}} \\ &= \frac{1}{3} S_\lambda(\tau_\lambda) + \frac{1}{5}\frac{d^2 S_\lambda(\tau_\lambda)}{d\tau_\lambda^2} + \frac{1}{7}\frac{d^4 S_\lambda(\tau_\lambda)}{d\tau_\lambda^4} + \cdots . \end{aligned} \tag{10.13}$$

repectively.

$$\boxed{\begin{aligned} I_\lambda(\tau_\lambda,\theta) &= S_\lambda(\tau_\lambda) + \frac{1}{w}\frac{dS_\lambda(\tau_\lambda)}{d\tau_\lambda} \\ J_\lambda(\tau_\lambda) &= S_\lambda(\tau_\lambda) \\ H_\lambda(\tau_\lambda) &= \frac{1}{3}\frac{dS_\lambda(\tau_\lambda)}{d\tau_\lambda} \\ K_\lambda(\tau_\lambda) &= \frac{1}{3} S_\lambda(\tau_\lambda) \end{aligned}} \tag{10.14}$$

10.1.3 Two-Stream Formalism

Eddington introduced a two-stream approximation, in which the specific intensity is separated into a outward stream, $I_\lambda^{\rm out}(\tau_\lambda,\theta)$, and an inward stream, $I_\lambda^{\rm in}(\tau_\lambda,\theta)$. To obtain $I_\lambda^{\rm out}(\tau_\lambda,\theta)$, we set $\tau_\lambda' = \infty$ corresponding to $0 \le \theta \le \pi/2$, which enforces $w > 0$. To obtain $I_\lambda^{\rm in}(\tau_\lambda,\theta)$, we set $\tau_\lambda = 0$ and $\tau_\lambda' = \tau_\lambda$, corresponding to $\pi/2 \le \theta \le \pi$, which enforces $w < 0$. We must thus define $w = -\sec\theta$ for $I_\lambda^{\rm in}(\tau_\lambda,\theta)$. That is

$$I_\lambda(\tau_\lambda,\theta) = \begin{cases} I_\lambda^{\rm out}(\tau_\lambda,\theta) & 0 \le \theta \le \pi/2\,, \quad w = +\sec\theta\,, \quad (\tau_\lambda,\infty) \\ I_\lambda^{\rm in}(\tau_\lambda,\theta) & \pi/2 \le \theta \le \pi\,, \quad w = -\sec\theta\,, \quad (0,\tau_\lambda) \end{cases} \tag{10.15}$$

Application to Eq. 10.6 yields

$$\boxed{\begin{aligned} I_\lambda^{\rm out}(\tau_\lambda,\theta) &= \int_{\tau_\lambda}^{\infty} S_\lambda(t_\lambda) \exp\left\{-w\left(t_\lambda - \tau_\lambda\right)\right\} w\, dt_\lambda \qquad (w>0) \\ I_\lambda^{\rm in}(\tau_\lambda,\theta) &= \int_0^{\tau_\lambda} S_\lambda(t_\lambda) \exp\left\{-w\left(t_\lambda - \tau_\lambda\right)\right\} (-w)\, dt_\lambda \qquad (w<0) \end{aligned}} \tag{10.16}$$

Note that $t_\lambda - \tau_\lambda < 0$ for $I_\lambda^{\rm in}(\tau_\lambda, \theta)$, which might lead one to infer exponential growth of $S_\lambda(t_\lambda)$. However, because $w < 0$ for $I_\lambda^{\rm in}(\tau_\lambda, \theta)$, the argument of the exponent is negative. Note that the emergent specific intensity observed at angle θ from the surface normal is

$$I_\lambda(0,\theta) = \int_0^\infty S_\lambda(t_\lambda) \exp\left\{-w\left(t_\lambda - \tau_\lambda\right)\right\} w\, dt_\lambda \qquad (w > 0) \tag{10.17}$$

In the two-stream approximation, the mean intensity

$$J_\lambda(\tau_\lambda) = \frac{1}{4\pi} \oint I_\lambda(\tau_\lambda, \theta)\, d\Omega = \frac{1}{4\pi} \int_0^{2\pi} \int_0^\pi I_\lambda(\tau_\lambda, \theta) \sin\theta\, d\theta\, d\phi\,, \tag{10.18}$$

is written

$$J_\lambda(\tau_\lambda) = J_\lambda^{\rm out}(\tau_\lambda) + J_\lambda^{\rm in}(\tau_\lambda)\,. \tag{10.19}$$

For the outward steam of the specific intensity, we have

$$\begin{aligned} J_\lambda^{\rm out}(\tau_\lambda) &= \frac{1}{4\pi} \int_0^{2\pi} \int_0^{\pi/2} I_\lambda^{\rm out}(\tau_\lambda, \theta) \sin\theta\, d\theta\, d\phi \\ &= \frac{1}{2} \int_0^{\pi/2} I_\lambda^{\rm out}(\tau_\lambda, \theta) \sin\theta\, d\theta \\ &= \frac{1}{2} \int_1^\infty I_\lambda^{\rm out}(\tau_\lambda, w) \frac{dw}{w^2} \qquad (w > 0) \end{aligned} \tag{10.20}$$

where the last step follows from $w = +\sec\theta$, from which $dw = \sec\theta \tan\theta d\theta = w^2 \sin\theta d\theta$ yields $\sin\theta d\theta = dw/w^2$. For the limits, when $\theta = 0$ we have $w = 1$ and when $\theta = \pi/2$ we have $w = \infty$. Substituting $I_\lambda^{\rm out}(\tau_\lambda, \theta)$ yields

$$J_\lambda^{\rm out}(\tau_\lambda) = \frac{1}{2} \int_{\tau_\lambda}^\infty S_\lambda(t_\lambda) \left[\int_1^\infty \exp\left\{-w\left(\tau_\lambda - t_\lambda\right)\right\} \frac{dw}{w}\right] dt_\lambda \tag{10.21}$$

At each t_λ, we integrate over all w (polar angles from $0 \to \pi/2$). The integral over w is the exponential integral

$$E_n(x) = \int_1^\infty \exp\{-wx\} \frac{dw}{w^n}\,, \tag{10.22}$$

where n is the order. For the mean intensity, $n = 1$. Similarly, applying the substitution $w = -\sec\theta$ (polar angles from $\pi/2 \to \pi$), we obtain,

$$J_\lambda^{\rm in}(\tau_\lambda) = \frac{1}{2} \int_0^{\tau_\lambda} S_\lambda(t_\lambda) \left[\int_1^\infty \exp\left\{-w\left(t_\lambda - \tau_\lambda\right)\right\} \frac{dw}{w}\right] dt_\lambda \tag{10.23}$$

Note that $x = \tau_\lambda - t_\lambda$ for the outward stream ($w > 0$) and $x = t_\lambda - \tau_\lambda$ for the inward stream ($w < 0$). In compact notation,

$$\boxed{\begin{aligned} J_\lambda^{\rm out}(\tau_\lambda) &= \frac{1}{2} \int_{\tau_\lambda}^\infty S_\lambda(t_\lambda) E_1\left(t_\lambda - \tau_\lambda\right) dt_\lambda \\ J_\lambda^{\rm in}(\tau_\lambda) &= \frac{1}{2} \int_0^{\tau_\lambda} S_\lambda(t_\lambda) E_1\left(\tau_\lambda - t_\lambda\right) dt_\lambda \end{aligned}} \tag{10.24}$$

Similar arguments for the Eddington flux

$$H_\lambda(\tau_\lambda) = \frac{1}{4\pi} \oint I_\lambda(\tau_\lambda, \theta) \cos\theta \, d\Omega = \frac{1}{4\pi} \int_0^{2\pi} \int_0^{\pi} I_\lambda(\tau_\lambda, \theta) \frac{\sin\theta}{w} \, d\theta \, d\phi \,, \quad (10.25)$$

and for the mean momentum

$$K_\lambda(\tau_\lambda) = \frac{1}{4\pi} \oint I_\lambda(\tau_\lambda, \theta) \cos^2\theta \, d\Omega = \frac{1}{4\pi} \int_0^{2\pi} \int_0^{\pi} I_\lambda(\tau_\lambda, \theta) \frac{\sin\theta}{w^2} \, d\theta \, d\phi \,, \quad (10.26)$$

yield

$$\boxed{\begin{aligned} H_\lambda^{\rm out}(\tau_\lambda) &= \frac{1}{2} \int_{\tau_\lambda}^{\infty} S_\lambda(t_\lambda) E_2\left(t_\lambda - \tau_\lambda\right) dt_\lambda \\ H_\lambda^{\rm in}(\tau_\lambda) &= \frac{1}{2} \int_0^{\tau_\lambda} S_\lambda(t_\lambda) E_2\left(\tau_\lambda - t_\lambda\right) dt_\lambda \end{aligned}} \quad (10.27)$$

and

$$\boxed{\begin{aligned} K_\lambda^{\rm out}(\tau_\lambda) &= \frac{1}{2} \int_{\tau_\lambda}^{\infty} S_\lambda(t_\lambda) E_3\left(t_\lambda - \tau_\lambda\right) dt_\lambda \\ K_\lambda^{\rm in}(\tau_\lambda) &= \frac{1}{2} \int_0^{\tau_\lambda} S_\lambda(t_\lambda) E_3\left(\tau_\lambda - t_\lambda\right) dt_\lambda \end{aligned}} \quad (10.28)$$

Equations 10.24, 10.27, and 10.28 are known as the Schwarzschild-Milne equations, which are homogeneous Volterra integral equations of the first ($n = 1$) and second kind ($n > 1$). The kernals of the Volterra integral equations are various orders, n, of the exponential integral, $E_n(x)$.

10.1.3.1 Exponential Integrals

Exponential integrals obey the recursion relation

$$E_{n+1}(x) = \frac{1}{n} \left[e^x - x E_n(x)\right] \quad (10.29)$$

A computationally expedient polynomial approximation for $E_1(x)$, accurate to an error less than 2×10^{-7}, has been tabulated by Abromowitz & Stegun (1964),

$$E_1(x \leq 1) = -\ln(x) + \sum_{m=0}^{5} a_m x^m \,, \quad E_1(x > 1) = \frac{1}{x e^x} \left\{ \frac{\sum_{m=0}^{4} b_m x^m}{\sum_{m=0}^{4} c_m x^m} \right\} . \quad (10.30)$$

The polynomial coefficients are listed in Table 10.1.

Table 10.1: Coefficients for $E_1(x)$

m	a_m	b_m	c_m
0	−0.57721566	0.2677737343	3.9584969228
1	+0.99999193	8.6347608952	21.0996530827
2	−0.24991055	18.0590169730	25.6329561486
3	+0.05519968	8.5733287401	9.5733223454
4	−0.00976004	1.0000000000	1.0000000000
5	+0.00107857	⋯	⋯

10.2 Isotropic Two-Stream Approximation

$$\begin{aligned} J_\lambda(\tau_\lambda) &= \frac{1}{4\pi}\oint I_\lambda(\tau_\lambda)\,d\Omega \\ &= \frac{1}{2}\left[\int_0^{\pi/2} I_\lambda^{\rm out}(\tau_\lambda)\sin\theta\,d\theta + \int_{\pi/2}^{\pi} I_\lambda^{\rm in}(\tau_\lambda)\sin\theta\,d\theta\right] \\ &= \frac{1}{2}I_\lambda^{\rm out}(\tau_\lambda)\Big[-\cos\theta\Big]_0^{\pi/2} + \frac{1}{2}I_\lambda^{\rm in}(\tau_\lambda)\Big[-\cos\theta\Big]_{\pi/2}^{\pi} \\ &= \frac{1}{2}\left[I_\lambda^{\rm out}(\tau_\lambda) + I_\lambda^{\rm in}(\tau_\lambda)\right] \end{aligned} \tag{10.31}$$

$$\begin{aligned} H_\lambda(\tau_\lambda) &= \frac{1}{4\pi}\oint I_\lambda(\tau_\lambda)\cos\theta\,d\Omega \\ &= \frac{1}{2}\left[\int_0^{\pi/2} I_\lambda^{\rm out}(\tau_\lambda)\cos\theta\sin\theta\,d\theta + \int_{\pi/2}^{\pi} I_\lambda^{\rm in}(\tau_\lambda)\cos\theta\sin\theta\,d\theta\right] \\ &= \frac{1}{2}I_\lambda^{\rm out}(\tau_\lambda)\left[\frac{1}{2}\sin^2\theta\right]_0^{\pi/2} + \frac{1}{2}I_\lambda^{\rm in}(\tau_\lambda)\left[\frac{1}{2}\sin^2\theta\right]_{\pi/2}^{\pi} \\ &= \frac{1}{4}\left[I_\lambda^{\rm out}(\tau_\lambda) - I_\lambda^{\rm in}(\tau_\lambda)\right] \end{aligned} \tag{10.32}$$

$$\begin{aligned} K_\lambda(\tau_\lambda) &= \frac{1}{4\pi}\oint I_\lambda(\tau_\lambda)\cos^2\theta\, d\Omega \\ &= \frac{1}{2}\left[\int_0^{\pi/2} I_\lambda^{\rm out}(\tau_\lambda)\cos^2\theta\sin\theta\, d\theta + \int_{\pi/2}^{\pi} I_\lambda^{\rm in}(\tau_\lambda)\cos^2\theta\sin\theta\, d\theta\right] \\ &= \frac{1}{2}I_\lambda^{\rm out}(\tau_\lambda)\left[-\frac{1}{3}\cos^3\theta\right]_0^{\pi/2} + \frac{1}{2}I_\lambda^{\rm in}(\tau_\lambda)\left[-\frac{1}{3}\cos^3\theta\right]_{\pi/2}^{\pi} \\ &= \frac{1}{6}\left[I_\lambda^{\rm out}(\tau_\lambda) + I_\lambda^{\rm in}(\tau_\lambda)\right] \end{aligned} \tag{10.33}$$

$$\boxed{\begin{aligned} J_\lambda(\tau_\lambda) &= \frac{1}{2}\left[I_\lambda^{\rm out}(\tau_\lambda) + I_\lambda^{\rm in}(\tau_\lambda)\right] \\ H_\lambda(\tau_\lambda) &= \frac{1}{4}\left[I_\lambda^{\rm out}(\tau_\lambda) - I_\lambda^{\rm in}(\tau_\lambda)\right] \\ K_\lambda(\tau_\lambda) &= \frac{1}{6}\left[I_\lambda^{\rm out}(\tau_\lambda) + I_\lambda^{\rm in}(\tau_\lambda)\right] \end{aligned}} \tag{10.34}$$

from which we obtain the Eddington relation

$$\boxed{K_\lambda(\tau_\lambda) = \frac{1}{3}J_\lambda(\tau_\lambda)} \tag{10.35}$$

10.3 Moments of the Transfer Equation

Recapping, where $d\tau_\lambda = \chi_\lambda dr$ and $w = \sec\theta$,

$$\boxed{\begin{aligned} \frac{1}{w}\frac{dI_\lambda(\tau_\lambda)}{d\tau_\lambda} &= I_\lambda(\tau_\lambda) - S_\lambda(\tau_\lambda) \\ \frac{dH_\lambda(\tau_\lambda)}{d\tau_\lambda} &= J_\lambda(\tau_\lambda) - S_\lambda(\tau_\lambda) \\ \frac{dK_\lambda(\tau_\lambda)}{d\tau_\lambda} &= H_\lambda(\tau_\lambda) \end{aligned}} \tag{10.36}$$

In strict thermal equilibrium with no scattering, $J_\lambda(\tau_\lambda) = S_\lambda(\tau_\lambda)$, which yields

$$\frac{dH_\lambda(\tau_\lambda)}{d\tau_\lambda} = 0\,. \tag{10.37}$$

That is, there is no flux gradient under the assumption of thermal equilibrium. This has important consequences.

10.4 Grey Approximation

We assume that the opacity is independent of wavelength. In so doing we replace the opacity with an average value, $\bar{\chi}$, (to be discussed below). Under this assumption optical depth is wavelength independent and there is a one-to-one mapping between intervals in optical depth and physical depth, i.e., $d\tau = \bar{\chi} dr$.

Integrating the specific intensity, source function, and higher moments over all wavelengths, we define

$$I(\tau) = \int_0^\infty I_\lambda(\tau) d\lambda \tag{10.38}$$

$$S(\tau) = \int_0^\infty S_\lambda(\tau) d\lambda \tag{10.39}$$

$$J(\tau) = \int_0^\infty J_\lambda(\tau) d\lambda \tag{10.40}$$

$$K(\tau) = \int_0^\infty K_\lambda(\tau) d\lambda \tag{10.41}$$

The grey transfer equation is then obtained via integration over all wavelenghts,

$$\frac{1}{w} \int_0^\infty \frac{dI_\lambda(\tau)}{d\tau} d\lambda = \int_0^\infty \left[I_\lambda(\tau) - S_\lambda(\tau) \right] d\lambda \tag{10.42}$$

$$\frac{d}{w\, d\tau} \int_0^\infty I_\lambda(\tau) d\lambda = \int_0^\infty I_\lambda(\tau) d\lambda - \int_0^\infty S_\lambda(\tau) d\lambda \tag{10.43}$$

yielding,

$$\frac{1}{w} \frac{dI(\tau)}{d\tau} = I(\tau) - S(\tau) \tag{10.44}$$

Similarly, for the first moment, we obtain

$$\frac{d}{d\tau} \int_0^\infty H_\lambda(\tau) d\lambda = \int_0^\infty \left[J_\lambda(\tau) - S_\lambda(\tau) \right] d\lambda \tag{10.45}$$

yielding,

$$\frac{dH(\tau)}{d\tau} = J(\tau) - S(\tau) \tag{10.46}$$

In strict thermal equilibrium with no scattering, $J(\tau) = S(\tau)$, which yields

$$\frac{dH(\tau)}{d\tau} = 0\,. \tag{10.47}$$

That is, there is no flux gradient under the assumption of thermal equilibrium. This has important consequences. For the second momemt, we obtain,

$$\frac{d}{d\tau} \int_0^\infty K_\lambda(\tau) d\lambda = \int_0^\infty H_\lambda(\tau) d\lambda \tag{10.48}$$

which yields,

$$\frac{dK(\tau)}{d\tau} = H(\tau) \tag{10.49}$$

Recapping, in equilibrium, we have

$$\boxed{\begin{aligned} \frac{1}{w}\frac{dI(\tau)}{d\tau} &= I(\tau) - S(\tau) \\ \frac{dH(\tau)}{d\tau} &= 0 \\ \frac{dK(\tau)}{d\tau} &= H(\tau) \end{aligned}} \tag{10.50}$$

From the two-stream approximation, we recover

$$\boxed{\begin{aligned} J(\tau) &= \frac{1}{2}\left[I^{\text{out}}(\tau) + I^{\text{in}}(\tau)\right] \\ H(\tau) &= \frac{1}{4}\left[I^{\text{out}}(\tau) - I^{\text{in}}(\tau)\right] \\ K(\tau) &= \frac{1}{6}\left[I^{\text{out}}(\tau) + I^{\text{in}}(\tau)\right] \\ K(\tau) &= \frac{1}{3}J(\tau) \end{aligned}} \tag{10.51}$$

with $\tau = 0$ "surface" boundary condition $J(0) = \frac{1}{2}I^{\text{out}}(0)$, $H(0) = \frac{1}{4}I^{\text{out}}(0)$, and $K(0) = \frac{1}{6}I^{\text{out}}(0)$, with

$$I^{\text{out}}(0) = \int_0^\infty S_\lambda(t_\lambda)\exp\{-wt_\lambda\}\,w\,dt_\lambda \tag{10.52}$$

with $w = \sec\theta$.

Integrating $dH(\tau)/d\tau = 0$, we obtain H is a constant, independent of optical depth. Integrating $dK(\tau)/d\tau = H$, we obtain

$$K(\tau) = H\tau + C\,. \tag{10.53}$$

To obtain the constant we invloke the $\tau = 0$ "surface" boundary condition $K(0) = \frac{1}{3}J(0)$, yielding $C = \frac{1}{3}J(0)$. From $J(0) = \frac{1}{2}I^{\text{out}}(0)$ and $H = \frac{1}{4}I^{\text{out}}(0)$, we obtain $J(0) = 2H$, yielding $C = \frac{2}{3}H$,

$$K(\tau) = H\left\{\tau + \frac{2}{3}\right\}\,. \tag{10.54}$$

Since $J(\tau) = 3K(\tau)$, we have

$$J(\tau) = H\left\{2 + 3\tau\right\}\,. \tag{10.55}$$

We can now obtain expressions for the specific intensities $I^{\rm out}(\tau)$ and $I^{\rm in}(\tau)$. The sum of

$$\begin{aligned} 2J^{\rm out}(\tau) &= I^{\rm out}(\tau) + I^{\rm in}(\tau) \\ 4H &= I^{\rm out}(\tau) - I^{\rm in}(\tau) \end{aligned} \tag{10.56}$$

yeilds $2I^{\rm out}(\tau)$ and the difference yields $2I^{\rm in}(\tau)$. Substituting Eq. 10.55 for $J(\tau)$, we obtain

$$\boxed{\begin{aligned} I^{\rm out}(\tau) &= H\,(4+3\tau) \\ I^{\rm in}(\tau) &= 3H\tau \end{aligned}} \tag{10.57}$$

Assuming a blackbody source function in thermal equilibrium, and recognizing that $H = F(\tau)/4\pi$, the Eddington flux is independent of τ, we have $H = F(0)/4\pi$, where $F(0) = \sigma T_*^4$, yielding

$$H = \frac{\sigma T_*^4}{4\pi}\,. \tag{10.58}$$

where T_* is the measured temperature of the star (a quantity which we define more precisely below). From Eq. 10.55, we have

$$J(\tau) = H\,\{2+3\tau\} = \frac{\sigma T_*^4}{4\pi}\,\{2+3\tau\}\ . \tag{10.59}$$

In thermal equilibrium with no scattering, we have shown that

$$J(\tau) = S(\tau) = B[T(\tau)] = \frac{\sigma T^4(\tau)}{\pi}\,. \tag{10.60}$$

Substituting for $J(\tau)$, we obtain

$$\frac{\sigma T^4(\tau)}{\pi} = \frac{\sigma T_*^4}{4\pi}\,\{2+3\tau\}\ , \tag{10.61}$$

which simplifies to

$$T^4(\tau) = \frac{3}{4}T_*^4\left\{\tau + \frac{2}{3}\right\}\ . \tag{10.62}$$

Note that at $\tau = 2/3$, we obtain $T(2/3) = T_*$. We now define the temperature at $\tau = 2/3$ is the "effective temperature", $T_{\rm eff}$, and write

$$\boxed{T^4(\tau) = \frac{3}{4}T_{\rm eff}^4\left\{\tau + \frac{2}{3}\right\}\ .} \tag{10.63}$$

Hopf function, $q(\tau)$,

$$q(\tau) = q(\infty) - \frac{1}{2\sqrt{3}}\int_0^{\pi/2}\frac{\exp\{-\tau\sec\theta\}}{f(\theta)g(\theta)}\sin\theta\,d\theta \tag{10.64}$$

where

$$\begin{aligned} q(\infty) &= \frac{6}{\pi^2} + Q \\ g(\theta) &= \left[1 - \frac{\cos\theta}{2} \ln\left\{\frac{1+\cos\theta}{1-\cos\theta}\right\}\right] + \frac{\pi^2 \cos^2\theta}{4} \\ f(\theta) &= \frac{\exp\{T\}}{(1+\cos\theta)^{1/2}} \end{aligned} \tag{10.65}$$

where

$$\begin{aligned} Q &= \frac{1}{\pi}\int_0^{\pi/2} \left[\frac{3}{\theta^2} - \frac{1}{1-\theta\cot\theta}\right] d\theta \\ T &= \frac{1}{\pi}\int_0^{\pi/2} \frac{\theta \tan^{-1}(\cos\theta\tan\theta)}{1-\theta\cot\theta} d\theta \end{aligned} \tag{10.66}$$

Table 10.2: The Hopf Function $q(\tau)$

τ	$q(\tau)$	τ	$q(\tau)$
0.00	0.577351	0.8	0.693534
0.01	0.588236	1.0	0.698540
0.03	0.601242	1.5	0.705130
0.05	0.610758	2.0	0.707916
0.10	0.627919	2.5	0.709191
0.20	0.649550	3.0	0.709806
0.30	0.663365	3.5	0.710120
0.40	0.673090	4.0	0.710270
0.50	0.680240	5.0	0.710398
0.60	0.685801	∞	0.710446

10.5 Mean Opacity

10.5.1 Flux Weighted Mean

$$-\frac{dK}{dz} = \bar{\chi}H = \int_0^\infty \chi_\lambda H_\lambda d\lambda \tag{10.67}$$

yielding

$$\bar{\chi} = \frac{1}{H}\int_0^\infty \chi_\lambda H_\lambda d\lambda \tag{10.68}$$

This form recovers the K integral, leading to correct values of radiation pressure and radiation forces. Thus, practicle for hot (early-type) stars. However, it does not transform for $dH/dz = 0$. The flux weighted require a priori knowledge of

H_λ, so that $\bar{\chi}$ cannot be solved until after the transfer equation is solved (which would require an iterative scheme).

10.5.2 The Rosseland Mean

$$\frac{1}{\chi_\lambda}\frac{dK_\lambda}{dz} = -H_\lambda \tag{10.69}$$

We have

$$-\int_0^\infty \frac{1}{\chi_\lambda}\frac{dK_\lambda}{dz}d\lambda = \int_0^\infty H_\lambda d\lambda \tag{10.70}$$

$$\frac{1}{\bar{\chi}} = \frac{\displaystyle\int_0^\infty \frac{1}{\chi_\lambda}\frac{dK_\lambda}{dz}d\lambda}{\displaystyle\int_0^\infty \frac{dK_\lambda}{dz}d\lambda} \tag{10.71}$$

From $K_\lambda = J_\lambda/3$, and in equilibrium $J_\lambda = S_\lambda = B_\lambda$, we obtain

$$\frac{dK_\lambda}{dz} = \frac{1}{3}\frac{dB_\lambda}{dz} = \frac{1}{3}\frac{dB_\lambda}{dT}\frac{dT}{dz} \tag{10.72}$$

yields

$$\bar{\chi}^{-1} = \frac{\displaystyle\int_0^\infty \frac{1}{\chi_\lambda}\frac{dB_\lambda}{dz}d\lambda}{\displaystyle\int_0^\infty \frac{dB_\lambda}{dz}d\lambda} \tag{10.73}$$

where the temperature gradient $\frac{1}{3}dT/dz$ pulls out of the integrals and cancels. From

$$\int_0^\infty \frac{dB_\lambda}{dz}d\lambda = \frac{4\sigma T^3}{\pi} \tag{10.74}$$

we obtain

$$\bar{\chi}^{-1} = \frac{\pi}{4\sigma T^3}\int_0^\infty \frac{1}{\chi_\lambda}\frac{dB_\lambda}{dz}d\lambda \tag{10.75}$$

The Rossland mean provides the highest weight where χ_λ is smallest, which is where radiation transport dominates. However, like the flux weighted mean, it does not transform $dH/dz = 0$, so it is not a self-consistent solution to the Grey problem.

Chapter 11

Continuum Cross Sections

11.1 Recapping Continuous absorption cross sections

11.1.1 Hydrogen

$\alpha^{bf}_{HI}(\lambda)$= bound-free neutral hydrogen (summer over all excitation states) (Boltzman) [cm^2 per neutral hydrogen]
Characterized by $\sim \lambda^3$ between series edges 911.5, 3646, 8203.6, 14084Å, etc and a "saw-tooth" shape due to series edges.

$\alpha^{ff}_{HI}(\lambda)$ = free-free neutral hyrdogen (averaged over velocities of electron pool) [cm^2 per neutral hydrogen]
Characterized by proportinally $\eta_e \lambda^3 T^{-1/2}$; most important in IR

$\alpha^{bf}_{H-}(\lambda)$ = bound-free H$^-$ion [cm^2 per H$^-$ion]
To convert to per neutral hydrogen, multiply by $\frac{\eta_{H-}}{\eta_{HI}}$ (Saha ratio)
Charaterized by rise from 1000–8500 Å, peaking at $\sim$ 8800 Å , then declining to the ionization edge at 16,421 Å; dominant opacity in cool stars; sensitive to metalicity; reduces Balmer decrement.

$\alpha^{ff}_{H-}(\lambda)$ = free-free H$^-$ion [cm^2 per HI atom!]
note: cross section already in units of per HI atom
Characterized by proportionality $\eta_e T \lambda$; most important in IR; it becomes dominant H$^-$ opacity for $\lambda \geq 16,000$ Å.

11.1.2 Helium

$\alpha^{bf}_{HeI}(\lambda)$ = bound-free neutral helium [cm^2 per HeI atom] (Boltzman, summed over n$\leq$ 3) to convert tp [er neutral hydrogen, multiply by $\frac{\eta_{HeII}}{\eta_{HI}}$
(abundance + saha)

Characterized by λ^3 proportionality betweeb series edges (like neutral hydrogen) edges at 504,629,7932,14380 Å etc.

$\alpha^{ff}_{HeI}(\lambda)$ = free-free neutral helium [cm^2 per HeI atom] to convert to per neutral hydrogen, multiply by $\frac{\eta_{HeI}}{\eta_{HI}}$ (abundance + saha)
Characterized by $\eta_e\lambda^3 T^{-1/2}$; behaves like $\alpha^{ff}_{HI}(\lambda)$ scaled by quantum defect factor.

$\alpha^{bf}_{HeII}(\lambda), \alpha^{ff}_{HeII}(\lambda)$ = bound-free and free-free HeII [cm^2 per HeII ion] to convert to per neutral hydrogen, multiply by $\frac{\eta_{HeII}}{\eta_{HI}}$ (abundance + Saha)
Both characterized by behavior identical to $\alpha^{bf}_{HI}(\lambda)$ and $\alpha^{ff}_{HI}(\lambda)$, respectively but scaled by $\mathrm{Z}^2_{He}(\frac{N_{He}}{N_H})$ for f-f and by $\mathrm{Z}^4_{He}(\frac{N_{He}}{N_H})$ for b-f.

$\alpha^{ff}_{He^-}(\lambda)$ = free-free He$^-$ ion [cm^2 per He$^-$ ion] to convert to per neutral hydrogen, multiply by $\frac{\eta_{He^-}}{\eta_{HI}}$ (abundance + saha)
Charaterized by $\eta_e\lambda$T proportionslity; important only in cool stars in IR
$*$ No closed form solution; polynomial fit <u>includes</u> stimulated emission factor.

$\alpha^{bf}_{He^-}(\lambda)$ = bound-free He$^-$ ion (NEGLIGIBLE)

11.1.3

The absorption coefficient is defined as
$\begin{cases} for\ a\ given\ continous\ process \\ for\ a\ given\ absorber,\ denoted\ i \end{cases}$

$K_\lambda = n_i\alpha_i(\lambda) \qquad [\mathrm{cm}^{-1}]$
where as n_i is the number density of absorber [cm^{-3}]

The mass absorption coefficient is defined as
$\mathrm{K}'_\lambda = \frac{n_i}{\rho_i}\alpha_i(\lambda) = \frac{x_i}{A_i m_{amu}}\alpha_i(\lambda) \qquad [\mathrm{cm}^2\mathrm{g}^{-1}]$

where as ρ_i is the mass density of absorber and x_i is the mass fraction of absorber and A_i is the atomic "weight" of absorber

The scattering coefficient is defined as
$\sigma^e_\lambda = n_e\sigma_e$ Thompson scattering [cm^{-1}]
$\sigma^R_\lambda = n_i\sigma_R(\lambda)$ Reyleigh Scattering {for a given absorber i} [cm^{-1}]

or mass scattering coefficient
$\sigma^e_\lambda = \frac{n_e}{\rho_e}\sigma_e = \frac{x_e}{m_e}\sigma_e$ Thompson scattering [cm^{2}g^{-1}]
$\sigma^R_\lambda = \frac{n_i}{\rho_i}\sigma_R(\lambda) = \frac{x_i}{A_i m_{amu}}\sigma_R(\lambda)$ Reyleigh scattering [cm^{2}g^{-1}]

11.2 Total Continous Absorption Cross Section and Opacity

The total opacity is X_λ=(1-$e^{-\frac{hc}{\lambda KT}}$)$\sum_{i=1} K_i + \sigma_\lambda^e + \sum_{i=1} \sigma_\lambda^R$
optical depth at λ_1

$$\boxed{\tau_\lambda = \int X_\lambda ds}$$

(1-e$^{\frac{hc}{\lambda KT}}$) = stimulated emission factor; applies to all non-scattering processes.

$\sum_{i=1} K_i$ = sum over all continuous absorption processes $\imath$

σ_λ^e = electron scattering (λ independent)

$\sum_{i=1} \sigma_\lambda^R$ = sum over all Rayleigh scatters

for mass opacity $X_\lambda^{'}$ $\boxed{n_i \rightarrow \frac{n_i}{\rho} = \frac{x_i}{A_i m_{amv}}}$

$\tau(\lambda) = \int X_\lambda^{'} \rho ds$

example:

$$\boxed{\begin{array}{l}\sum_{i=1} k_i = \sum_{i=1} n_i \alpha_i(\lambda) = n_{HI}\alpha_{HI}^{bf}(\lambda) + n_{HI}\alpha_{HI}^{ff}(\lambda) + n_{H^-}\alpha_{H^-}^{bf}(\lambda) + \\ n_{HI}\alpha_{HI}^{ff}(\lambda) + n_{H_eI}\alpha_{H_eI}^{bf}(\lambda) + n_{H_eI}\alpha_{H_eI}^{ff}(\lambda) + \\ n_{H_eII}\alpha_{H_eII}^{bf}(\lambda) + n_{H_eII}\alpha_{H_eII}^{ff}(\lambda) + [1 - e^{\frac{-hc}{\lambda kT}}]^{-1} n_{H_e^-}(\lambda) + \cdots metals\end{array}}$$

recall $\alpha_{H_e^-}^{ff}(\lambda)$ already includes stimulated emission factor.
similar example for Reyleigh scattering

NOTE: each density must be solved for using Saha, which requires n_e and T!

In terms of neutral hydrogen...

$$\boxed{\sum_{i=1} K_i = n_{HI} \sum \frac{n_i}{n_{HI}} \alpha_i(\lambda)}$$

for example:

$$\frac{n_{HeI}}{n_{HI}} = 10^{(A^2_{He-12})}[1+n_e^{-1}\Phi_{HI}(T)][1+n_e^{-1}\Phi_{HeI}(T)+n_e^{-2}\Phi_{HeII}(T)\Phi_{HeI}(T)]^{-1} \tag{11.1}$$

$\rightarrow$ Where we have shown how this ratio $\frac{n_L}{n_{HI}}$ can be written for each (see ex. above)
respective continuous absorption process. [ALWAYS REMEMBER He^- f,f in-

cludes the stimulated emission factor]!∗

11.3 Continuous Absorption in Stellar Atmospheres

metals dominate in the UV for
$\lambda < 2500\mathring{A}$

here, "per H atom" means per neutral hydrogen atom not total H.

11.4 Continuous Absorption bound-free hydrogenic atoms

Kramers' (semi-classical)

$$\boxed{\alpha_n^{bf}(\nu) = \frac{2^4}{3\sqrt{3}}\frac{e^2}{m_e c}\frac{R^2}{h^2}\frac{1}{n^6\nu^3}g_{II}(n) \quad \alpha_n^{bf}(\lambda) = \frac{2^4}{3\sqrt{3}}\frac{e^2}{m_e c^4}\frac{R^2}{h^2}\frac{\lambda}{n^5}g_{II}(n)} \tag{11.2}$$

units of α are cm^2. [cm^2 per neutral hydrogenic atom in excitation level n.]

where g_{II} in $\alpha_n^{bf}(\nu)$is a bound-free Gaunt Factor(accounts for quantum - wave mechanics correction) and g_{II} in α_n^{bf} is approximately unity

where N is the reduced electron mass

$R = Z^2(\frac{N}{me})R_\infty \Rightarrow$ Rydbergs' constant $\qquad R_\infty = \frac{m_e e^4}{2h^2} = \frac{2\pi^2 e^4 m_e}{h^2}$

$g_{II}(n) = 1\text{-}[\frac{\frac{121}{700}(1-\epsilon_n^2)}{n^{\frac{2}{3}}(1+\epsilon_n^2)^{\frac{2}{3}}}] \qquad \epsilon_n = \frac{\nu}{\nu_n} - 1 = \frac{\lambda_n}{\lambda} - 1$

where ϵ_n is the fractional measure of energy of ejected electron (now in a continum state), ν_n and λ_n are the cutoff energies

$\nu_n = \frac{R}{hn^2} \qquad \lambda_n = \frac{n^2 hc}{R}$

$\{\alpha_n^{bf}(\nu) = 0 \quad \nu < \nu_n \qquad \alpha_n^{bf}(\lambda) = 0 \quad \lambda < \lambda_n\}$

numerical versions (accounting for nuclear charge + mass of hydrogenic atom)

$\alpha_n^{bf}(\nu) = A_o\frac{g_{II}(n)}{n^5\nu^3} \qquad A_o = 2.8154 \times 10^{29} Z^4(\frac{N}{m_e})^2 \qquad [cm^2 H_z^3]$

$\alpha_n^{bf}(\lambda) = A_o'\frac{\lambda^3}{n^5}g_{II}(n) \qquad A_o' = 1.0449 \times 10^{-26} Z^4(\frac{N}{m_e})^2 \qquad [cm^2\mathring{A}^{-3}]$

$\Big\{cm^2$ *per neutral H in excitation level n*

• Kromers' cross section (with Gaunt factor included) is more accurate for increasing ϵ_n (far from the ionization edge).

• The above Gaunt factor is the first term in an expansion formula.

Kramers 1923, Phil. mag. V46,p836

• Fully accurate cross-section (cm^2 per neutral H in excitation level n)

$$\boxed{\alpha_n^{bf} = A_o^{\text{“}} \frac{n^3 k^8 P_n(K)}{(k^2+n^2)^{2n+2}} \frac{exp\{4 - 4k\tan^{-1}(\frac{n}{k})\}}{1 - exp\{-2\pi k\}}} \tag{11.3}$$

where

$$k = n(\frac{\nu}{\nu_n} - 1)^{\frac{-1}{2}} = n(\frac{\lambda_n}{\lambda} - 1)^{\frac{-1}{2}} \tag{11.4}$$

note: $\frac{\nu}{\nu_n} = \frac{\lambda_n}{\lambda}$

$A_o^{''} = \frac{2^7}{3}\frac{\pi e^2 h}{m_e c R} exp\{-4\} = 6.304 \times 10^{-18} Z^{-2} (\frac{N}{m_e})^{-1}$ cm^2

and where P_n(k) for n=1,2,3,15
$P_1(k) = 1$
$P_2(k) = (3K^2 + 4)(5k^2 + 4)$
$P_3(k) = (13k^4 + 78k^2 + 81)(29k^4 + 126k^2 + 81)$
$\Big\{$*Polynomials* $P_n(k)$ *these polynomials and generating formula are given in Menzel & Pekeris* (1935, *MN*

ex. consider n = 1, we can obtain a ″fairly ″simple form:

$\frac{n^3 k^8 P_n(k)}{(k^2+n^2)^{2n+2}} \xrightarrow{(n=1)} \frac{(k^2)^4}{(k^2+1)^4} = (\frac{\nu_1}{\nu})^4$ $\nu_1 = \frac{R}{h}$ = ionization edge for n=1

we obtain

$$\boxed{\alpha_1^{bf}(\nu) = A_o^{''}(\frac{\nu_1}{\nu})^4 \frac{exp\{4-4(\frac{\nu}{\nu_1}-1)^{\frac{-1}{2}} \tan^{-1}[(\frac{\nu}{\nu_l}-1)^{\frac{1}{2}}]\}}{1-exp\{-2\pi(\frac{\nu}{\nu_l}-1)^{\frac{-1}{2}}\}}}$$

[cm^2 per ground state neutral H] n=1 ionization bound-free absorption cross section (lyman series edge)

- ionization from higher n levels (excited electrons) yield much more complex closed expressions, but they can be written out.

- for $\alpha_1^{bf}(\lambda)$, replace $\frac{\nu}{\nu_1}$ with $\frac{\lambda_1}{\lambda}$; the constant A_o'' is unaltered (change is unitless).

11.4.1 Comparison of hydrogenic bound-free absorption cross sections

• Kramers' formula overestimates α_n^{bf} near the ionization edges

• H_eII is hydrogenic (single electron); the cross section for H_eII is therefore expressed using the hydrogen cross section but with scaling $Z^4(\frac{N_{H_e}}{N_H})^2$ appropriate for helium. (see inset)
(appearing in constant A_o, N_{H_e} = reduced mass of electron in helium)

◯ $\alpha_{H_eII}^{bf}(\lambda) \approx 4\alpha_H^{bf}(\lambda)$

$\lambda_n(H_eII) \simeq \frac{1}{4}\lambda_n(H)$

11.4.2 TOTAL

We can account for number of hydrogens in n=1 (ground state) and in excited states n=2,3,4,etc. in order to get the opacity (bound-free absorption coefficient) j=0, k=1 (neutral hydrogen)

$$\boxed{\alpha_{HI}^{bf}(\lambda) = \sum_{i=1}^{\infty}(\frac{n_{i01}}{n_{01}})\alpha_i^{bf}(\lambda) = \sum_{i=1}^{\infty}\frac{g_{i01}}{\nu_{01}(T)}\ \alpha_i^{bf}(\lambda)exp\{-\frac{X_{i01}}{kT}\}}$$

cm^2 per neutal hydrogen see Grey p152 for approximations

$\frac{\eta_{i01}}{\eta_{01}}$ = Boltzman
$g_{i01} = g_n = 2n^2$
$\nu_{01}(T) \simeq 2$

• Starting with

$$\boxed{\alpha_{HI}^{bf}(\lambda) = \sum_{i=1}^{\infty}(\frac{n_{i01}}{n_{01}})\alpha_i^{bf}(\lambda) = \sum_{i=1}^{\infty}\frac{g_{i01}}{\nu_{01}(T)}\alpha_1^{bf}(\lambda)exp\{-\frac{X_{i01}}{kT}\}}$$

using Kramers' formula, we have
$\nu_{01}(T) = Z \quad X_{i01} = X_n$
$g_{i01} = g_n = 2n^2$
$\alpha_i^{bf}(\lambda) = A_o^{'}\frac{\lambda^3}{n^5}g_{II}(n)$
notation change from $\imath$ to n for hydrogen

and obtain

$$\boxed{\alpha_{HI}^{bf}(\lambda) = A_o^{'}\lambda^3 \sum_{i=1}^{\infty} \frac{g_{II}(n)}{n^3} exp\{-\frac{X_n}{kT}\}} \quad \text{(cm}^2 \text{ per neutral hydrogen atom)}$$

IMPORTANT

$$\begin{cases} recall\ that\ \ \alpha_n^{bf}(\lambda) = 0 \quad for \quad \lambda > \lambda_n \quad \lambda_n = \frac{n^2 hc}{R} \ \ i.e,\ for \lambda > \lambda_3 \ \ the \\ n = 1 \ \ n = 2, \ \ and \ \ n = 3 \ \ contributions\ are\ null. \end{cases}$$

• from this summation, note that the λ tails to the blue in higher order n contributions add to the curves and peaks of the lower order n cross sections. Thus, the sum must be carried out to large n even for the n that correspond to visible wavelengths (i.e, n=2).

• Employ a simplification developed by Unsold (1955) - recognize that from $X_n = R(1-\frac{1}{n^2})$ that $dX_n = 2R\frac{dn}{n^3}$ we see that $\exp\{-\frac{X_n}{kT}\}\frac{dn}{n^3} = \frac{1}{2R} exp\{-\frac{X_n}{kT}\} dx_n$

$$\boxed{NOTE: n = \infty \quad X_I = X_\infty = R \quad Thus,\ R\ can\ be\ replaced\ by\ X_I}$$

thus, for some n = m+1,

$$\boxed{\sum_{n=m+1}^{\infty} \frac{1}{n^3} exp\{-\frac{X_n}{kT}\} = \frac{1}{2R} \int_{X_{m+1}}^{X_I} exp\{-\frac{X}{kT}\} dX = \frac{kT}{2X_I}[exp\{-\frac{X_{m+1}}{kT}\} - exp\{-\frac{X_I}{kt}\}]}$$

We have

$$\boxed{\alpha_{HI}^{bf}(\lambda) = A_o^{'}\lambda^3 \{\sum_{n=1}^{m} \frac{g_{II}(n)}{n^3} exp\{-\frac{X_n}{kT}\} + \frac{kT}{2X_I}[exp\{-\frac{X_{m+1}}{kT}\} - exp\{-\frac{X_I}{kT}\}]\}}$$

cm^2 per netural hydrogen atom

$X_I = R \qquad X_{m+1} = R[1 - \frac{1}{(m+1)^2}]$

$m = n_o + a \qquad a$ = integer on order of few to several

$*$ because lower n cross sections do not contribute to higher n cross sections, if you are interested in wavelengths $\lambda > \lambda_3$ for example, then one begins the sum from n_o=4 and chooses in to be $m=n_n+a$. Where a is integer.

11.5 Continuous Absorption free-free hydrogenic atoms

• Menzel's (semi-classical)

$\alpha^{bf}_{k\ell}(\nu, v)dv = \frac{2}{3\pi\sqrt{3}} \frac{n_e h_e^2}{m_e^3 c} \frac{R}{\nu^3} \frac{dv}{v} g^{k\ell}_{III}(\nu, v)$
cross-section for absorption from electron free state ık to free state ıℓ

for an electron interacting with a photon of hν, where the electron is initially in unbound hyperbolic ″orbit ″ı ℓ with velocity in the interval $v \to v + dv$
several of the constants in α come from statisteal weight of the free electron
$g_e(v)dv = \frac{8\pi}{h^3} n_e^{-1} m_e^3 v^2 dv$

g_{III} func of ν,v $\begin{cases} k = [\frac{R}{h\nu + \frac{1}{2}mv^2}]^{\frac{1}{2}} \\ \ell = [\frac{R}{\frac{1}{2}mv^2}]^{\frac{1}{2}} \end{cases}$

in compact notation

$\alpha^{ff}_{k\ell}(\nu, v)dv = A_o^{'''} \frac{n_e}{\nu^3} \frac{dv}{v} g^{k\ell}_{III}(\nu, v) \qquad A_o^{'''} = 1.8016 \times 10^{14} Z^2 (\frac{N}{m_e})$

to obtain the cross section, we integrate over all electron velocities weighted by their distribution (Maxwellien, f(v))

$\alpha^{ff}_{k\ell}(\nu, T) = \int_0^\infty \alpha^{bf}_{H\ell}(\nu, v)\mathrm{f(v)dv} = 4\pi A_o^{'''} \frac{n_e}{\nu^3} (\frac{m_e}{2\pi KT})^{\frac{3}{2}} \int_0^\infty g^{k\ell}_{III}(\nu, v) exp\{-\frac{mev^2}{kT}\}\mathrm{vdv}$

[NOTE: not v^2]

let $x = \frac{1}{2} \frac{m_e v^2}{kT}$ then $vdv = (\frac{kT}{m_e})dx$

the integral becomes: Where ν is a function of x.

$\int_0^\infty g^{k\ell}_{III}(\nu, x) exp(-x) dx \equiv \bar{g}_{III}(\nu, T)$

which is known as the thermally average Gaunt factor

• thus we have

$$\boxed{\alpha^{ff}_{k\ell}(\nu, T) = A_o^{'''} \frac{n_e}{\nu^3} (\frac{2}{\pi} \frac{m_e}{kT})^{\frac{1}{2}} \bar{g}_{III}(\nu, T) = B_o \frac{n_e}{\nu^3} T^{\frac{-1}{2}} \bar{g}_{III}(\nu, T)}$$

cm^2 per netural hydrogen

the devil is in $\bar{g}_{III}(\nu, T)$! but it is of order unity.

$B_o = (\frac{2m_e}{\pi k})^{\frac{1}{2}} A_o^{'''} = 3.6923 \times 10^8 Z^2 (\frac{N}{m_e})$

$\rightarrow$ NOTE: to obtain $\alpha^{bf}_{k\ell}(\lambda, T)$ simply substitute $\nu = \frac{c}{\lambda}$; results in $\begin{cases} A^{\lambda}_{o} = \frac{A^{\nu}_{o}}{c^3} \\ B^{\lambda}_{o} = \frac{B^{\nu}_{o}}{c^3} \end{cases}$

• the thermally averaged Gaunt factor is complex, involving the evalvation of the hypergeometric function using complex numbers
- recall that the quantum mechanical treatment is involved to get the absorption coeffient, where the Gaunt factor is simply algebraically factored out from the semi-classic expression.

• diagram shows $\alpha^{bf}_{k\ell}(\lambda, T)$ and $\bar{g}_{III}(\lambda, T)$, where $\bar{g}_{III}$ is interpolated from the calculations by Sutherland (1998, MNRAS, 300, 321).
$*>$ in stellar photoshers $\bar{g}_{III} \approx 1 - 1.1$
$*>$ free-free absorption cross section is about 10^{-4} to 10^{-6} of bound-free

free-free absorption cross-sec $\leftarrow | \rightarrow$ Thermal Averaged Gaunt factor.

NOTE: hotter stars have smaller $\alpha^{bf}_{k\ell}(\lambda, T)$ - electrons moving faster on average yield smaller interaction cross section.

• for $\mathrm{H}_e II$, shape identical, normalization scales by $\mathrm{Z}^2(\frac{N}{m_e}) \approx 4$

• A DOMINANT OPACITY IN STARS WITH T$\leq$ 8000K!!

• In atomspheres with sufficient electron density and cool enough temperatures neutral hydrogen can capture a second electron. It is weakly bound.

- there is only a single state with unity statistical weight ($\mathrm{g}_{H^-} = 1, \nu_{H^-}(T) = 1$)

- the ionization energy is X_{I,H^-}=0.755eV.

• the calculation of $\alpha^{bf}_{H^-}(\lambda)$ is very complicated, involving overlap integrals of the H^- bound state wave function with the wave function of the free electron.....(we will not cover this!) NO CLOSED FORM SOLUTION.

• Polynomial fits have been extensively utilized using the fit of Wishart(1979, MNRAS, 187, 59)

$\alpha^{bf}_{H^-}(\lambda) = 10^{-18} \sum_{i=0}^{6} a_i \lambda^i$ [cm^2 per H^- atom] with λ in units $\mathring{A}$

where

$a_o = 1.99654 \quad a_1 = -1.18267 \times 10^{-5} \quad a_2 = 2.64243 \times 10^{-6}$
$a_3 = -4.40524 \times 10^{-10} \quad a_4 = 3.23992 \times 10^{-14} \quad a_5 = -1.39568 \times^{-18}$
$a_6 = 2.78701 \times 10^{-23}$

• to express $\alpha^{bf}_{H^-}(\lambda)$ on same scale as neutral hydrogen, which is custom, we must multiply by $\frac{n_{H^-}}{n_{HI}}$, which is obtained using the Saha Equation

$\frac{n_{J+1}}{n_J} = n_e^{-1}\Phi_J$ where $\Phi_J = C_\Phi T^{\frac{3}{2}} \frac{U_{J+1}(T)}{U_J(T)} exp\{-\frac{X_{IJ}}{kT}\}$
$C_\Phi = 2(\frac{2\pi m_e k}{h^2})^{\frac{3}{2}} = 4.83 \times 10^{15} cm^{-3} K^{\frac{-3}{2}}$

for H^-(=j) and HI(=j+1), we have

$\frac{nH^-}{n_{HI}} = \frac{n_e}{\Phi_{H^-}}$ with $U_{HI}(T) = 2,\ U_{H^-}(T) = 1,\ X_{I,H} = 0.755eV$
$\alpha^{bf}_{\frac{H^-}{HI}}(\lambda) = \frac{n_{H^-}}{n_{HI}} \alpha^{bf}_{H^-}(\lambda)$ cm^2 per neutral hydrogen atom

• shape of the H^- bound-free cross section

• H^- is the prominent opacity in the continum for the sun.

• from Saha n_{H^-} SOME SYMBOL n_e, so increases linearly with electron density/pressure. It is thus sensitive to the density of electron donars, which at cooler temperature is not domincated by the ionization of hydrogen (which would minimize the amility of H^- to form!). The donar are metals with low ionization potentials (Ca, Na, etc) with $X_I < 13.6$ eV.

$\alpha^{bf}_{\frac{H^-}{HI}}(\lambda)$ sensitive to metallicity.

• since $\alpha^{bf}_{\frac{H^-}{HI}}(\lambda)$ increases moving redward across the Balmer jump, it reduces the continum above the jump and therefore reduced the size of the Balmer jump. Thus, Balmer jump is also n_e and metallicity sensitive (not just T).

• As discussed for the bound-free absorption, the H^- free-free process is a siginificant opacity source in cooler stars and is enchaned with increased electron density, which is sensitive to metallicity.

• Again, the compution is complex with no simple closed form expression

• use empirical fit to data of Bell & Berrington (1987, J. PLys Atomic mol. Phys., 20,801)

$*$ the fits is to data computed per neutral hydrogen (not per H^- atom) $*$

$$\alpha^{ff}_{\frac{H^-}{HI}}(\lambda) = n_e kT \times 10^{f_\theta(\lambda)-26} \tag{11.5}$$

cm^2 per neutral hydrogen atom

where $f_\theta(\lambda) = f_0(\lambda) + f_1(\lambda) log\theta + f_2(\lambda) log^2\theta$

$f_k(\lambda) = \sum_{\imath=0}^{4} a_{k\imath} log^\imath \lambda$

NOTE: this parameterization includes to "correction" for stimulated emission λ is in units of $\mathring{A}$

$$a_{k\imath} = \begin{array}{|ccccc|} -2.2763 & -1.6850 & 0.76661 & -0.053346 & 0.000 \\ 15.2827 & -9.2846 & 1.99381 & -0.142631 & 0.000 \\ -197.789 & 190.266 & -67.9775 & 10.6913 & -0.6215 \end{array}$$

• note the direct proportionality to n_e and T (also note: $P_e = n_e kT$
this cross section becomes important in G and F stars.

∗ NOTE 1: Bell + Berrington formula gives cross section of H^- free per neutral hydrogen - so no need for Saha conversion.

11.5.1 Belmer Decrement

Handout Fig 10 p.115 of Lang.

$$D_B = log[\frac{I(< 3650)}{I(> 3650)}] \tag{11.6}$$

why $\begin{cases} D_B \downarrow \ as \ T \uparrow \\ D_B \downarrow \ as \ n_e \downarrow \end{cases}$ $\boxed{D_B = D_B(n_e, T)}$

The Balmer Decrement provides independent measure of (n_e,T) pairs, but can not provide n_e, or T separately. But, T is medsuable in other ways.
BTW, this T is the temperature of electron plasma! T_e, not Teff.

11.6 Continuum Scattering

• process in which photon is not detroyed, but direction is redirected through some change in frequency (small) can occur.
• in stellar atomspheres the two most important types of scattering are Electron Scattering and Rayleigh Scattering

11.6.1 Electron Scattering

also known as Thompson Scattering.

can be derived from the classical electron oscillator cross section

$$\sigma_e(w) = \frac{8\pi e^4 w^4}{3m_e^2c^4} \frac{1}{(w^2 - w_o^2)^2 + \gamma^2 w^2} \tag{11.7}$$

where as w_o is resonance frequency and γ is the damping constant
for free electron $w_o = 0$ and $\gamma = 0$

we have

$$\boxed{\sigma_e = \frac{8\pi}{3}(\frac{e^2}{m_e c^2})^2 = 6.65 \times 10^{-25} \quad cm^2 \;\; per \;\; electron}$$

NOTE: frequency independent

$$* \boxed{Per \;\; neutral \;\; HI \quad \alpha_e = \frac{n_e}{n_{HI}}\sigma_e}$$

Also note that $\frac{e^2}{m_e c^2}$ is the classical radius of the electron

$\rightarrow$ regime in which applies are for $h_\nu << m_e c^2$, which applies normal stellar atmospheres.

11.6.2 Rayleigh Scattering

this is the process by which photons scatter off of atoms with bound electrons, or molecules that are bound. For ν much less than the transition frequencies in the atom/molecules. A transition occurs with frequency w_o with oscillator strength f_o, then for $w << w_o$, the classical oscillator cross section reduces to $[(w^2 - w_o^2)^2 >> \gamma^2 w^2]$

$$\boxed{\sigma_R(w) = \frac{8\pi}{3}(\frac{e^2}{m_e c^2})^2 f_o \frac{w^4}{(w^2 - w_o^2)^2} \quad cm^2 \;\; per \;\; scatter}$$

when $w << w_o$ $\sigma_R(w) \propto w^4$, $w = 2\pi\nu = 2\pi\frac{c}{\lambda}$
$\sigma_R(\lambda) \propto \lambda^{-4}$
then $(w^2 - w_o^2)^2$ is large and slowly changing with w.

11.7 Continuous Absorption

11.7.1 HeliumII bound free

∗ we begin with HeII because it is hydrogenic and the hydrogen bound-free cross section applies-

$\alpha^{bf}_{H_eII,n}(\lambda) = 1.0449 \times 10^{-26} Z^4_{H_E} (\frac{N_{He}}{m_e})^2 \ \frac{\lambda^2}{n^5} g_{II}(n)$ [cm^2 per HeII atom in excited state n]

$N_{H_e} = \frac{m_e}{1+\frac{m_e}{m_{He}}}$ = reduced electron mass in helium
$Z^2_{H_e} = 4$ = atomic "change" number of Helium
g_{II}(n) = Gaunt factor = identical to that of hydrogen

- accounting for summation over all n states

$$\alpha^{bf}_{H_eII} = CZ^4_{H_E}(\frac{N_{H_e}}{m_e})^2\lambda^3\{\sum_{n=1}^{m}\frac{g_{II}(n)}{n^3}exp\{\frac{-X_{n,H_eII}}{kT}\}+\frac{kT}{2X_{I,H_eII}}[exp\{-\frac{X_{m,H_eII}}{kT}\}-exp\{-\frac{X_{I,H_eII}}{kT}\}]\} \tag{11.8}$$

where $c = 1.0449 \times 10^{-26}$ cm^2 $\mathring{A}^{-3}$

and

$$\alpha^{bf}_{H_eII}(\lambda) = [cm^2 per H_eII atom] \tag{11.9}$$

$$X_{n,HeII} = Z^2(\frac{N_{He}}{m_e})R_\infty(1-\frac{1}{n^2}) \tag{11.10}$$

$$X_{I,HeII} = Z^2(\frac{N_{He}}{m_e})R_\infty \tag{11.11}$$

- note that we hace invoked the Unsold integral for n=m+1
- it is customary to obtain cross section per neutral hydrogen thus, we desire

$$\alpha^{bf}_{\frac{HeII}{HI}}(\lambda) = \frac{n_{HeII}}{n_{HI}}\alpha^{bf}_{HeII}(\lambda) = \frac{n_{HeII}}{n_{He}}\frac{n_{He}}{n_H}\frac{n_H}{n_{HI}}\alpha^{bf}_{HeII}(\lambda) \tag{11.12}$$

$$\frac{n_{He}}{n_H} = 10^{(A^{-12}_{He})} \tag{11.13}$$

$$\frac{n_H}{n_{HI}} = (\frac{n_{HI}}{n_H})^{-1} = [\frac{n_{HI}}{n_{HI}+n_{HI}}]^{-1} = [\frac{1}{1+\frac{n_{HII}}{n_{HI}}}]^{-1} = 1+n_e^{-1}\phi_{HI} \tag{11.14}$$

$$\frac{n_{HeII}}{n_{He}} = \frac{\frac{n_{HeII}}{n_{HeI}}}{1 + \frac{n_{HeII}}{n_{HeI}} + (\frac{n_{HeIII}}{n_{HeII}})(\frac{n_{HeII}}{n_{HeI}})} = \frac{n_e^{-1}\phi_{HeI}}{n_e^{-1}\phi_{HeI} + n_e^{-2}\phi_{HeII}\phi_{HeI}} \quad (11.15)$$

cm^2 per neutral hydrogen

NOTE: $\alpha^{bf}_{\frac{HeII}{HI}}$ is on the order of 10% of α^{bf}_{HI} in regine where HeII is prominent ion of He and HI is small.

11.7.2 HeliumI bound-free

• HeI is multielectron, so non-hydrogenic treatment the treatment explorts the energy structure of HeI, which has

$$\begin{cases} X_{I,HeI} = 24.59eV \;\; ground \;\; state \;\; ionization \;\; energy \\ X_2 = 19.72eV \;\; mean \;\; excitation \;\; of \;\; n = 2 \;\; (recall \;\; X_1 = 0, \;\; ground \;\; state) \\ X_1 = 23.03eV \;\; mean \;\; excitation \;\; energy \;\; of \;\; n = 3 \end{cases}$$

note that excitation energies are very close to ground state ionization; thus, excited electrons are not highly bound- they can be treated like a quasi-hydrogenic atom for which the loosely bound electron sees an quasi-cloumb potential with some "effective" nuclear charge. The approximation holds well for $n \geq 3$.

$$\begin{cases} ionization \;\; edge \;\; of \;\; ground \;\; stat \;\; \lambda_1 = 504.19 \;\mathring{A} \;\; (FUV) \\ ionization \;\; edge \;\; of \;\; n = 2 \;\; state \;\; \lambda_2 = 2544 \;\mathring{A} \;\; (NUV) \\ ionization \;\; edge \;\; of \;\; n = 3 \;\; state \lambda_3 = 7932 \;\mathring{A} \;\; (optical) \end{cases}$$

Where (FUV) and (NUV) do not play a role in the optical spectrum.

• Summing from n=3 to n=m

$$\alpha^{bf}_{HeI}(\lambda) = \sum_{n=3}^{m} \frac{g_n}{U_{HeI(T)}} \alpha^{bf}_{HeI,n}(\lambda) exp\{-\frac{X_{n,HeI}}{kT}\} \;\; (n \geq 3) \quad (11.16)$$

cm^2 per HeI atom

where,

$$\frac{g_n}{U_{HeI(T)}} = 4n^2 \quad (11.17)$$

$$\alpha^{bf}_{HeI,n}(\lambda) = CZ^4_{eff,n}(\frac{N_{He}}{m_e})^2 \frac{\lambda^3}{n^5} g_{II}(n) \quad (11.18)$$

with, $C = 1.0449 \times 10^{-26} cm^2 \mathring{A}^{-3}$

NOTES:

$$\begin{cases} \bullet\ We\ \ will\ \ assume \\ g_{II}(n) \approx 1 (n \geq 3) \\ within\ \ few\ \ \% \\ \bullet\ also\ \ recall\ \ \alpha^{bf}_{HeI,n}(\lambda) = 0 \\ for \lambda > \lambda_n \\ \lambda_n = \frac{n^2 hc}{R} = \frac{n^2 hc}{Z^2_{He}} (\frac{N_{He}}{m_e}) R_\infty \end{cases}$$

• Applying Unsold and substituting

$$\boxed{\alpha^{bf}_{HeI}(\lambda) = 4C(\frac{N_{He}}{m_e})^2 \lambda^3 \{\sum_{n=3}^{m} \frac{Z^4_{eff,n}}{n^3} exp\{\frac{-X_{n,HeI}}{kT}\} + Z^2_{eff,1} \frac{kT}{X_{I,HeI}} [exp\{\frac{-X_{m+1,HeI}}{kT}\} - exp\{\frac{-X_{I,HeI}}{kT}\}]\}}$$

we need to choose m and then have the data for all n states below and including m+1

• not in sum $Z^4_{eff,n}$

• in front of 2_{nd} term $Z^2_{eff,1}$ $X_{I,HeI} = X_{I,1} = 24.590eV$

• from Vardya (1964, ApJs,8,277)

the n levels are not degenerate for different L states of HeI
the X_n,$X_{I,n}$, and λ for tese data are weighted for the various L states (see Gortrian diagram)

• Vardya recommends summing up to $\boxed{m = 9}$
• to obtain the cross section per meutral hydrogen

$$\alpha^{bf}_{\frac{HeI}{HI}}(\lambda) = \frac{n_{HeI}}{n_{HI}} \alpha^{bf}_{HeI}(\lambda) = \frac{n_{HeI}}{n_{He}} \frac{n_{He}}{n_H} \frac{n_H}{n_{HI}} \alpha^{bf}_{HeI}(\lambda)$$

cm^2 per neutral hydrogen

$$\frac{n_{He}}{n_H} = 10^{(\mathring{A}_{ne-12})}$$

$$\frac{n_{He}}{n_{HI}} = 1 + n_e^{-1} \phi_{HI}$$

$$\frac{n_{HeI}}{n_{He}} = \frac{1}{1 + n_e^{-1} \phi_{HeI} + n_e^{-2} \phi_{HeII} \phi_{HeI}}$$

• bound-free HeI is fairly negligible in stars of all temperatures (in the optical) because by the time HeI has a signigicant fraction in the n=3 excitation state, the majority of it is ionized to HeII!

11.7.3 He free-free (HeII,HeI)

$$B_o^\lambda = \frac{B_o}{c^3} = \frac{3.6923 \times 10^8}{(3 \times 10^{10})^3} = 1.3675 \times 10^{-23} \tag{11.19}$$

so that,
(HI)

$$\alpha_{k\ell}^{ff}(\lambda) = 1.3675 \times 10^{-23} Z^2 (\frac{N}{m_e}) n_e \lambda^3 T^{\frac{-1}{2}} \bar{g}_{III}(\lambda, T) \tag{11.20}$$

for hydrogen this is cm^2 per neutral hydrogen

• Since HeII is hydrogenic, the cross section immediately applies
(HeII)

$$\alpha_{HeII}^{ff} = 1.3675 \times 10^{-23} Z_{HeII}^2 (\frac{N_{He}}{m_e}) n_e \lambda^3 T^{\frac{-1}{2}} \bar{g}_{III}(\lambda, T) \tag{11.21}$$

cm^2 per HeII atom

to convert to cm^2 per neutral hydrogen atom

$$\alpha_{\frac{HeII}{HI}}^{ff}(\lambda) = \frac{n_{HeII}}{n_{HI}} \alpha_{HeII}^{ff}(\lambda) = \frac{n_{HeII}}{n_{He}} \frac{n_{He}}{n_H} \frac{n_H}{n_{HI}} \alpha_{HeII}^{ff}(\lambda) \tag{11.22}$$

cm^2 per neutral hydrogen

where,

$$\frac{n_{HeII}}{n_{HI}} = 10^{(\mathring{A}_{Hr}^{-12})} (1 + n_e^{-1} \phi_{HI}) [\frac{n_e^{-1} \phi_{HeI}}{1 + n_e^{-1} \phi_{HeI} + n_e^{-2} \phi_{HeII} \phi_{HeI}}] \tag{11.23}$$

as worked out for $\alpha_{HeII}^{bf}(\lambda)$

• HeI is not hydrogenic, however it is well approximated by introducing a quatum "defect" factor of $\exp\{-\frac{\Delta X}{kT}\}$ where $\Delta X = 10.93eV$.

(HeI)

$$\alpha_{HeI}^{ff} = exp\{-\frac{\Delta X}{kT}\} 1.3675 \times 10^{-23} Z_{HeII}^2 (\frac{N_{He}}{m_e}) n_e \lambda^3 T^{\frac{-1}{2}} \bar{g}_{III}(\lambda, T) \tag{11.24}$$

cm^2 per HeI atom

to convert to cm^2 per neutral hydrogen atom

$$\alpha^{ff}_{\frac{HeI}{HI}}(\lambda) = \frac{n_{HeI}}{n_{HI}}\alpha^{ff}_{HeI}(\lambda) = \frac{n_{HeI}}{n_{He}}\frac{n_{He}}{n_H}\frac{n_H}{n_{HI}}\alpha^{ff}_{HeI}(\lambda) \tag{11.25}$$

cm^2 per neutral hydrogen

where,

$$\frac{n_{HeI}}{n_{HI}} = 10^{(\mathring{A}^{-12}_{He^-})}(1 + n_e^{-1}\phi_{HI})[\frac{1}{1 + n_e^{-1}\phi_{HeI} + n_e^{-2}\phi_{HeII}\phi_{HeI}}] \tag{11.26}$$

as worked out for $\alpha^{bf}_{HeI}(\lambda)$

11.7.4 He^- free free

• in cool stars with relatively high n_e, a third electron can become bound to neutral He (HeI). This negatively charged ion is known as He^-.

• there is only one bound level with ionization potential energy $19eV$. (thus, the binding energy is $-19eV$). The population of this level is in fact quite rare. Thus, bound-free absorption from He^- is negligible. But free-free can make a contribution to the continuous absorption at redder wavelengths in cool stars.

• There is no closed form solutions form the overlap integrals, so use parameterized fir to John(1994,MNRAS, 269,871)[Table 2]

$$\alpha^{ff}_{He^-}(\lambda) = n_e kT 10^{f_\theta(\lambda)-26} \tag{11.27}$$

cm^2 per He^- ion

where

$$f_\theta(\lambda) = f_o(\theta) + f_1(\theta)log\lambda + f_2(\theta)log^2\lambda + f_3(\theta)log^3\lambda \tag{11.28}$$

in units of $\mathring{A}$

$f_k(\theta) = \sum_{\imath=0}^{4} a_{k\imath}\theta^\imath$

$$a_{k\imath} = \begin{matrix} 9.66736 & -71.7642 & 105.29576 & -56.49259 & 10.69206 \\ -10.50614 & 48.20802 & -70.43363 & 37.80099 & -7.15445 \\ 2.74020 & -10.62144 & 15.50518 & -8.33845 & 1.57960 \\ -0.19923 & 0.77485 & -1.13200 & 0.60994 & -0.11564 \end{matrix}$$

the parameterization is good to 1% for $5000 \leq \lambda \geq 150000\mathring{A}$ and $0.5 \leq \theta \geq 2.0$. The stimulated emission factor is included in the polynomials.

$$\alpha^{ff}_{\frac{He^-}{HI}}(\lambda) = \frac{n_{He^-}}{n_{HI}}\alpha^{ff}_{He^-}(\lambda) = \frac{n_{He^-}}{n_{He}}\frac{n_{HeI}}{n_H}\frac{n_H}{n_{HI}}\alpha^{ff}_{He^-}(\lambda) \tag{11.29}$$

cm^2 per neutral hydrogen

Where,
$\frac{n_{HeI}}{n_{He^-}} = n_e^{-1}\phi_{He^-}$
$U_{He^-}(T) = 1$
$X_{I,He^-} = 19eV$

The importance of gravity ⇒ Pressure!

$$g = \frac{GM_\star}{R_*^2} \tag{11.30}$$

G = 6.6742×10^{-8} $cm^3 g^{-1} s^{-1}$
$M_\odot$ = 1.9892×10^{33}g
$R_\odot$ = 6.95997/$times10^{10}$ cm
$g_\odot$ = 2.738×10^4 $\frac{cm}{s^2}$ cm/s^2

often expressed $\log(g_\odot) = 4.438 \approx 4.4$

$$\boxed{log(\frac{g_\star}{g_\odot}) = log(\frac{M_*}{M_\odot}) - 2log(\frac{R_*}{R_\odot})}$$

determining log(g) is one way to get $\frac{M_*}{R_*^2}$

11.8 In Hydrostatic equilibrium

$F_{down} = F_{up}$

(P+dp)dA + gdm = PdA

defining ρ = mass density = $\frac{dm}{dV} = \frac{dm}{dxdA}$

dm = ρdxdA
$\rho = \sum m_\imath n_\imath = \sum \frac{n_\imath A_\imath m_{amu}}{X_\imath}$
$A_\imath$ = atomic weight
$m_\imath$ = mass
$n_\imath$ = number density [atoms cm^{-3}]
$X_\imath$ = mass fraction

we have,
(P + dP)dA + gρdxdA = PdA

$$\boxed{\text{giving} \quad \frac{dP}{dx} = -g\rho}$$

$$\boxed{\text{g is important! P}\propto g}$$

• can assume g≠g(x) in atmosphere, but not for stellar structure!
• we will see, P and ρ covered through equation of state and detailed balancing of particle densities and ionization conditions.
• also, PRESSURE BROADENING of absorption lines (nearest neighbor effects)

$$\frac{dP}{dx} = -\rho p \qquad P = \frac{\rho}{NM_{amu}} kT \quad (ignoring \;\; radiation) \tag{11.31}$$

• $\mathrm{NM}_{amu} =< M >_{ave}$ of all particles including electrons.
• N≡ mean molecular weight (depends on ionization condition)
•$P = n_{tot}kT = (n_N + n_e)kT$
•$n_{tot} = \frac{\rho}{NM_{amu}}$

thus

$$\frac{dP}{dx} = -\frac{PNM_{amu}}{kT} g \tag{11.32}$$

$$\frac{dP}{P} = -g\frac{NM_{amu}}{kT} dx \tag{11.33}$$

yielding (general solution),

$$P(x) = P(x_o) exp\{-\frac{M_{amu}}{k} \int_{x_o}^{x} \frac{Ng}{T} dx\} \tag{11.34}$$

technically $N = N(x) \;\; g = g(x)$ and $T = T(x)$

if they are constant then,

$$P(x) = P(x_o) exp\{-\frac{NM_{amu}g}{kT}(x - x_o)\} = P(x_o) exp\{-\frac{(x - x_o)}{H}\} \tag{11.35}$$

idealized solution
where H is scale height $H = \frac{kt}{NM_{amu}g}$
- atmospheres are not isothermal with physical depth x.
- atmosphere have changing N, which depend upon ionization fractions with physical depth x.
- though the gravity is also varying with physical depth x, it can be treated as a constant with little loss of accuracy.

11.9 Importance of Pressure

consider the mean distance between particles. $< r >$

$$n = \frac{1}{\frac{4}{3}\pi < r >^3} = \frac{P}{kT} \quad \rightarrow \quad < r >= [\frac{3kT}{4\pi P}]^{\frac{1}{3}} \tag{11.36}$$

or

$$< r > \propto [\frac{T}{P}]^{\frac{1}{3}} \tag{11.37}$$

as P goes up $< r >$ decreases! Particles influence each other more.

11.10 Qualitative Overview: Pressure Broadening

$$< r >= [\frac{3kT}{4\pi P}]^{\frac{1}{3}} \tag{11.38}$$

$\frac{1}{2}m < v^2 >= \frac{3}{2}kT \qquad < v^2 >= \int_0^\infty v^2 f(v)dv$
where f(v) is Maxwell-Boltzman speed distribution

$$< r >= [\frac{m < r^2 >}{4\pi P}]^{\frac{1}{3}} \tag{11.39}$$

Many Methods, but consider "impact" perturbation approach.

1. electric magnetic fields of neighbors influence the frequencies of transitions via

$$\Delta w = C_n R^{-n} \tag{11.40}$$

w = 2πv = $\frac{2\pi c}{\lambda}$ n=integer

2. the pertrubing ions pass by the target atom with average velocity

$$v =< v^2 >^{\frac{1}{2}} = \{\frac{8kT}{\pi}(\frac{1}{m_A} + \frac{1}{m_p}\}^{\frac{1}{2}} \tag{11.41}$$

where v is the center of mass, m_A is atom and m_p is pertruber.
with closest approach ρ_o (not density!) this results in an impulse of duration

$$\tau = \frac{1}{\pi \rho_o^2 n_{tot} v} \tag{11.42}$$

$$\rho_o = [\frac{2\pi C_n}{v} \int_{\frac{-\pi}{2}}^{\frac{\pi}{2}} cos^{n-2}\theta d\theta]^{\frac{1}{(n-1)}} \tag{11.43}$$

where n is an integer
which causes a shift in the energy of the atom

3. the funtional form of the change in the transition energy is of the form (Lorentzian)

$$\Delta E = \frac{\frac{1}{\pi\tau}}{(w - w_o)^2 + (\frac{1}{\tau})^2} \tag{11.44}$$

which results in significant line broadening in wings of lines $\sim \frac{1}{(w-w_o)^2}$
$*$ the values of n and C_n depends upon the type of perturbation

11.11 Pressure Broadening

The value of n (the power index $\Delta w = C_n R^{-n}$) applies for the physical effect of the perturbation

n=2 Linear Stark (first order electrical) Effects Hydrogen, Perturders are protons and electrons
n=3 Resonance Broadening Effects all atoms, Perturbers are like atoms
n=4 Quadratic Stark (second order electrical) Effects non-hydrogen atoms, Perturbers are protons and electrons
n=6 Van der Waals force Effects all atoms, Perturbers are all non-like atoms mostly hydrogen perturbing non-hydrogen

n=2
Linear Stark Effect: Dominates the broadening of hydrogen lines. It requires a slightly different treatment. The broadening is characterized by a narrow Gaussian core and very broad Lorentzian wings due to high velocities (short impulse times) because perturbers are protons and electrons (light particles).

n=3
Resonance broadening: Important mostly for hydrogen - hydrogen interactions. It dominants the lowest order hydrogen lines, particularly the Hα line. It is neglible in comparison to Linear Stark (n=2) for Hβ and higher.

NOTE: Since Linear Stark and Resonance broadening effect hydrogen lines, they are important in stars for which hydrogen is in its first excited state but not ionized. Thus they are important broadening mechanism in A,F and G stars.

n=4
Quadratic Stark Effect: Important for broadening line in non-hydrogenic atoms (i.e. HeI, etc) due to perturbations by electrons (and somewhat protons). Most effective with high electron density, meaning in highly ionized atmospheres. Thus, important in hot, early type stars.

n=6
Van der Waals Interactions: Important for non-hydrogenic atoms perturbed ny neutral hydrogen atoms. It is the dominant source of pressure broadening in cooler-F, G, and hotter

Important for CaII H+K, and NaI H+K, also MgIb and FeI, etc.

11.12 Collisional Broadening (Impact Treatment)

• In the impact approximation (theory), the electric field of a "colliding" particle is treated as a photon originating at the perturbing particle and terminating at the atom being perturbed.
The photon is thus truncated over a path length cΔt. So, we can treat the photon as being "trapped" in a "box".
A truncated sinisoidal wave has an electric field spectrum.

$$E_v(\Delta t) = E_o sinc[\pi \Delta t(v - v_o)] \tag{11.45}$$

where v_o is the frequency of the non-truncated photon (the sinisoidal frequency) and the intensity is

$$I_v(\Delta t) = E_v^*(\Delta t) \times E_v(\Delta t) = E_o^2 sinc^2[\pi \Delta t(v - v_o)] \tag{11.46}$$

The fourier transform of $I_v(\Delta t)$ provides the frequency power spectrum Fv for a given Δt, yielding.

$$F(v) = [\frac{sin[\pi \Delta t(v - v_o)]}{\pi(v - v_o)}]^2 = (\Delta t)^2 [\frac{sin[\pi \Delta t(v - v_o)]}{\pi \Delta t(v - v_o)}]^2 \tag{11.47}$$

• To obtain the full frequency redistribution function of the effect of many random impulses (or collisions) we must integrate over the impulse times weighted by the probability if a collision occuring in the interval dΔt

$$f_p(v) = \int_{-\infty}^{\infty} F(v) dP(\Delta t) \tag{11.48}$$

where dP(Δt) is the probability element in interval Δt

• we need to compute dP(Δt)...
define P(Δt) = probability of a collision in Δt
p(Δ t) = probability of no collision in Δt
then $p(\Delta t) = 1 - P(\Delta t)$
where Δt_o is the average time between collisions

in interval dΔt, the probability of no collision is (to first order)

$$p(\Delta t + d\Delta t) = p(\Delta t) - p(\Delta t) \frac{d\Delta t}{\Delta t_o} \tag{11.49}$$

the probability of no collision decreases with time(intuitive)

comparing to the Taylor expansion

$$p(\Delta t + d\Delta t) = p(\Delta t) + \frac{dp}{d\Delta t} d\Delta t + ... \tag{11.50}$$

we see that

$$\frac{dp}{d\Delta t} = -\frac{p(\Delta t)}{\Delta t_o} \tag{11.51}$$

or

$$\frac{dp}{p(\Delta t)} = -\frac{d\Delta t}{\Delta t_o} \tag{11.52}$$

integrating, we have

$$p(\Delta t) = exp\{-\frac{\Delta t}{\Delta t_o}\} \tag{11.53}$$

From p(Δt) = 1-P(Δt)

$$P(\Delta t) = 1 - exp\{-\frac{\Delta t}{\Delta t_o}\} \tag{11.54}$$

from which we obtain

$$dP(\Delta t) = exp\{-\frac{\Delta t}{\Delta t_o}\}\frac{d\Delta t}{\Delta t_o} \tag{11.55}$$

• Thus, the integral for fp(v) is

$$f_p(v) = 2\int_{-\infty}^{\infty} (\Delta t)^2 [\frac{sin[\pi \Delta t(v - v_o)]}{\pi \Delta t(v - v_o)}] exp\{-\frac{\Delta t}{\Delta t_o}\}\frac{d\Delta t}{\Delta t_o} \tag{11.56}$$

which has analytic soultion

$$f_p(v) = \frac{2(\frac{1}{\Delta t_o})}{4\pi^2(v - v_o)^2 + (\frac{1}{\Delta t_o})^2} = \frac{1}{\pi}\frac{\frac{1}{2\pi\Delta t_o}}{(v - v_o)^2 + (\frac{1}{2\pi\Delta t_o})^2} \tag{11.57}$$

• The frequency redistribution function is a Lorenztian, L(v), with $\boxed{y = \frac{1}{2\pi\Delta t_o}}$

note

$$\int_0^{\infty} f_p(v)dv = \int_0^{\infty} L(v)dv = \frac{1}{\pi}\int_0^{\infty} \frac{y}{(v - v_o)^2 + y^2} dv = 1 \tag{11.58}$$

f(v) normalized

- Note the identical form to the natural broadening cross section

$$\alpha_n \propto \frac{(\frac{\pi}{4\pi})}{(v-v_r)^2+(\frac{\pi}{4\pi})^2} \tag{11.59}$$

so, writing $\gamma_o = \frac{2}{\Delta t_o}$, the pressure broading redistribution function is

$$f_p(v) = \frac{1}{\pi}\frac{(\frac{\gamma_o}{4\pi})}{(v-v_o)^2+(\frac{\gamma_o}{4\pi})^2} \tag{11.60}$$

HWHM $= \frac{\gamma_o}{4\pi}$
FWHM $= 2(\frac{\gamma_o}{4\pi}) = \frac{\gamma_o}{2\pi}$
Amplitude $= \frac{1}{\pi}(\frac{\gamma_o}{4\pi}) = \frac{\gamma_o}{4\pi^2}$

- what remains is to determine the value of $\gamma_o = \frac{2}{\Delta t_o}$

- From standard mean free path calculations

$$\frac{1}{\gamma_o} = \frac{\Delta t_o}{2} = \frac{1}{2}\frac{1}{n_c < \sigma >< v >} \tag{11.61}$$

$$< \sigma >= \frac{\int_0^\infty \sigma(v)dv}{\int_0^\infty dv} \tag{11.62}$$

where σ(v) is the interaction cross-section (where all the physics lurks)
$< v >$ is the average (not most probable) velocity of the interaction(center of mass frame)
n_c is number density of pertrubing(colliding) particles

In actvality

$$\gamma_o = \frac{2}{\Delta t_o} = 2n_c \int_0^\infty v f(v)\sigma(v)dv \tag{11.63}$$

the cross section weighted by Maxwellian velocity distribution

- Simplified Approach

$$< v >= \{\frac{8kT}{\pi}(\frac{1}{m_a}+\frac{1}{m_c})\}^{\frac{1}{2}} \tag{11.64}$$

center of mass average velocity in T.E.
we now need to compute $< \sigma(v) >\equiv< \sigma >$, the cross section of the pertuibation

- this will depend upon the type of electromagnetic perturbation. We designate these types by the subscript n; so we need to find σ_n, which will then yield γ_n.

• classically $\sigma_n = \pi\rho_n^2$ where ρ is the "interaction" impact parameter
-it is a physical distance [cm], but ut includes the interaction physics for the perturbetion of type "n".

then

$\boxed{\gamma_n = 2\pi\rho_n^2 n_c < v >}$
we need the "interaction" impact parameter.

• $\boxed{FORMSOFTHEPERTURBATIONS}$

1. Linear Stark Effect (n=2)
- Electric dipole interation. Where the dipole electric field scales as R^{-2} , thus $\boxed{n = 2}$ and the energy shift of the level in the atom goes as

$$\delta E_i = \frac{h}{2\pi} K_i R^{-2} \tag{11.65}$$

R = distance to perturbing ion/electron
and the energy shift of transition i→j goes as

$$\Delta E_{ij} = \frac{h}{2\pi} K_{ij} R^{-4} \tag{11.66}$$

2. Quadratic Stark Effect (n=4)
- electric quadrapole interaction (required when dipole interaction nulls). The electric field scales as R^{-4},thus $\boxed{n = 4}$ and the energy shift goes as

$$\Delta E_{ij} = \frac{h}{2\pi} K_{ij} R^{-4} \tag{11.67}$$

In the Linear Stark Effect, the otherwise energy degenerate levels split symmetrically about the unshifted level. (energy splits). The broadening is due to the magnitude of the spliting - multiple transitions now occur between these multiple levels, resulting in the broadening It is symmetric about unshifited line. In the Quadratic Stark Effect the spliting is one sided (to lower energies) realitive to the unshifted line - thus, the broadening is asymmetric about the line center.

3. Resonance Broadening (n=3) (like atoms/ions) - combined Linear Stark in resonance with the transition energy in the affected atom/ion. Interaction goes as R^{-3}, thus $\boxed{n = 3}$ and

$$\Delta E_{ij} = \frac{h}{2\pi} k_{ij} R^{-3} \tag{11.68}$$

4. Van der Waals (n=6) - interaction between neutral particles. These atoms have internal electric moments (dipoles, quadrapoles, etc) and they induce dipoles in each other. The induced moment goes as R^{-3} and the interaction of the moments goes as R^{-6}, thus $\boxed{n = 6}$, and

$$\Delta E_{ij} = \frac{h}{2\pi} K_{ij} R^{-6} \tag{11.69}$$

$\longrightarrow$ Recall earlier notes outlining the atom/ions most strongly affected by each of these different forms of the perturbations (REVIEW THEM)

• $\boxed{GETTING\ \ THE\ \ "INTERACTION"\ \ IMPACT\ \ PARAMETER\ \rho_n}$

recall $\gamma_n = 2\pi\rho_n^2 n_c < v >$

ρ_n is obtained from the total energy shifts of the levels, but interms of the frequency shift $\Delta v = \frac{\Delta E}{h}$
for a given transition, the total shift (called the phase shift) over the "impact" is

$$n_{ij} = \frac{2\pi}{h} \int_{-\infty}^{\infty} \Delta v_{ij} dt = k_{ij} \int_{-\infty}^{\infty} \frac{dt}{R^n} = k_{ij} \int_{-\infty}^{\infty} \frac{dt}{[\rho_n^2 + (< v > t)^2]^{\frac{n}{2}}} \tag{11.70}$$

from $R^2 = \rho_n^2 + (< v > t)^2$

re-arranging...

$$\frac{1}{[\rho_n^2 + (< v > t)^2]^{\frac{n}{2}}} = \frac{1}{[\rho_n^2\{1 + (\frac{<v>t}{\rho_n})^2\}]^{\frac{n}{2}}} = \frac{1}{\rho_n^n} \frac{1}{[1 + (\frac{<v>t}{\rho_n})^2]^{\frac{n}{2}}} \tag{11.71}$$

we obtain $\rightarrow$

$$n_{ij} = \frac{k_{ij}}{\rho_n^n} \int_{-\infty}^{\infty} \frac{dt}{[1 + (\frac{<v>t}{\rho_n})^2]^{\frac{n}{2}}} = \frac{k_{ij}}{< v > \rho_n^{n-1}} \int_{-\infty}^{\infty} \frac{(\frac{<v>}{\rho_n})}{[1 + (\frac{<v>}{\rho_n})^2 t^2]^{\frac{n}{2}}} dt \tag{11.72}$$

$$I_n = \int_{-\infty}^{\infty} \frac{x}{(1 + x^2 t^2)^{\frac{n}{2}}} dt \tag{11.73}$$

where $\boxed{\pi \ \ n = 2 \qquad 2 \ \ n = 3 \qquad \frac{\pi}{2} \ \ n = 4 \qquad \frac{3\pi}{8} \ \ n = 6}$

n=2	n=3	n=4	n=6
$\gamma_n \propto T^{\frac{3}{2}}$	$\gamma_n \propto T^{-1}$	$\gamma_n \propto T^{-\frac{5}{8}}$	$\gamma_n \propto T^{-\frac{7}{10}}$

$x = \frac{<v>}{\rho_n}$

so we have

$$n_{ij} = \frac{k_{ij}}{< v > \rho_n^{n-1}} I_n \tag{11.74}$$

or

$$\rho_n^2 = \{\frac{k_{ij} I_n}{n_{ij} < v >}\}^{\frac{2}{n-1}} \tag{11.75}$$

finally yielding

$$\gamma_n = 2\pi\rho_n^2 n_c < v >= 2\pi n_c \{\frac{k_{ij} I_n}{n_{ij} < v >}\}^{\frac{2}{n-1}} < v >= 2\pi n_c \{\frac{k_{ij} I_n}{n_{ij}}\}^{\frac{2}{n-1}} < v >^{\frac{n-3}{n-1}} \tag{11.76}$$

invoking, average velocity

$$< v >= \{\frac{8kT}{\pi}(\frac{1}{m_a} + \frac{1}{m_c})\}^{\frac{1}{2}} \tag{11.77}$$

and

$$P_c = n_c kT \rightarrow n_c = \frac{P_c}{kT} \tag{11.78}$$

where P_c is the partial pressure of the perturbing atom or electrons

we obtain

$$\gamma_n = 2\pi P_c T^{-\frac{n+1}{2(n-1)}} \{\frac{k_{ij} I_n}{n_{ij}}\}^{\frac{2}{n-1}} [\frac{8k}{\pi}(\frac{1}{m_a} + \frac{1}{m_c})]^{\frac{n-3}{2(n-1)}} \tag{11.79}$$

$\gamma_n \propto P_c$ the "damping constant" is linear proportional with pressure
Thus we call this "pressure broadening"

$\gamma_n \propto T^{-\frac{n+1}{2(n-1)}}$ weakly inverse proportional to T.

11.13 Pressure Broadening

11.13.1 Impact theory Parameter

K_{ij} - To fully specify γ_n for a given transition in a given atom/ion we need the values of k_{ij}. They are specific to a give transition within a given atom/ion. They can be computed from Quantum Theory for some cases, but many are measured (but not all!).

n_{ij} - Also required is the value n_{ij}, the total phase shift of the "photon in a box" over the duration of the impact. The "interaction" impact parameter is proportional to $n_{ij}^{\frac{-2}{n-1}}$. Thiss has remained an arbitrary parameter of impact theory. $n_{ij} = 1$ radian is nominally adopted.

Collisional Therory is one of many approaches, most are more sophisticated and better account for the spatial distribution of a "sea" of perturbing particles as well as polarization of the gas (The Debye Shielding) An entire cause could be dedicated to pressure broadening.

• example: NaI D_2D, lines
(n=4), Quadaratic Stark)
NaI D_2 $\lambda 5890 log k_{ij} = -15.17$
NaI D_1 $\lambda 5896 log k_{ij} = -15.33$

(n=6, Van der Waals)
$k_{ij} = 3 \times 10^{-29}[(x_I - x_\ell - \frac{hc}{\lambda})^{-2} - (x_I - x_\ell)^{-2}]$
(from Unsold 1955)
X_I = ionization potential
X_ℓ = excitation potential (lower state)
λ = transition wavelength

Chapter 12

Cross Sections

12.1 Defining cross sections

The cross section is derived from a classical picture of particle interactions. Because observations measure the time average of many individual events, it is useful to describe particle interactions as probabalistic and employ a statistical treatment.

As illustrated in Figure 12.1, consider a beam of cross sectional area A_b comprising monoenergetic particles with number density n_b and velocity v_b. In a unit time interval $t \to t + dt$, the beam volume element is $A_b(v_b dt)$ and this volume element contains $dN_b = n_b A_b v_b dt$ particles. The particle flux [particles s^{-1} cm^{-2}] is

$$F_b = \frac{1}{A_b}\frac{dN_b}{dt} = \frac{n_b A_b v_b}{A_b} = n_b v_b \,, \tag{12.1}$$

Allow the beam to intersect a target of thickness L with particle density n_{T}. The number of target particles that can potentially interact with the beam is $N_{\mathrm{T}} = n_{\mathrm{T}} A_b L$, as schematically illustrated as the filled points in Figure 12.1. From the point of view of the incoming beam, illustrated in Figure 12.1b, if the projected "interaction area" of a target particle is σ, then each potentially interacting target particle has fractional interaction area σ/A_b.

The probability that a single beam particle will interact with a target particle is the product $N_{\mathrm{T}}(\sigma/A_b)$. Note that his requires that the units of σ are cm^2 $\mathrm{particle}^{-1}$ (i.e., incident beam particle). Geometrically, this probability is the ratio of the total interaction area of all potentially interacting target particles to the area of the beam (see Figure 12.1b). The probability can also be expressed as the ratio of the number of *interacting* beam particles per unit time, dN_i/dt, to the number of incident beam particles per unit time, dN_b/dt. Equating, we have

$$\frac{dN_i/dt}{dN_b/dt} = N_{\mathrm{T}}\frac{\sigma}{A_b} \,. \tag{12.2}$$

We have assumed that a given beam particle can interact with only a single

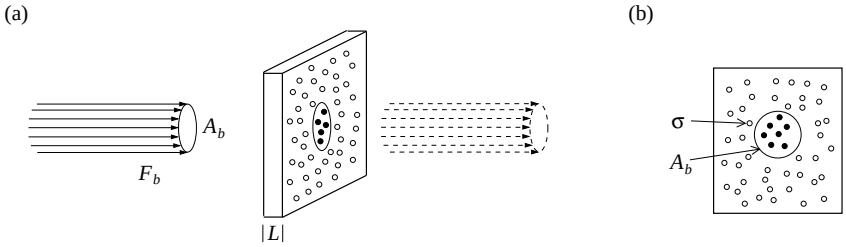

Figure 12.1: (a) The schematic of an incident beam of cross sectional area A_b striking a target of thickness L. The incident beam flux is $F_b = n_b v_b$, where n_b. The number of potentially interacting target particles (filled points) is $N_{\rm T} = n_{\rm T} A_b L$. The post-target beam flux is reduced, as illustrated with the dashed lines. (b) The face-on view of the target illustrating the projected area of the beam (region over which interactions can take place) and of the individual target particle cross section, σ.

target particle (once a beam particle is absorbed or scattered it is removed from the beam) and that no target particle is shadowed by other target particles. Rearranging, we obtain

$$N_{\rm T}\sigma = \frac{dN_i/dt}{(1/A_b)(dN_b/dt)} = \frac{\mathcal{P}}{F_b}\,, \tag{12.3}$$

where $\mathcal{P} = dN_i/dt$ is the rate, or power, at which particles are removed from the beam. We see that a cross section is defined as the ratio of the power at which particles are removed from the beam per potential target particle to the particle flux of the beam. Since the units of $\mathcal{P}$ are [particles sec^{-1}] and the units of F_b are [particles cm^{-2} sec^{-1}], the units of $N_{\rm T}\sigma$ are [cm^2].

12.1.1 Pure absorption

For pure absorption, we assume no scattering, only removal of particles from the beam. The power at which particles are removed from the beam, dN_b/dt, is the negative of the power at which particles interact with the beam, yielding $dN_b/dt = -dN_i/dt$. Thus, $\mathcal{P} = -dN_b/dt = -A_b dF_b$, where dF_b is the change in the beam flux. Substituting into Eq. 12.3 yields $N_{\rm T}\sigma = -A_b(dF_b/F_b)$. From $N_{\rm T} = n_{\rm T} A_b L$, and rearranging, we obtain

$$\frac{dF_b}{F_b} = -n_{\rm T} L\sigma\,, \tag{12.4}$$

a differential equation with solution

$$F_b = F_b(0)\exp\left\{-n_{\rm T} L\sigma\right\}\,, \tag{12.5}$$

where F_b is the post-target beam flux and $F_b(0)$ is the beam flux incident on the target. Note that the product $n_{\rm T} L = N$ is the column density of interacting target particles.

If the particles in the monoenergetic beam are photons of frequency ω with electric field amplitude E_0, then the particle flux, $F_b = n_b v_b$, can be replaced by the flux of monochromatic radiative energy. This is most simply accomplished by substituting the radiative energy density, $E_0^2/8\pi$, for the particle density, and substituting the speed of light for the particle velocity, giving

$$F_\omega(0) = \frac{c}{8\pi} E_0^2 \,. \tag{12.6}$$

Following the identical treatment used to obtain Eq. 12.5, we find that the absorption of a radiative beam obeys,

$$F_\omega = F_\omega(0) \exp\left\{-N\sigma(\omega)\right\} \,, \tag{12.7}$$

where $N = n_{\scriptscriptstyle T} L$ is the column density and $\sigma(\omega)$ is the absorption cross section at frequency ω.

12.1.2 Pure scattering

In the case of pure scattering, the particles are deflected into various directions relative to the incident beam. The resulting angular distribution of scattered particle flux may not be isotropic, which provides insights into the scattering physics. We thus must invoke a differential cross section, $d\sigma(\phi,\theta)/d\Omega$, which is the cross section for scattering into angle ϕ, θ into a solid angle element $d\Omega$.

A schematic of the differential cross section is presented in Figure 12.2, which is a diagram showing particles deflected into solid angle elements in various directions, each defined by the angle ϕ and θ with respect to the incident beam. The total cross section is defined as the integral of the differential cross section over all solid angles

$$\sigma = \oint \frac{d\sigma(\phi,\theta)}{d\Omega} = \int_0^{2\pi}\int_0^{\pi} \frac{d\sigma(\phi,\theta)}{d\Omega} \sin\theta \, d\theta \, d\phi \,. \tag{12.8}$$

The relationship between total cross section and the power removed from the beam are identical for pure scattering and pure absorption, i.e., Eq. 12.3. What is fundamentally different between absorption and scattering, however, is the that the power removed from the beam due to scattering is redistributed as particle flux over all solid angles.

As defined in Eq. 12.3, let $\mathcal{P} = dN_i/dt$ denote the beam particle interaction rate. For non-isotropic scattering, the rate at which particles are scattered into the (ϕ,θ) direction within a solid angle $d\Omega$ is written in terms of the differential scattered power distribution, $d\mathcal{P}(\phi,\theta)/d\Omega = dN_i(\phi,\theta)/dt d\Omega$. Analagous to Eq. 12.2, the probability that a single beam particle will interact with a target particle and be scattered into the (ϕ,θ) direction within a solid angle $d\Omega$ is

$$\frac{d\mathcal{P}(\phi,\theta)/d\Omega}{dN_b/dt} = N_{\scriptscriptstyle T} \frac{d\sigma(\phi,\theta)/d\Omega}{A_b} \,. \tag{12.9}$$

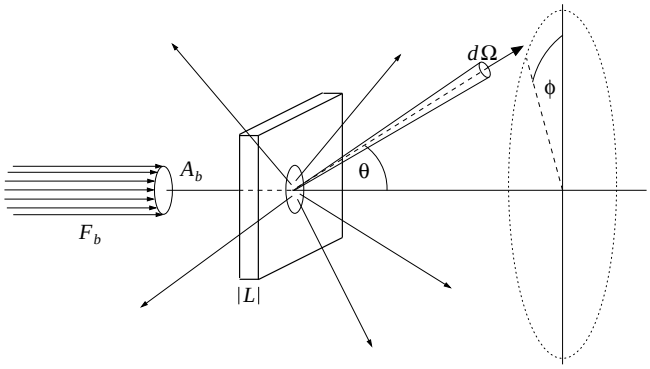

Figure 12.2: A schematic of scattering of particles in an incident beam of cross sectional area A_b and particle flux F_b by a target of thickness L. An individual particle is scattered into the direction defined by the angle pair ϕ, θ, where the beam direction is the polar axis of the coordinate system with origin at the center of scattering. The differential scattering cross section, $d\sigma(\phi,\theta)/d\Omega$ is defined as the effective iteraction area per per interacting target particle per unit solid angle for particles scattered into a solid angle element $d\Omega$ in the ϕ, θ direction.

Rearranging, we have,

$$N_{\text{T}}\, d\sigma(\phi,\theta)/d\Omega = \frac{d\mathcal{P}(\phi,\theta)/d\Omega}{(1/A_b)dN_b/dt} = \frac{1}{F_b}\, d\mathcal{P}(\phi,\theta)/d\Omega\,. \tag{12.10}$$

Integrating over all solid angles,

$$N_{\text{T}}\sigma = \frac{1}{F_b}\oint \frac{\mathcal{P}(\phi,\theta)}{d\Omega}\, d\Omega = \frac{\mathcal{P}}{F_b}\,, \tag{12.11}$$

where the total scattering cross section, σ, is given by Eq. 12.8. Thus, the integration over the angular redistribution of the power removed from the beam provides the a definition of the total scattering cross section that is identical to Eq. 12.3.

The differential scattered power distribution, $d\mathcal{P}(\phi,\theta)/d\Omega$, is related to the scattered flux distribution via the relation $d\mathcal{P}(\phi,\theta) = \mathbf{F}(r,\phi,\theta)\cdot\mathbf{dA}$, evaluated at radial distance r from the scattering center at the location of the area element. Assuming the projectiles of the scattered particles are radial and the normal to the area element is also radial,

$$\mathcal{P} = \oint \frac{d\mathcal{P}(\phi,\theta)}{d\Omega}\, d\Omega = \oint_r \frac{\mathcal{F}(r,\phi,\theta)dA}{d\Omega} d\Omega = \oint_r \mathcal{F}(r,\phi,\theta)\, dA. \tag{12.12}$$

For r much greater than the beam radius, the radial component of the scattered flux scales as r^{-2} and the surface area of the sphere scales as r^2; thus, the total scattered power integrated over all solid angles (Eq. 12.12) is independent of r.

In astronomical experiments, a detector at great distance r from the scattering center has a finite collecting area, A_d, and thus subtends a finite solid

angle $\Omega_d = A_d/r^2$. Thus, only the scattered flux at the detector, F_d, can be measured. In such scenarios, Eq. 12.11 is written

$$N_{\rm T} \iint_{\Omega_d} \frac{d\sigma(\phi,\theta)}{d\Omega} d\Omega = \frac{1}{F_b} \iint_{A_d} F_d(r,\phi,\theta)\, dA\,. \tag{12.13}$$

If we assume the total scattering cross section is σ and that the scattering is isotropic, then the differential cross section is $d\sigma/d\Omega = \sigma/4\pi$. The solid angle of the detector a distance r from the center of scattering is A_d/r^2, and the left hand side of Eq. 12.13 simplifies to $N_{\rm T}\sigma A_d/4\pi r^2$. Evaluating the right hand side, the observed flux over the detector area is $\mathcal{P}_d = F_d A_d$. Equating, we have $N_{\rm T}\sigma(A_d/4\pi R^2) = F_d A_d/F_b$. Since the number of target $N_{\rm T} = n_{\rm T} A_b L = N A_b$, we have the measured flux at the detector,

$$F_d = N\sigma \frac{A_b F_b}{4\pi r^2} = N\sigma \frac{P_b}{4\pi r^2}\,, \tag{12.14}$$

in terms of the column density of scatterers, N, where $P_b = A_b F_b$ is the power of the beam, dN_b/dt. If the particles in the monoenergetic beam are photons of frequency ω and electic field amplitude E_0, then beam flux [erg s^{-1} cm^{-2}] is $F_\omega = (c/8\pi)E_0^2$, and the power of the beam is $P_\omega = A_b F_\omega$ [erg s^{-1}]. The power is commonly refered to as the luminosity, L_ω, yielding

$$F_\omega = N\sigma(\omega) \frac{L_\omega}{4\pi r^2}\,. \tag{12.15}$$

Note that the factor 4π applies under the assumption of isotropic scattering.

Chapter 13

The Classical Oscillator

The classical oscillator is an ideal scenario of an isolated electron that is being accelerated by an oscillating electric field. The scenario serves as a analog to the oscillating probability distribution (square of the wave function) during an atomic transition. Here, our goal is to derive the cross section of the classical oscillator. Recall that the cross section is defined as the rate of energy (power) [erg s^{-1}] absorbed from a beam per unit flux in the beam [erg s^{-1} cm^{-2}] and has units cm^2.

To compute the rate at which energy is removed *from* a photon beam by a classical oscillator, we invoke energy conservation and equate the power radiated by a sinusoidal accelerating electron (thus the term classical oscillator) to the power removed from the incidient beam. We solve the cross section in four steps by deriving the radiative power of (1) an electron undergoing general acceleration, (2) a simple harmonic oscillator, (3) a damped harmonic oscillator, and (4) a damped oscillator with a sinusoidal forcing function. The latter scenario is used to derive the cross section of the classical oscillator by dividing the power by the beam flux. The results of will be compared to the atomic natural absorption cross section discussed in Chapter 4.

13.1 Accelerating Electron

Consider an electron undergoing acceleration at the origin of a spherical coordinate system and that the acceleration is parallel to the polar axis (which we will denote $\hat{\mathbf{k}}$ direction). The instantaneous monochromatic energy density [erg cm^{-3} Hz^{-1}] of the electric and magnetic field vectors a distance r from the electron are

$$\begin{aligned} \mathbf{E}_\omega(r,t) &= \frac{e}{c^2}\frac{\ddot{x}(t)}{r}\sin\theta\,\hat{\mathbf{\Theta}} \\ \mathbf{B}_\omega(r,t) &= \frac{e}{c^2}\frac{\ddot{x}(t)}{r}\sin\theta\,\hat{\mathbf{\Phi}}\,, \end{aligned} \tag{13.1}$$

where we use the notation $\omega = 2\pi\nu = 2\pi c/\lambda$, and where the polar angle θ is the angle between the radial vector $\mathbf{r} = r\,\hat{\mathbf{r}}$ and the acceleration vector, $\ddot{\mathbf{x}}(t) = \ddot{x}(t)\,\hat{\mathbf{k}}$. The instantaneous flux at distance r from the accelerating charge is given by the Poynting vector [erg s^{-1} cm^{-2}],

$$\mathbf{S}_\omega(r,t) = \frac{c}{4\pi}\,[\mathbf{E}_\omega(r,t) \times \mathbf{B}_\omega(r,t)] = \frac{e^2}{4\pi c^3}\frac{\ddot{x}^2(t)}{r^2}\sin^2\theta\,\hat{\mathbf{r}}\,. \tag{13.2}$$

The macroscopic radially directed flux is the time average of the Poynting vector,

$$\mathbf{F}_\omega(r,t) = \langle \mathbf{S}_\omega(r,t)\rangle = \frac{e^2}{4\pi c^3}\frac{\sin^2\theta}{r^2}\left\langle \ddot{x}^2\right\rangle\,\hat{\mathbf{r}}\,, \tag{13.3}$$

where we denote the time average of $\ddot{x}^2(t)$ with the notation $\left\langle \ddot{x}^2\right\rangle$. If the acceleration is cyclic, then the computation of the time average is straight forward, as will be described below in § 13.2 for a harmonic oscillator.

To obtain the cycle averaged instantaneous monochromatic power [erg s^{-1} Hz^{-1}] radiated over all solid angles, we compute

$$\mathcal{P}_\omega = \oint_r \mathbf{F}_\omega(r,t)\cdot\mathbf{dA} = \oint_r \langle \mathbf{S}_\omega(r,t)\rangle\cdot\mathbf{dA}\,, \tag{13.4}$$

where $\mathbf{dA} = r^2\sin\theta\,d\theta\,d\phi\,\hat{\mathbf{r}}$. Since $\mathbf{F} \propto r^{-2}$ and $\mathbf{dA} \propto r^2$, the power is independent of r. We have

$$\mathcal{P}_\omega = \frac{e^2}{4\pi c^3}\left\langle \ddot{x}^2\right\rangle \int_0^{2\pi}\int_0^{\pi} \sin^3\theta\,d\theta\,d\phi\,, \tag{13.5}$$

Using the substitution $\mu = \cos\theta$, so that $\sin^2\theta = 1-\mu^2$ and $d\mu = -\sin\theta\,d\theta$, the integral evaluates to $8\pi/3$, yielding

$$\boxed{\mathcal{P}_\omega = \frac{2e^2}{3c^3}\left\langle \ddot{x}^2\right\rangle\,.} \tag{13.6}$$

Thus, the total radiative power, i.e., the radially directed radiative flux passing through a surface subtending all 4π steradians of solid angle, generated by an accelerating electron is proportional to the time average of the square of the acceleration. Thus, what is required to compute the radiative power is a solution to the equation of motion for the electron, from which the time average of the square of the acceleration is determined.

13.2 Simple Oscillator

Harmonic oscillation is defined by acceleration, $\ddot{x}(t)$, that is proportional and opposite to the instantaneous displacement, i.e., $-kx(t)$, where k is a constant of proportionality which can be interpreted as the force acting on the electron

per unit displacement. Balancing forces, the equation of motion for harmonic oscillation of an electron is

$$\ddot{x}(t) + \omega_0^2 x(t) = 0\,, \tag{13.7}$$

where $\omega = \sqrt{k/m_e}$ is the eigenfrequency. Assuming $x(t) = \exp\{\lambda t\}$, we obtain the characteristic polynomial $\lambda^2 + \omega_0^2 = 0$, from which $\lambda = \pm i\omega_0$; there are two general solutions and they are complex conjugates of one another. Employing the superposition principle[1],

$$x(t) = \tilde{C}\exp\{i\omega_0 t\} + \tilde{C}^*\exp\{-i\omega_0\}\ , \tag{13.8}$$

where $\tilde{C} = A + iB$ is complex and $\tilde{C}^* = A - iB$ is the complex conjugate of $\tilde{C}$, where A is the real part of $\tilde{C}$ and B is the imaginary part. Employing the general identity[2],

$$\exp\{\pm i\omega_0\} = \cos\omega_0 t \pm i\sin\omega_0 t\,, \tag{13.9}$$

we rewrite the solution as $x(t) = 2A\cos\omega_0 t$, where $2A$ is the amplitude, which depends upon the intial conditions. If the initial condition at $t = 0$ is that the electron is at maximum displacement, $x(0) = x_0 = 2A$, the solution is

$$x(t) = x_0\cos\omega_0 t\,. \tag{13.10}$$

To obtain the total radiative power, we compute the time average of the acceleration for insertion into Eq. 13.6. The time derivitives of $x(t)$ are $\dot{x}(t) = -\omega_0 x_0\cos\omega_0 t$ and $\ddot{x}(t) = -\omega_0^2 x_0\sin\omega_0 t$. Over a single cycle period $\mathcal{T} = 2\pi/\omega_0$, from $t_1 = t - \mathcal{T}/2$ to $t_2 = t + \mathcal{T}/2$, centered on arbitrary time t and separated by exactly a single oscillation cycle such t_1 and t_2 arise at the same phase in adjacent cycles, we have

$$\big\langle \ddot{x}^2\big\rangle = \frac{1}{\mathcal{T}}\int_{t_1}^{t_2}\ddot{x}^2(t)\,dt = \frac{\omega_0^4 x_0^2}{\mathcal{T}}\int_{t_1}^{t_2}\cos^2\omega_0 t\,dt = \frac{\omega_0^4 x_0^2}{2}\,. \tag{13.11}$$

Thus, the total radiative power of a simple harmonic oscillating electron is

$$\boxed{\mathcal{P}_\omega = \frac{2e^2}{3c^3}\big\langle\ddot{x}^2\big\rangle = \frac{e^2\omega_0^4 x_0^2}{3c^3}\,.} \tag{13.12}$$

13.3 Damped Oscillator

Since the accelerating electron is radiating electromagnetic energy, the amplitude of the harmonic oscillations will decay over time. Thus, for the classical

[1]For linear ordinary differential equations, the form of the solution can be written as the sum of individual solutions.

[2]We remind the reader that each complex number $\tilde{C} = A + iB$ has a complex conjugate $\tilde{C}^* = A - iB$, such that $C^2 = \tilde{C}^*\tilde{C} = (A - iB)(A + iB) = A^2 + B^2$. Also, a complex number can be written $\tilde{C} = C\exp i\theta = C(\cos\theta + i\sin\theta)$, where $A = C\cos\theta$ and $B = C\sin\theta$. The ratio of the imaginary part to the real part is $B/A = \tan\theta$.

oscillator scenario, we can view the electric field generated by the accelerating electron as providing a damping force. The damping is interpreted as a radiation reaction force that is proportional to the instantaneous velocity,

$$\mathbf{F}_\gamma(t) = -m_e\gamma\dot{\mathbf{x}}(t)\,, \tag{13.13}$$

where γ is called the damping constant.

The equation of motion with damping is

$$\ddot{x}(t) + \gamma\dot{x}(t) + \omega_0^2 x(t) = 0\,. \tag{13.14}$$

As with the simple harmonic oscillator, if we again assume $x(t) = \exp\{\lambda t\}$, we obtain the characteristic polynomial $\lambda^2 + \gamma\lambda + \omega_0^2 = 0$, which has two roots, $\lambda = -\gamma/2 \pm \sqrt{(\gamma/2)^2 - \omega_0^2}$; there are three general solutions depending upon the ratio $(\gamma/2)/\omega_0$. We consider the "underdamped" case in which $\gamma/2 < \omega_0$, which yields $\lambda = -\gamma/2 \pm i\sqrt{\omega_0^2 - (\gamma/2)^2}$. The underdamped condition is the only one of the three in which oscillations are manifest. We again employ the superposition principle to obtain

$$x(t) = \exp\left\{-\frac{\gamma}{2}t\right\}\left[\tilde{C}\exp\{i\omega t\} + \tilde{C}^*\exp\{-i\omega t\}\right], \tag{13.15}$$

where $\omega = \sqrt{\omega_0^2 - (\gamma/2)^2}$. The real part of the eigenvalues govern the rate of decay and the imaginary part is the angular frequency of the damped oscillation. From Eq. 13.9, and applying the boundary condition of maximum displacement x_0 at $t = 0$, we have

$$x(t) = x_0\exp\left\{-\frac{\gamma}{2}t\right\}\cos\omega t\,. \tag{13.16}$$

Note that the damped oscillation frequency, ω, is shorter than the eigenfrequency, ω_0. The electron oscillates with a longer cycle time than the simple harmonic oscillator and the amplitude decays with an e-folding time of $\gamma/2$.

We obtain the decay rate γ by recognizing the fact that, averaged over a single cycle, the rate of work done on the electron by the radiation reaction force is equal to the negative of the radiative power loss, $\mathcal{P}_\omega$,

$$\frac{dW_\gamma}{dt} = \langle\mathbf{F}_\gamma\cdot\dot{\mathbf{x}}\rangle = -\mathcal{P}_\omega\,, \tag{13.17}$$

where $\mathcal{P}_\omega$ is taken from Eq. 13.6. The time average of $\mathbf{F}_\gamma(t)\cdot\dot{\mathbf{x}}(t)$ over a single oscillation cycle is

$$\langle\mathbf{F}_\gamma\cdot\dot{\mathbf{x}}\rangle = -m_e\gamma\,\langle\dot{\mathbf{x}}\cdot\dot{\mathbf{x}}\rangle = -m_e\gamma\,\frac{1}{\mathcal{T}}\int_{t_1}^{t_2}\dot{x}^2(t)\,dt\,, \tag{13.18}$$

and the radiative power loss is

$$\mathcal{P}_\omega = \frac{2e^2}{3c^3}\,\langle\ddot{x}^2\rangle = \frac{2e^2}{3c^3}\,\frac{1}{\mathcal{T}}\int_{t_1}^{t_2}\ddot{x}^2(t)\,dt\,, \tag{13.19}$$

where , $\mathcal{T} = 2\pi/\omega$, and where $t_1 = t - \mathcal{T}/2$ and $t_2 = t + \mathcal{T}/2$ are evaluated at identical phases in the oscillation centered on t.

The remaining steps to obtain the damping constant γ are to compute the first and second time derivitives of Eq. 13.16, perform the integrations in Eqs. 13.18 and 13.19, equate the rate of work done and the power loss (via Eq. 13.17) and solve for γ. Because of the decay of the damped oscillator amplitude with time, the symmetry of $x(t)$, $\dot{x}(t)$, and $\ddot{x}(t)$ for a simple oscillator is broken at times t_1 and $t_2 = t_1 + \mathcal{T}$. Thus, the integrals are non trivial. The mathematics are simplified with little loss of generality by assuming $\gamma \ll \omega_0$. Under this condition the damped oscillation frequency, ω, can be approximated by the eigenfrequency, ω_0, because the damping rate of the amplitude is negligible over a single cycle period $\mathcal{T} \simeq 2\pi/\omega_0$. Thus, the solution for the damped oscillator (Eq. 13.16) used to perform the integrations can be approximated using the simple oscillator[3] (Eq. 13.10). Applying this assumption, the integral in Eq. 13.18 evaluates to $\omega_0^2 x_0^2/2$ and the integral in Eq. 13.19 evaluates to $\omega_0^4 x_0^2/2$. Equating Eqs. 13.18 and 13.19,

$$-m_e\gamma\frac{\omega_0^2 x_0^2}{2} = -\frac{2e^2}{3c^3}\frac{\omega_0^4 x_0^2}{2}\,. \tag{13.20}$$

we find the damping constant,

$$\boxed{\gamma = \frac{2e^2\omega_0^2}{3m_e c^3} = 6.2664\times 10^{-24}\,\omega_0^2\ \text{sec}^{-1}\,.} \tag{13.21}$$

Clearly, the assumption $\gamma \ll \omega_0$ is well founded.

13.4 Forced Damped Oscillator

Consider an electron embedded in a monchromatic plane wave beam in which the oscillating electric field with amplitude E_0 and polarization $\mathbf{E}_0 = E_0\hat{\mathbf{k}}$. Placing the electron at $r = 0$, the force acting on the electron is

$$\mathbf{F}_\omega(t) = e\mathbf{E}_0\cos\omega t\,, \tag{13.22}$$

where $\omega = 2\pi\nu = 2\pi c/\lambda$ is the angular frequency. The equation of motion governing the electron is that of a damped harmonic oscillator, but with a driving force

$$\ddot{x}(t) + \gamma\dot{x}(t) + \omega_0^2 x(t) = F(t) = \frac{e}{m_e}E_0\cos\omega t\,, \tag{13.23}$$

[3]Most treatments (e.g., **???**) carry out the mathematical formalism to show that the radiative reaction force is proportional to $\dddot{x}(t)$, which is difficult to interprete. Following this result, the assumption of a simple harmonic oscillator is *then* applied in order to obtain $\dddot{x}(t) = -\omega^2\dot{x}(t)$. The reader is referred to other works if such details are sought. Here, to simplify obtaining the result, we begin with the assumption $\gamma \ll \omega_0$ and obtain the identical expression for γ.

where the damping force arises from the radiative power loss of the electron (the radiative reaction force discussed in § 13.3), with γ given by Eq 13.21.

The solution to Eq. 13.23 has a transitory solution followed by a steady state solution. The steady state solution is obtained most readily in the complex plane. Since any real quantity can be expressed as a component of a complex quantity (following Eq. 13.9), we can rewrite the driving force, Eq. 13.22, as a real plus imaginary part[4],

$$F(t) = \tilde{F}\exp\{i\omega t\} = \tilde{F}\left(\cos\omega t + i\sin\omega t\right) \qquad \tilde{F} = F_0\exp\{i\phi\}\ , \tag{13.24}$$

where $\tilde{F}$ is a complex coefficient with amplitude $F_0 = (e/m_e)E_0$ and phase modulation $\exp\{i\phi\} = \cos\phi + i\sin\phi$. We also write the (yet to be determined) position as real and imaginary parts

$$x(t) = \tilde{x}\exp\{i\omega t\} = \tilde{x}\left(\cos\omega t + i\sin\omega t\right) \qquad \tilde{x} = x_0\exp\{i\phi\}\ , \tag{13.25}$$

where $\tilde{x}$ is complex with amplitude x_0 and phase $\exp\{i\phi\}$. The full expression for the complex solution for the electron motion is

$$x(t) = \tilde{x}\exp\{i\omega t\} = x_0\exp\{i\phi\}\exp\{i\omega t\} = x_0\exp\{i(\omega t+\phi)\}\,. \tag{13.26}$$

The real part of Eq. 13.26 is taken as the steady-state solution to Eq. 13.23. Thus,

$$x(t) = x_0\cos(\omega t+\phi)\,, \tag{13.27}$$

for which we need to determine the amplitdue x_0 and phase angle ϕ. From Eq. 13.25, the derivitives of $x(t)$ are

$$\dot{x}(t) = i\omega\tilde{x}\exp\{i\omega t\} \qquad \ddot{x}(t) = (i\omega)^2\tilde{x}\exp\{i\omega t\}\ . \tag{13.28}$$

Substitution into Eq. 13.23 and subsequent cancellation of the $\exp\{i\omega t\}$ terms yields

$$(i\omega)^2\tilde{x} + (i\omega)\gamma\tilde{x} + \omega_0^2\tilde{x} = \tilde{F}\,. \tag{13.29}$$

Solving for $\tilde{x}$ provides the complex coefficient of $x(t)$,

$$\tilde{x} = \frac{\tilde{F}}{\omega_0^2 - \omega^2 + i\gamma\omega}\,, \tag{13.30}$$

which is interpreted as the amplitude of the phase modulation. The electron

[4]See footnote 2 of this appendix. A slight difference here is that for ease of solution, we write Eqs. 13.24 and 13.25 as the product two complex numbers (i.e., we multiple by a complex coefficient). This accounts for the fact that the electron motion will not be in phase with the driving force (the complex coefficient is the phase lag term).

oscillation amplitude is obtained from $x_0^2 = \tilde{x}^* \tilde{x}$, yielding

$$\begin{aligned} x_0 &= \left[\frac{\tilde{F}^*}{(\omega_0^2 - \omega^2 - i\gamma\omega)} \cdot \frac{\tilde{F}}{(\omega_0^2 - \omega^2 + i\gamma\omega)} \right]^{1/2} \\ &= \left[\frac{F_0 \exp\{-i\phi\}}{(\omega_0^2 - \omega^2 - i\gamma\omega)} \cdot \frac{F_0 \exp\{i\phi\}}{(\omega_0^2 - \omega^2 + i\gamma\omega)} \right]^{1/2} \\ &= \frac{F_0}{\left[(\omega^2 - \omega_0^2)^2 + \gamma^2\omega^2\right]^{1/2}} \\ &= \frac{(e/m_e)E_0}{\left[(\omega^2 - \omega_0^2)^2 + \gamma^2\omega^2\right]^{1/2}} \, . \end{aligned} \tag{13.31}$$

where $\tilde{x}^*$ and $\tilde{F}^*$ are the complex conjugates of $\tilde{x}$ and $\tilde{F}$. Note that the amplitude of the electron oscillation depends upon the driving force frequency, ω, and has maximum $\gamma(e/m_e)E_0\omega_0$ when $\omega = \omega_0$ (a phenomonon called resonance), where E_0 is the amplitude of the oscillating electric field of the incident beam. Substituting for x_0 in Eq. 13.27, we have

$$x(t) = \frac{(e/m_e)E_0 \cos(\omega t + \phi)}{\left[(\omega^2 - \omega_0^2)^2 + \gamma^2\omega^2\right]^{1/2}} \, . \tag{13.32}$$

Thus, we see that, once steady state is achieved, the electron oscillates at the frequency of the electic field of the incident beam. Furthermore, the oscillation is out of phase with the electric field by phase angle ϕ, which can easily be shown to be $\phi = -\tan^{-1}[\gamma\omega/(\omega_0^2 - \omega^2)]$. For underdamped conditions near resonance, the electron lags the electric field by $\phi \simeq \pi/2$.

Following the steps taken in § 13.2, we employ Eq. 13.6 to obtain the total power radiated over all solid angles from the time average of the real part of the electron acceleration, $\ddot{x}(t) = -\omega^2 x(t)$. Carrying out the time average (see Eq. 13.11), we obtain $\langle \ddot{x} \rangle = \omega^2 x_0^2/2$, from which we find the steady state power of electromagentic energy emitted by the electron

$$\boxed{\mathcal{P}_\omega = \frac{e^4\omega^4}{3m_e^2c^3} \frac{E_0^2}{\left(\omega^2 - \omega_0^2\right)^2 + \gamma^2\omega^2} \, .} \tag{13.33}$$

For $\omega = \omega_0$, the eigenfrequency of the system, the power is a maximum with $\mathcal{P}_{max} = (e^4\omega_0^2/3m_e^2c^3\gamma^2)E_0^2$.

13.5 Cross Section of the Classical Oscillator

From the principles of absorption and scattering cross sections discussed in Appendix 12, the total absorption (scattering) cross section per interacting particle

at frequency ω is defined as the power absorbed (scattered over all solid angles) from an incident beam normalized to the beam flux,

$$N_{\rm T}\sigma(\omega) = \frac{\mathcal{P}_\omega}{F_\omega}\,, \tag{13.34}$$

where we carry over the angular frequency notation for the classical oscillator and explicitely include the monochromatic frequency of the beam flux.

For the following, allow the beam to be polychromatic with the stipulation that the flux is constant at each frequency, i.e., that the specific intensity distribution is constant or the electric field amplitude is constant as a function of ω. The flux in the incident beam is then $F_\omega = (c/8\pi)E_0^2$ at all frequencies. As will be demonstrated below, this assumption is not required over a large range of frequencies, but only over an *extremely* narrow range centered on the eigenfrequency ω_0.

We equate the power radiated into all solid angles by the forced accelerating electron (given by Eq. 13.33) as the power scattered from the incident beam. Barring the radiation scattered back into the direction of the beam (which is effectively zero since the angular distribution of the scattered power is $d\mathcal{P}(\phi,\theta)/d\Omega \propto \sin^2\theta$, where $\theta = 0$ in the beam direction), the total power scattered over all solid angles is also equatable to the power absorbed from the beam.

The classical oscillator is a single electron, so that $N_{\rm T} = 1$. Since the flux in the incident beam is $F_\omega = (c/8\pi)E_0^2$, the frequency dependent total cross section for the classical oscillator is

$$\sigma(\omega) = \frac{\mathcal{P}_\omega}{F_\omega} = \frac{e^4\omega^4}{3m_e^2c^3}\,\frac{E_0^2}{\left(\omega^2-\omega_0^2\right)^2+\gamma^2\omega^2}\left(\frac{cE_0^2}{8\pi}\right)^{-1}\,, \tag{13.35}$$

which simplifies to,

$$\sigma(\omega) = \frac{8\pi e^4\omega^4}{3m_e^2c^4}\,\frac{1}{\left(\omega^2-\omega_0^2\right)^2+\gamma^2\omega^2}\,. \tag{13.36}$$

The behavior of Eq. 13.36 is such that the half-height full-width of $\sigma(\omega)$ is $\Delta\omega \simeq \gamma/2$. From Eq. 13.21, $\gamma/\omega_0^2 \simeq 6.3\times10^{-24}$, so that the fractional full width is $\Delta\omega/\omega_0 \simeq (\omega_0/2)(\gamma/\omega_0^2) \simeq 3.15\times10^{-24}\omega_0$. For ultraviolet and optical transitions, $\omega_0 \simeq 10^{16}$ sec^{-1} (for example, neutral hydrogen Lyα has $\omega_0 = 1.549\times10^{16}$ sec^{-1}), yielding $\Delta\omega/\omega_0 \simeq 10^{-8}$. Thus, Eq. 13.36 is highly peaked for the eigenfrequncy of atomic transitions (our assumption of a constant flux over this range is thus quite sound). We can thus apply the approximation

$$\left(\omega^2-\omega_0^2\right) = (\omega+\omega_0)\,(\omega-\omega_0) \simeq 2\omega_0\,(\omega-\omega_0)\,. \tag{13.37}$$

Invoking Eq. 13.37, and replacing all other appearances of ω in Eq. 13.36 with ω_0, we obtain

$$\sigma(\omega) = \frac{2\pi e^4\omega_0^2}{3m_e^2c^4}\,\frac{1}{\left(\omega-\omega_0\right)^2+(\gamma/2)^2}\,. \tag{13.38}$$

Since the relationship between the damping constant and the eigenfrequency is $\gamma = 2e^2\omega_0^2/3m_ec^3$, further manipulation yields

$$\boxed{\sigma(\omega) = \frac{2\pi e^2}{m_e c}\,\frac{\gamma/2}{\left(\omega-\omega_0\right)^2 + (\gamma/2)^2},} \tag{13.39}$$

Within a factor $1/\pi$, the second factor of Eq. 13.39 is known as the Cauchy probability distribution, Breit-Wigner distribution, or more commonly by physicists and astronomers as the Lorentz distribution (or Lorentzian),

$$\mathcal{L}(x) = \frac{1}{\pi}\,\frac{y}{(x-x_0)^2 + y^2}\,, \tag{13.40}$$

for which the peak amplitude is $1/\pi y$. Thus, y is known as the scale parameter. Note that the half-width at half-maximum, FWHM/2, is also given by y. The peak is at x_0, which is known as the location parameter. The area is unity

$$\frac{1}{\pi}\int_0^\infty \frac{y}{(x-x_0)^2 + y^2}\,dx = 1\,. \tag{13.41}$$

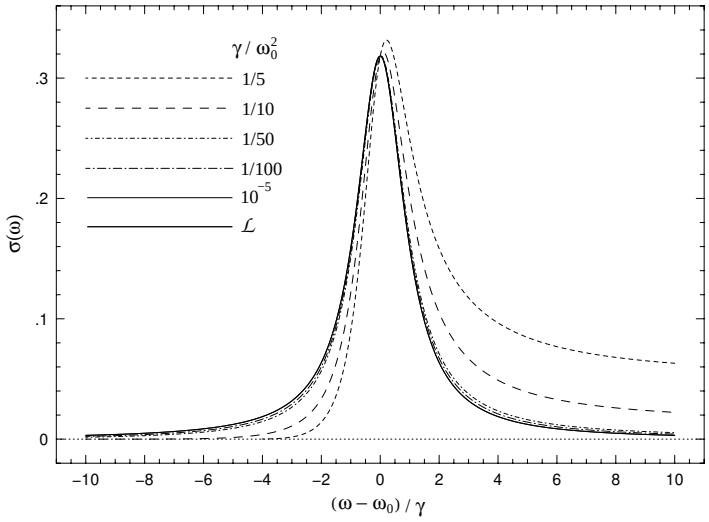

Figure 13.1: A comparison between the full expression of the cross section for the classical oscillator, $\sigma(\omega)$, as given by Eq. 13.36, and the Lorentzian version (designated $\mathcal{L}$ in the figure legend), given by Eq. 13.38 derived from the fact that $\gamma \ll \omega_0^2$. The amplitude of the curves have been normalized for ease of comparison. The shapes are independent of the value of ω_0; they depend only upon the ratio γ/ω_0^2. For $\gamma/\omega_0^2 \leq 10^{-5}$, the two functions differ by no more than 0.0002% at the peak and by no more than 0.3% well into the wings. Since $\gamma/\omega_0^2 \simeq 10^{-24}$ for the classical oscillator, the application of a Lorentzian is well founded.

In Figure 13.1, Eq. 13.36 is plotted for various values of γ/ω_0^2. As the ratio decreases, the function approaches the form of a Lorentzian, such that by

$\gamma/\omega_0^2 = 10^{-5}$, the fractional difference between the two functions never exceeds 0.3% within ten half-width at half maximum. For the classical oscillator, $\gamma/\omega_0^2 \simeq 10^{-24}$; the Lorentzian is an excellent approximation for the cross section.

In terms of frequency, we have $\Delta\omega = 2\pi\Delta\nu$, where $\Delta\omega = \omega - \omega_0$ and $\Delta\nu = \nu - \nu_0$; we can thus write Eq. 13.39 as

$$\boxed{\sigma(\nu) = \frac{e^2}{m_e c} \frac{\gamma/4\pi}{(\nu - \nu_0)^2 + (\gamma/4\pi)^2} \,.} \tag{13.42}$$

Applying Eq. 13.41, the integrated absorption coefficient over all frequencies is

$$\int_0^\infty \sigma(\nu)\, d\nu = \frac{\pi e^2}{m_e c} \,. \tag{13.43}$$

In terms of wavelength, we have $\Delta\omega = (2\pi c/\lambda_0^2)\Delta\lambda$, where $\Delta\lambda = \lambda - \lambda_0$; Eq. 13.39 can then be written

$$\boxed{\sigma(\lambda) = \frac{e^2}{m_e c} \frac{\lambda_0^2}{c} \frac{\gamma\lambda_0^2/4\pi c}{(\lambda - \lambda_0)^2 + (\gamma\lambda_0^2/4\pi c)^2} \,.} \tag{13.44}$$

The integrated absorption coefficient over all wavelengths is

$$\int_0^\infty \sigma(\lambda)\, d\lambda = \frac{\pi e^2}{m_e c} \frac{\lambda_0^2}{c} . \tag{13.45}$$

The integration of $\sigma(\nu)$ over all frequencies and of $\sigma(\lambda)$ over all wavelengths provides which is the total power removed from the beam per absorber per unit flux.